BEHAVIOR OF GEOCELL REINFORCED SANDY SOILS UNDER STATIC LOAD

A THESIS SUBMITTED TO
THE GRADUATE SCHOOL OF NATURAL AND APPLIED SCIENCES
OF
MIDDLE EAST TECHNICAL UNIVERSITY

BY

MUHARREM CAN ŞİMŞEK

IN PARTIAL FULFILLMENT OF THE REQUIREMENTS
FOR
THE DEGREE OF MASTER OF SCIENCE
IN
CIVIL ENGINEERING

DECEMBER 2017

Approval of the thesis:

BEHAVIOR OF GEOCELL REINFORCED SANDY SOILS UNDER STATIC LOAD

submitted by **MUHARREM CAN ŞİMŞEK** in partial fulfillment of the requirements for the degree of **Master of Science in Civil Engineering Department, Middle East Technical University** by,

Prof. Dr. Gülbin DURAL ÜNVER _____
Dean, Graduate School of **Natural and Applied Sciences**

Prof. Dr. İsmail Özgür YAMAN _____
Head of Department, **Civil Engineering**

Asst. Prof. Dr. Nejan HUVAJ SARIHAN _____
Supervisor, **Civil Engineering Dept., METU**

Examining Committee Members:

Prof. Dr. Erdal ÇOKÇA _____
Civil Engineering Dept., METU

Asst. Prof. Dr. Nejan HUVAJ SARIHAN _____
Civil Engineering Dept., METU

Prof. Dr. B. Sadık BAKIR _____
Civil Engineering Dept., METU

Asst. Prof. Dr. N. Kartal TOKER _____
Civil Engineering Dept., METU

Assoc. Prof. Dr. Cem AKGÜNER _____
Civil Engineering Dept., TED University

Date: December 20, 2017

I hereby declare that all information in this document has been obtained and presented in accordance with academic rules and ethical conduct. I also declare that, as required by these rules and conduct, I have fully cited and referenced all material and results that are not original to this work.

Name, Last Name: Muharrem Can ŞİMŞEK

Signature :

ABSTRACT

BEHAVIOR OF GEOCELL REINFORCED SANDY SOILS UNDER STATIC LOAD

ŞİMŞEK, Muharrem Can
M.S., Department of Civil Engineering
Supervisor: Asst. Prof. Dr. Nejan HUVAJ SARIHAN

December 2017, 118 pages

Geocell, which is mainly used in transportation and geotechnical engineering applications, is a three dimensional cellular geosynthetic product to provide all-around confinement by the interaction of infill soil, cell walls and cell geometry. Geocell prevents the lateral spreading of soil, provides increased stiffness, distributes the loads over a larger area and helps reducing the total and differential settlements, in other words it provides soil reinforcement and stabilization. This study comprises of laboratory model tests of geocell-reinforced sandy soil with different dimensions of geocells. Tests are conducted in a tank with dimensions of 1 m width, 1 m length and various heights depending on geocell height, where static loading is applied via a steel plate on the sand surface. Different geocell openings and cell heights are used. In addition, the load is applied at the center of the cell and at the intersection of polymer boundaries of geocells. 13 model tests are conducted to evaluate the amount of the contributions of the geocells with regards to height of the cell, width of the cell and loading location. The results are presented in terms of load versus settlement plots and bearing capacity and settlement performance of geocell reinforcement are investigated and compared to unreinforced conditions. It is observed that for a predetermined settlement value, presence of the geocells increased the bearing capacity of the footing

by 38% to 73% compared to unreinforced cases and reduced the settlements under a given pressure.

Keywords: geocell, laboratory test, plate load test, settlement, bearing capacity, improvement.

ÖZ

HÜCRESEL DOLGU SİSTEMİ İLE GÜÇLENDİRİLMİŞ KUMLU ZEMİNLERİN STATİK YÜK ALTINDA DAVRANIŞI

ŞİMŞEK, Muharrem Can
Yüksek Lisans, İnşaat Mühendisliği Bölümü
Tez Yöneticisi: Yrd. Doç. Dr. Nejan HUVAJ SARIHAN

Aralık 2017, 118 sayfa

Genellikle ulaştırma ve geoteknik mühendisliği uygulamalarında kullanılan hücresel dolgu sistemi, hücre içi dolgu malzemesi, hücre duvarı ve hücre geometrisinin etkileşimi ile zemin hareketinin her yönden sınırlandırılmasını sağlayan üç boyutlu, hücresel bir geosentetik üründür. Hücresel dolgu sistemi, zeminin yanal olarak yayılmasını engeller, rijitliğini arttırır, yükleri çok daha geniş bir alana dağıtarak toplam ve farklı oturmaların azalmasına yardımcı olur, diğer bir deyişle zeminin güçlendirilmesini ve stabilizasyonunu sağlar. Bu çalışma, farklı boyutlardaki hücresel dolgu sistemleri ile güçlendirilmiş kumlu zeminlerin laboratuvar model deneylerinden oluşmaktadır. Deneyler, 1.0 m genişliğinde, 1.0 m uzunluğunda ve hücresel dolgu sisteminin yüksekliğine göre değişen çeşitli yüksekliklerde, statik yüklemenin kum yüzeyinden çelik bir plaka vasıtasıyla uygulandığı bir tankta gerçekleştirilmiştir. Farklı hücre açıklıkları ve hücre yükseklikleri kullanılmıştır. Ek olarak, yük, hücrenin tam ortasına ve hücrelerin polimer kenarlarının kesiştiği yere uygulanmıştır. Hücresel dolgu sistemlerinde, hücrenin yüksekliği, genişliği ve yükün uygulanma noktasının iyileştirme miktarına etkisi 13 model deney ile belirlenmiştir. Sonuçlar, yük - oturma grafikleri olarak sunulmuş ve hücresel dolgu güçlendirmesinin taşıma gücü ve oturma performansı, güçlendirilmemiş durum ile karşılaştırılarak araştırılmıştır. Belirlenen bir

oturma değeri için, hücresel dolgu sistemi varlığının, güçlendirilmemiş durumlara kıyasla, temelin taşıma kapasitesini %38 ila %73 aralığında arttırdığı ve belirli bir basınç değeri altında oluşan oturmaları azalttığı gözlemlenmiştir.

Anahtar Kelimeler: hücresel dolgu sistemi, laboratuvar deneyi, plaka yükleme deneyi, oturma, taşıma gücü, iyileştirme.

To my family

ACKNOWLEDGMENTS

I would like to thank my supervisor Asst. Prof. Dr. Nejan Huvaj Sarıhan for her guidance, technical support and understanding. I am grateful to her for sharing her invaluable experience in every stage.

I would also like to thank Asst. Prof. Dr. N. Kartal Toker for his comments and guidance throughout this study.

I would like to thank my geotechnical engineering division instructors and my colleagues in METU. I learned many things from them throughout my graduate study.

I would like to express my special gratitude to my mother Nergis Şimşek, my father Enver Şimşek and my sister Cansu Mullaoğlu for their continuous support, encouragement and patience.

I would like to present my special thanks to my boss Dr. Özgür Yılmazer for his understanding and patience.

Finally, I would like to thank to staff of Soil Mechanics Laboratory of Civil Engineering Department of METU. I am also grateful to ALFA Testing Equipments, TENSAR International Corporation and GEOPLAS Co. Ltd. for their moral and material supports.

TABLE OF CONTENTS

LIST OF TABLES

LIST OF FIGURES

CHAPTER 1

INTRODUCTION

The development of transportation and geotechnical fields in the world, brings about a significant increase in the use of geosynthetics. Materials science developments in the last few decades has brought a new breath to the geosynthetics industry. Rapid and easy implementation, cost advantage, durability and material life time are the main determining factors in favor of application of geosynthetic materials by comparison to other methods.

Geocells come into prominence with their wide implementation areas. They are commonly used under the embankments constructed on weak soils, in the ballast of railways and in the gravel basements of unpaved roads to prevent differential settlement and also improve the bearing capacity. Geocells are also used as channel lining reinforcements for river valley projects, stability and erosion controls of slopes, construction of green walls and under the foundation of any structure.

The key benefit of geocells is to confine the fill inside three-dimensional polymeric honeycomb cells thus reduce the lateral movement of soil and form a stiffened mattress to distribute applied loads to a wider area (Han et al., 2008). A view of crushed stone filled perforated geocell is shown in Figure 1.1.

Figure 1.1 A view of crushed stone filled perforated geocell (Parvathi and Jayasree, 2017)

An estimated 20% of all roads in the world are paved (Tingle and Jersey, 2007) and according to the AASHTO (American Association of State Highway and Transportation Officials) report, approximately 20% of pavements fail due to insufficient structural strength (Mengelt et al., 2000). To remedy this problem, geocells have become increasingly widespread and especially preferred in road projects. They are effective in increasing the bearing capacity of the roads, while enabling faster application with easy deployment and transportation advantage, as demonstrated in Figure 1.2.

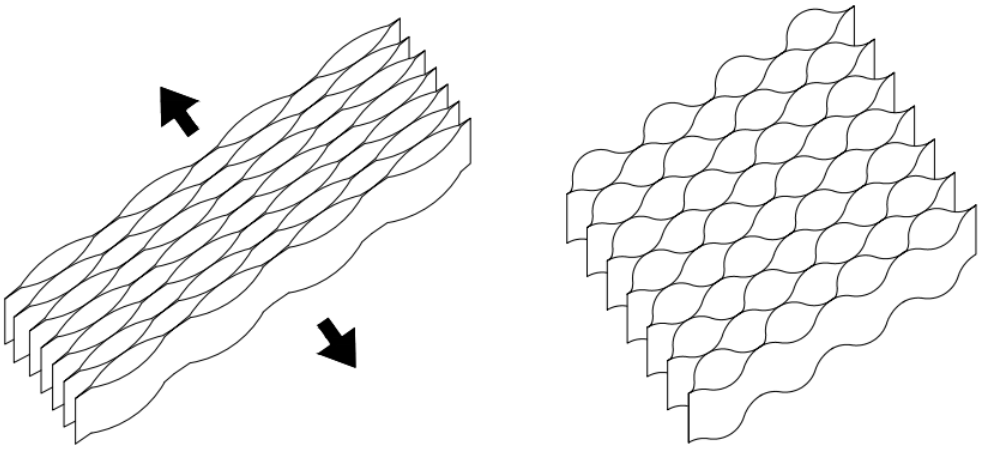

Figure 1.2 Typical view of geocells

According to the estimation of Koerner (2012) for the year 2010, geocomposite sales reached 400 million US Dollars. In recent years, usage of geocells have become popular in Turkey, but some uncertainties, deficiencies and also difficulties during design processes necessitate more research and effort. Accurate identification of geocell reinforced soil's behavior might make the design of structures more economical, safe and long-lasting. In this study, geocell reinforced and unreinforced laboratory tests were performed in a sandy soil and contribution of geocell to either bearing capacity or settlement is studied under static loads.

1.1 Problem Statement

Structures are not always constructed on solid grounds. Soils may need to be improved to increase their bearing capacity or to reduce settlements in major projects. Improvement of soils with geosynthetics has recently started to be preferred, thanks to their easy and fast implementation of them. Geocells are a three-dimensional form of geosynthetic materials with interconnected cells infilled with compacted soil. They have been successfully used worldwide to construct retaining walls, slopes and to reinforce road bases (Han et. al., 2008). Behavior of geocell reinforced soil can be affected by many factors such as height, width, thickness and material of geocell, as well as type and density of basement and infill soils. Geocell width and height are two major factors that influence the geocell performance the most. Effects of these factors on the load carrying capacity and also settlement performance of geocell-reinforced soil mattresses have been investigated by several researchers (Shin et al., 2017; Gurbuz and Mertol, 2012; Sitharam et al., 2005; Latha et. al, 2006; Emersleben and Meyer, 2008). However, most of the model experimental studies used only one cell and there is a need for studies with multiple geocells to better represent overall behavior in the field. Furthermore, the sizes of geocells that are used widely in the market have not been used in most of these studies, which developed the need to investigate that aspect of the topic. Additionally, geocells have bigger aperture sizes compared to other geosynthetics such as geogrids, geonets etc. Because of this, additional study is needed to investigate the effect of loading location (in the middle of the cell or at the

intersection of polymer cell boundaries) on the behavior of the geocell-reinforced soils, considering that different results could be obtained in the case of small area of loadings applied on geocells have big aperture sizes and this was not studied before.

1.2 Research Objectives

The main objective of this study is to understand the effects of some of the factors on the behavior of geocell reinforced soils, deformation and also bearing capacity characteristics of footings under static load. Other objectives are;

1) Investigation of the amount of improvement in the case of using different heights of geocells and different geocell openings.
2) Research on the effects of geocell width on the behavior of the bearing capacity of the footing.
3) Investigation of the significance of loading location by applying the load at the center and also intersection of the boundaries of the geocell.

In order to achieve the aims listed above, four series of static plate load tests were conducted. Contributions of the geocell usage on the bearing capacity performance of the footing were investigated by comparing with tests on unreinforced soil. Findings in this study can be helpful for developing a better understanding on geocell reinforced granular soil behavior. The results of this study are believed to be useful for further understanding of the design of geocell reinforced sands.

1.3 Scope

This study mainly investigates the effect of geocell reinforcement on the settlement and the bearing capacity characteristics of sandy soils. In Chapter 2, a literature review is presented. In Chapter 3, design and manufacturing process of test set up and usage of measuring sets are provided and also properties of used materials that are geocell and sand are specified and examined. In Chapter 4, details of laboratory model tests such as relative density determination, preparation of an experiment and results of static plate loading tests are presented. Amount of contribution of using geocells with

different cell height and cell width are examined. Additionally, significance of loading location are investigated by applying the load at the center of the cell and at the intersection of polymer boundaries of cells. Finally, in Chapter 5, consequences of the study are highlighted and topics for further studies are suggested.

CHAPTER 2

LITERATURE REVIEW

This chapter contains a literature review about geocell reinforced soils under three main titles. Firstly, general information about applications and usage areas of geocells are discussed, then studies performed in cohesionless and cohesive soils are examined.

2.1 Applications of Geocell

Geocell reinforcement is a lately developed technique in the area of soil reinforcement and comprises a three dimensional, polymeric, honeycomb-like structure of filled cells interconnected at joints. Because of its three dimensional nature, the geocell offers an all-round confinement to the encapsulated soil, and the interconnected filled cells form a panel that acts like a large mat and spreads the applied load over a larger area, instead of directly at the point of contact, leading to an improvement in the overall performance of the foundation (Sitharam et al., 2005).

Geocells are widely applied in geotechnical and transportation engineering, in areas such as controlling erosion of slopes and river banks, enhancing bearing capacities of pavements and footings, reinforcing soft grounds and slopes, and protecting shores and channel beds (Chen et al., 2013). Some schematic and photographic views of application areas of geocells are shown in Figure 2.1.

Figure 2.1 Applications of geocells (a: channel lining, retaining wall, erosion and slope protection, b: road and foundation basement, soft ground reinforcing, Terram, www.terram.com, last visited on September, 2017)

During the last 40 years geosynthetic reinforcement has greatly helped to improve the performance of paved and unpaved roads and become one of the established techniques for base course reinforcement (Giroud & Han 2004). Problems during design process and some unknowns about the behavior of geocell reinforced soils cause hesitation in the use of geocells but nevertheless it is observed that applications of geocells are increasing day by day.

2.2 Studies of Geocell in Cohesionless Soils

This section contains the studies performed on cohesionless soils in either static or repeated loading conditions. Each study is briefly summarized below.

Bathurst and Karpurapu (1993) carried out 23 large-diameter triaxial compression tests by using uniformly-graded silica sand and 100% crushed limestone. It was observed that geocell reinforced specimens showed greater strain-hardening response and shear strength. Reinforced and unreinforced specimens prepared in the same relative density

showed that they both have almost the same friction angle values but geocell reinforced specimens had bigger apparent cohesion due to geocell confinement as against unreinforced specimens. Geocell confinement effect was calculated from Elastic Membrane Theory proposed by Henkel and Gilbert (1952).

$$\Delta\sigma_3 = \frac{2M\varepsilon_c}{d}\frac{1}{(1-\varepsilon_a)} \quad (2.1)$$

$$\varepsilon_c = \frac{1-\sqrt{1-\varepsilon_a}}{1-\varepsilon_a} \quad (2.2)$$

$\Delta\sigma_3$, increased confining pressure

M, modulus of the membrane

ε_c, circumferential strain

ε_a, axial strain

d, original diameter of specimen

Likewise, strength of geocell-soil composite was described in terms of equivalent cohesion showed as c_r and calculated from Equation 3 to link with Mohr-Coulomb strength envelope shown in Figure 2.2. Predicted cohesion values were smaller than measured cohesion values. Recommended elastic membrane model is valid for single geocell reinforced specimens accordingly, in field applications of multi-cell geocells will give larger strength due to interactions between connected cells. In this way, it was emphasized that safer calculations and estimations can be carried out for designs.

$$c_r = \frac{\Delta\sigma_3}{2}\tan\left(\frac{\pi}{4}+\frac{\varphi}{2}\right) \quad (2.3)$$

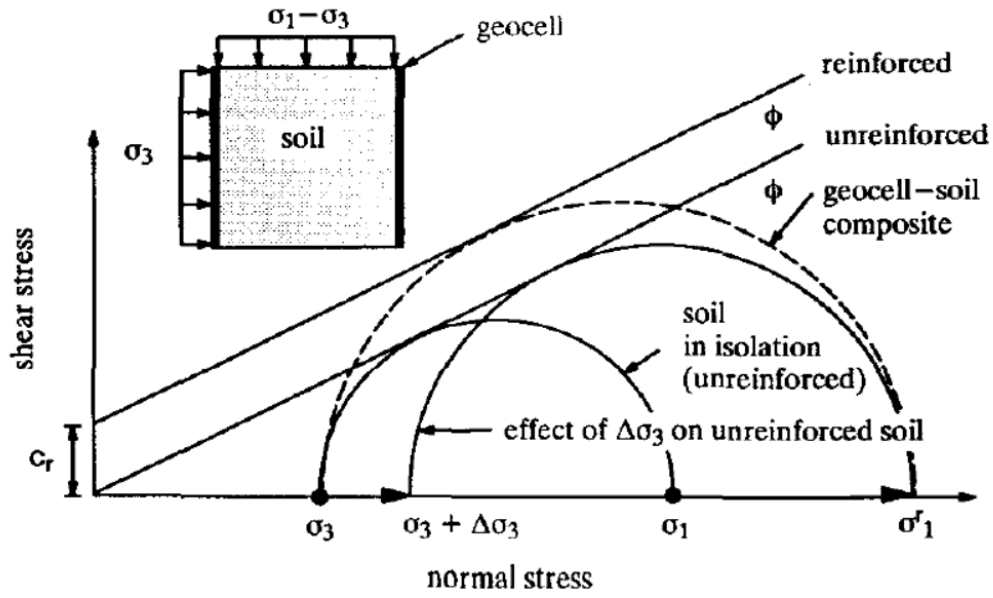

Figure 2.2 Mohr circle construction for calculation of equivalent cohesion for geocell-soil composites (Bathurst and Karpurapu 1993)

Rajagopal et al. (1999) investigated single and multiple geocell reinforced granular soil behavior with regards to strength and stiffness by performing a series of triaxial tests. Uniformly graded river sand and four different types of geosynthetics were used in tests. Failure mechanism was followed during tests and it was seen that failure starts from seam of outer cells to inner cells in multiple geocells due to the seam strength is lower than the strength of geosynthetic material. In a similar manner with Bathurst and Karpurapu (1993) and Chen at al. (2013), same friction angle values were obtained in both unreinforced and geocell reinforced conditions, while an obvious contribution of geocell reinforcement to cohesion was observed. Different configurations were used in tests, as shown in Figure 2.3. It was concluded that at least three interconnected cells represent real behavior of multiple cells which shown in Figure 2.4. Using four interconnected cells gave result very similar to three-cell condition, and it is speculated that more than four cells will also give similar results.

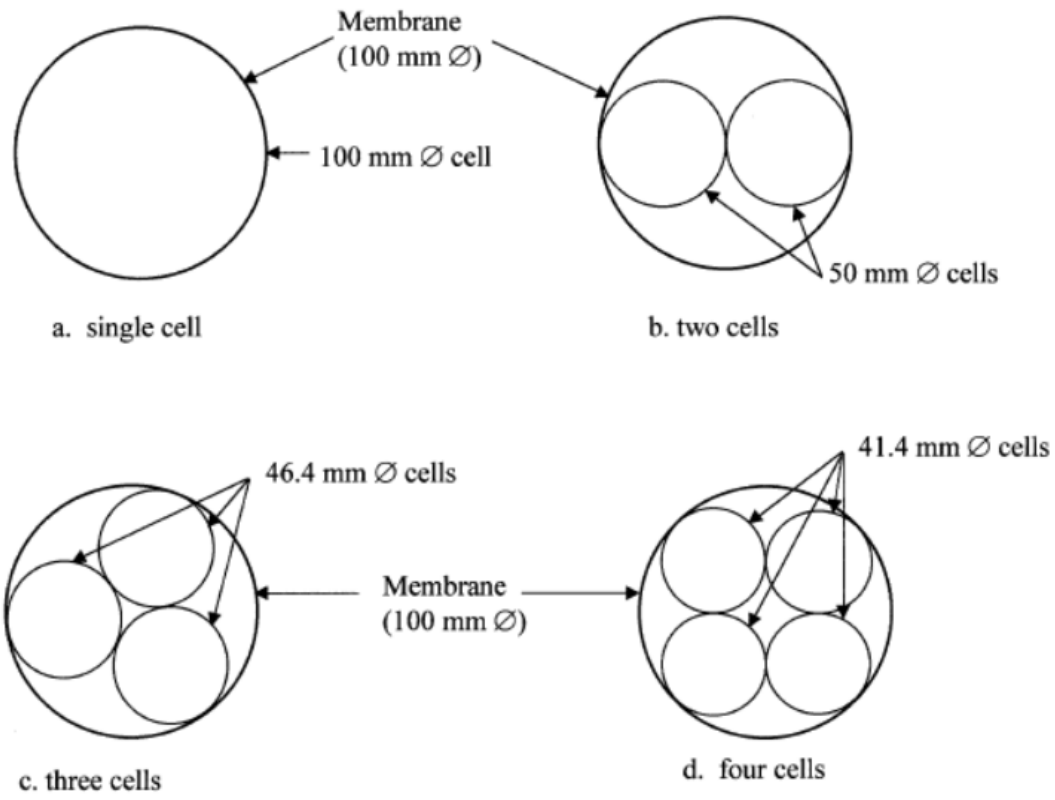

Figure 2.3 Different configurations of cells used in triaxial tests (Rajagopal et al., 1999)

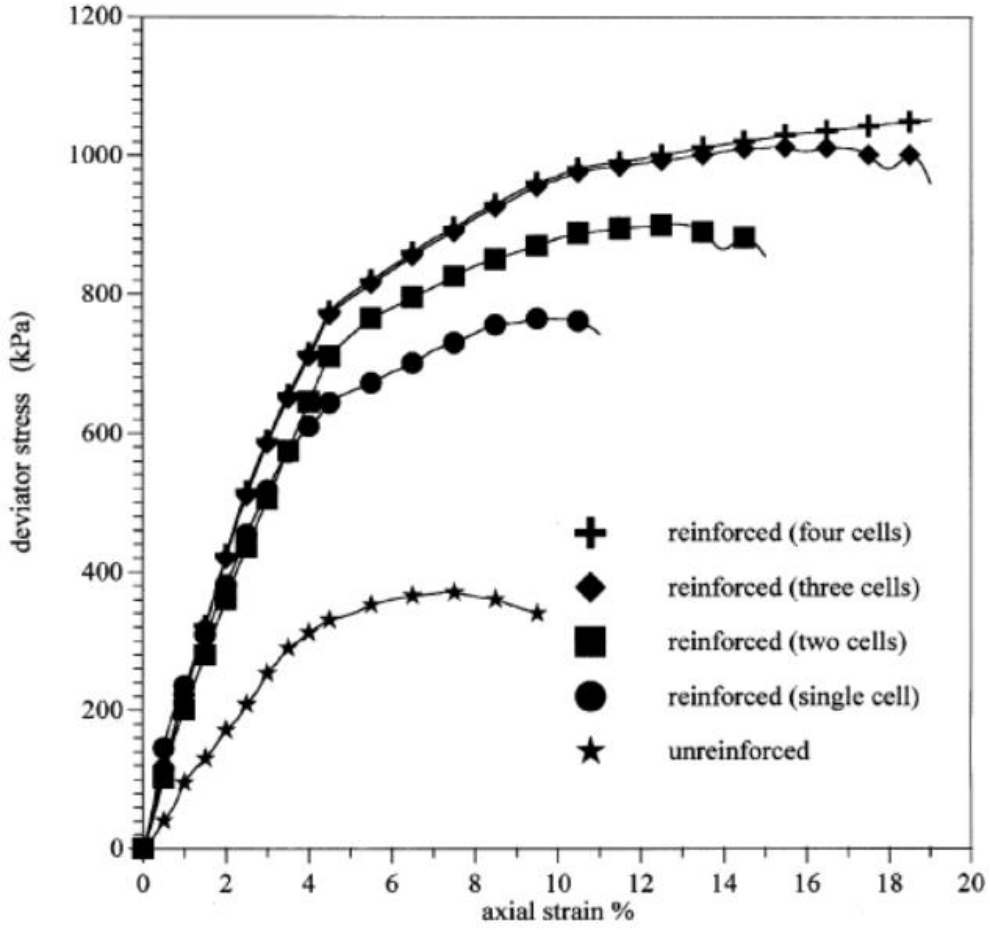

Figure 2.4 Stress-strain curves for sand with different configurations of geocells (confining pressure = 100 kPa) (Rajagopal et al., 1999)

Chen at al. (2013) performed several triaxial compression tests with geocell reinforced sand samples in different shape, size and number of cells to understand effects of these factors. They observed that cell size is the most important factor and there is an inversely proportional relation between the cell size and apparent cohesion. They have also researched the effect of the shape of the cells and found that circular cells have highest and hexagonal cells have lowest apparent cohesion. In addition, friction angle values of unreinforced and geocell-reinforced specimens were compared, and a small difference was observed. Hexagonal shape cells had the biggest friction angle due to number of corners.

Han et al. (2008) researched the behavior of single geocell reinforced sand under a vertical load by comparing experimental and numerical results. In experimental studies, poorly graded Kansas River sand and HDPE-made geocells which have 50 mm height, 210 mm length and 250 mm width were used. Rectangular loading plate was selected in dimensions (100 mm x 90 mm) to not to touch the sides of the geocell. Sand was compacted to 70% relative density. Two unreinforced and two reinforced tests were performed to ensure repeatability of tests. Because defining the load transfer mechanism was the aim, no subgrade was used in the tests. Schematic view of the test setup is shown in Figure 2.5.

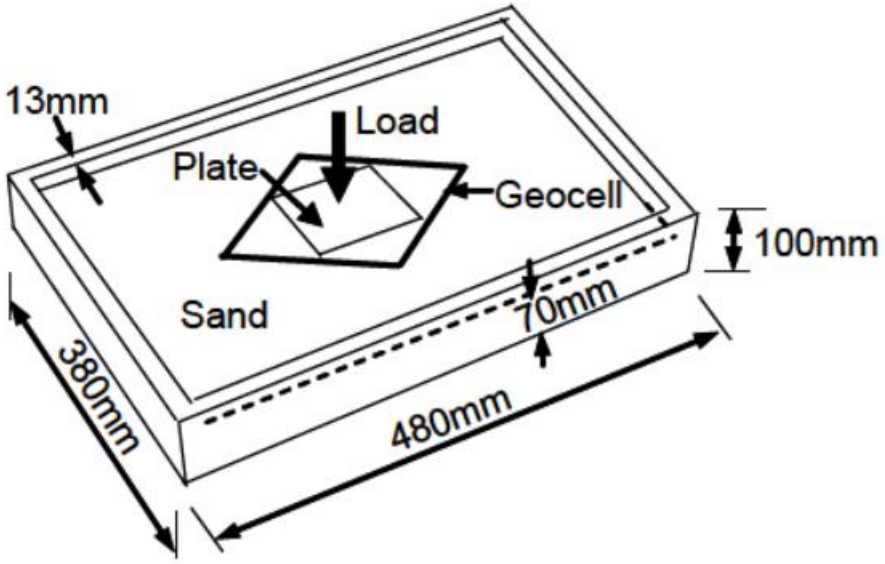

Figure 2.5 Test box and test setup (Han et al., 2007)

According to experimental test results, at the same deformation (1.25 mm), stress increased from 70 kPa to 115 kPa by using single geocell reinforcement. In the case of using multiple geocell reinforcement, it was speculated that a larger stress increment could be needed to reach the same deformation. Numerical analyses were done by using FLAC 3D which is finite difference modeling software. Sand was modeled as linearly elastic – perfectly plastic material and geocell was modeled as structural

(geogrid) elements. Vertical and horizontal displacements of soil were examined for both unreinforced and reinforced conditions. Forces in geocell walls, displacement of geocell and interface shear stresses between geocell and sand could be seen by using finite difference software, which are not possible by experimental studies. Matching experimental and numerical results were obtained (Figure 2.6).

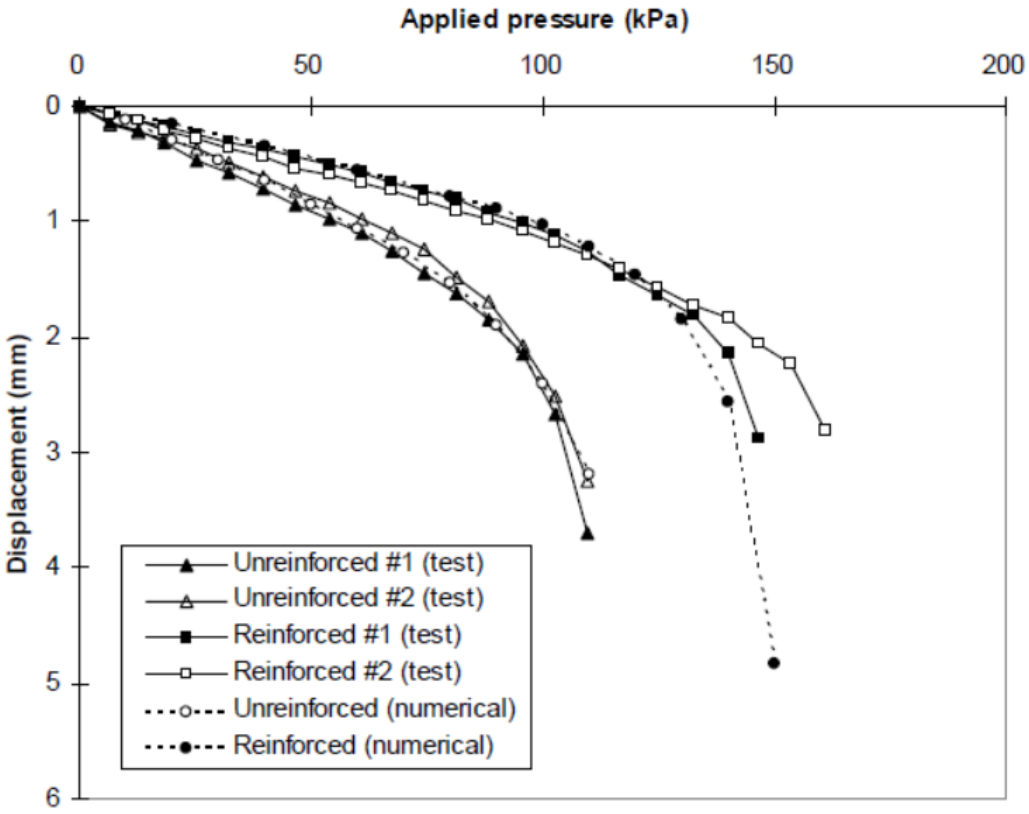

Figure 2.6 Results of plate load tests (Han et al., 2007)

Pokharel et al. (2009) investigated single-geocell-reinforced bases under static and repeated loads, by using two different infill soils (Kansas River sand and quarry waste) and novel polymeric alloy-made geocells with 100 mm height and 1.1 mm thickness. 60.5 cm x 60.5 cm testing tank and a circular steel loading plate with 15.2 cm diameter were used. Under static load condition, improvement factors were found as 1.75 and 1.50 for bearing capacity and stiffness, respectively, performed on Kansas River sand.

However, for quarry waste bases, no major effect is obtained due to presence of apparent cohesion compared to sand. Nevertheless, it was seen that single geocell reinforcement reduced permanent deformation roughly 1.5 times as compared to unreinforced condition on quarry waste basement. Under repeated load condition, Kansas River sand had a lower percentage of elastic deformation than quarry waste due to its sub-rounded particle and poor gradation.

Pokharel et al. (2010) investigated factors such as type, embedment, shape, quality of infill soil and geocell height, that affect the behavior of single-geocell-reinforced bases, using the same infill materials and test setup. 100 mm and 75 mm cell heights were used for one-layer and two-layer reinforcement, respectively. Performance of elliptical and circular shape of geocells were compared and circular shape geocell showed stiffer and stronger responses. A direct proportion was found between elastic modulus of geocell sheet and bearing capacity of reinforced bases. The effect of embedment of geocells was also examined. Geocells which are embedded and not embedded in sand were called confined and unconfined conditions, respectively. Unconfined geocell had a lower stiffness but a higher ultimate load capacity compared to confined geocell because of its lateral expansion. Multiple geocell reinforcement yielded greater stiffness and ultimate bearing capacity compared as single geocell reinforcement. Also, under static loading condition, cohesionless infill soil (Kansas River sand) had better performance with regard to a little cohesive soil (quarry waste). Unlike other studies, smaller test thickness was found to have higher ultimate bearing capacity, and it was explained as the stable bottom in the thinner section forced the failure surface to occur in a shallower depth and increased the bearing capacity.

Shin et al. (2017) investigated the effect of width, height and shape of geocell as well as the type of infill soils. They performed unreinforced and geocell reinforced tests and used four different infill soils (silty, sandy, gravel and weathered granite) on a silty soil base. A large scale testing tank that is 1400 mm in length, 1000 mm in width and 1400 mm in height was used. It was found when the ratio between cell width and height is approximately 1, geocell reinforcement performs better bearing capacity was obtained between 4 to 8 times that unreinforced ground in the case of using geocell

with width to height ratio of 0.83 filled by gravel, and also in the case of using geocell with width to height ratio of 1.25 filled by weathered granite. Stresses under loading plate were measured by earth pressure cells, thus vertical and horizontal load transfer mechanisms were investigated. In the reinforced case, load dispersion angle increased by about 15% and measurements seen in earth pressure cells decreased by about 50% to 60% compared to the unreinforced soil.

Shetgar and Sharma (2017) used a steel testing tank of 1000 x 1000 x 600 mm dimensions and two different types of loading plate: the first one was a circular shape with diameter of 100 mm, the second one was a 100 x 100 mm square. Better performance was observed when geocells with small cell openings were placed close to the surface or geocells with large cell openings were placed deeper (100 mm) from the surface, with respect to bearing capacity and settlement, independently from loading plate shape.

Dabiryan et al. (2017) investigated the effect of fiber cross section and cell shape on the bearing capacity of geocells made from polyester fibers. Poorly graded, rough grained silica sand was loaded by a 50 mm in wide and 340 mm in long rigid strip plate in a 800 mm in wide and long and 560 mm deep testing tank. The tank was filled by pre-calibrated sand raining system to keep the relative density of sand (72%) constant in all tests. It was obviously proved that increase in geocell height or decrease in cell aperture contribute to bearing capacity positively. Geocells made of different cross sections of fibers woven together performed better than geocells made of uniform cross sections, because friction between the fiber and soil is higher in the former. Ultimate strength of geotextile did not have a major role in bearing capacity of the system because the soil under the geocell reinforced zone failed before the rupture of the geotextile.

Wesseloo et al. (2009) performed a series of uniaxial compression tests with different sizes of geocell packs. 0.2 mm width HDPE type geocells and ML (USCS) type soil were used. They compared the behavior of single and multiple geocell behavior in their study. It was emphasized that, strength estimations (Bathurst and Karpurapu,

1993) based on single-geocell-reinforced structures are not applicable for multiple-geocell structures. Contrary to the results of the study performed by Rajagopal et al. (1999), strength decrease was observed while increasing in number of cells. However this might have been due to different modes of failure (seam failure vs material rupture).

Dash et al. (2001b) investigated the contribution of planar reinforcement load carrying capacity of geocell reinforced structures in their technical note. A testing tank in dimensions 1200 mm length, 332 mm width and 700 mm height is used. They carried out some tests by placing a planar reinforcement below or above the geocell, as well as putting a geotextile layer below the geocell and planar reinforcement under the geotextile. Planar reinforcement above the geocell layer condition and geotextile layer condition tests have not given a considerable improvement on the load carrying capacity of the system, because overburden pressure on these planar reinforcement layers were too small to generate enough frictional resistance. Best result was obtained by using planar reinforcement under the geocell layer. However, performance of the system was affected by the height of the geocell. Increase in geocell height made stiffer structures and it decreased the transferred load to planar reinforcement. The cumulative beneficial effect of geocell mattress and planar geogrid layer is found to be maximum for h/B=2 (h is height of geocell and B is width of footing), as shown in Figure 2.7.

In the second study by Dash et al. (2001a), in the same year, contributions of the parameters such as pocket size, height and width of geocell mattress, as well as pattern of geocell mattress, tensile stiffness of geocell material, relative density of soil and the depth of the top of geocell mattress on the performance of bearing capacity and settlement were investigated by performing eight series of tests. Poorly graded sand and three types of geogrid-made geocells were used. Load was applied in small increments till the footing settled by about 50 mm. It was emphasized that the load-settlement response is linear up to a settlement of about 5% of footing width in the unreinforced sand while this limit has gone up to about 20% when reinforced with geocell layer.

Ratio of settlement to footing width versus bearing pressure charts in terms of width and height of geocell are demonstrated in Figure 2.8 and Figure 2.9, respectively.

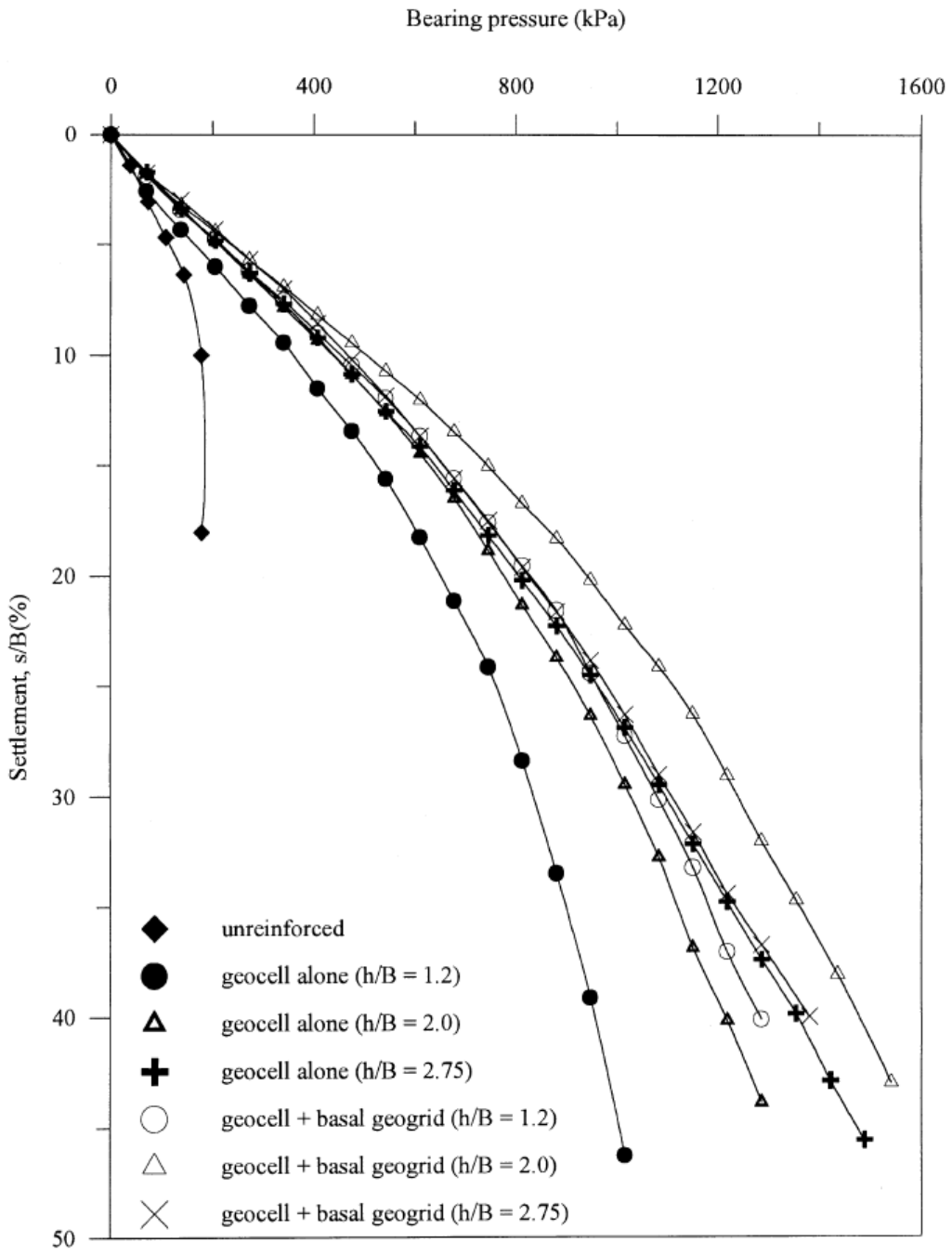

Figure 2.7 Bearing pressure-settlement responses of footings (Dash et al., 2001b)

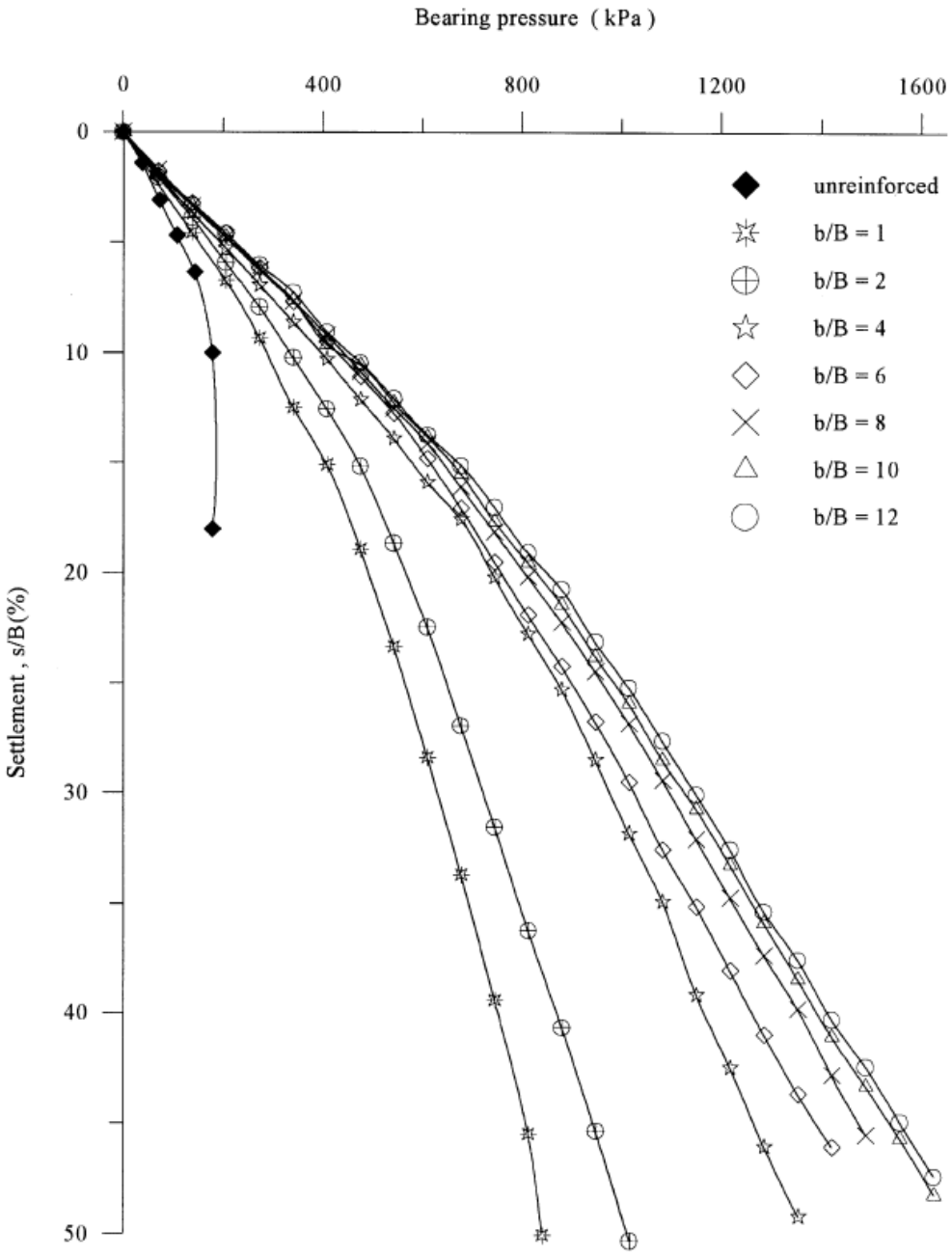

Figure 2.8 Variation of bearing pressure with settlement for different widths of geocell mattress (Dash et. al., 2001a)

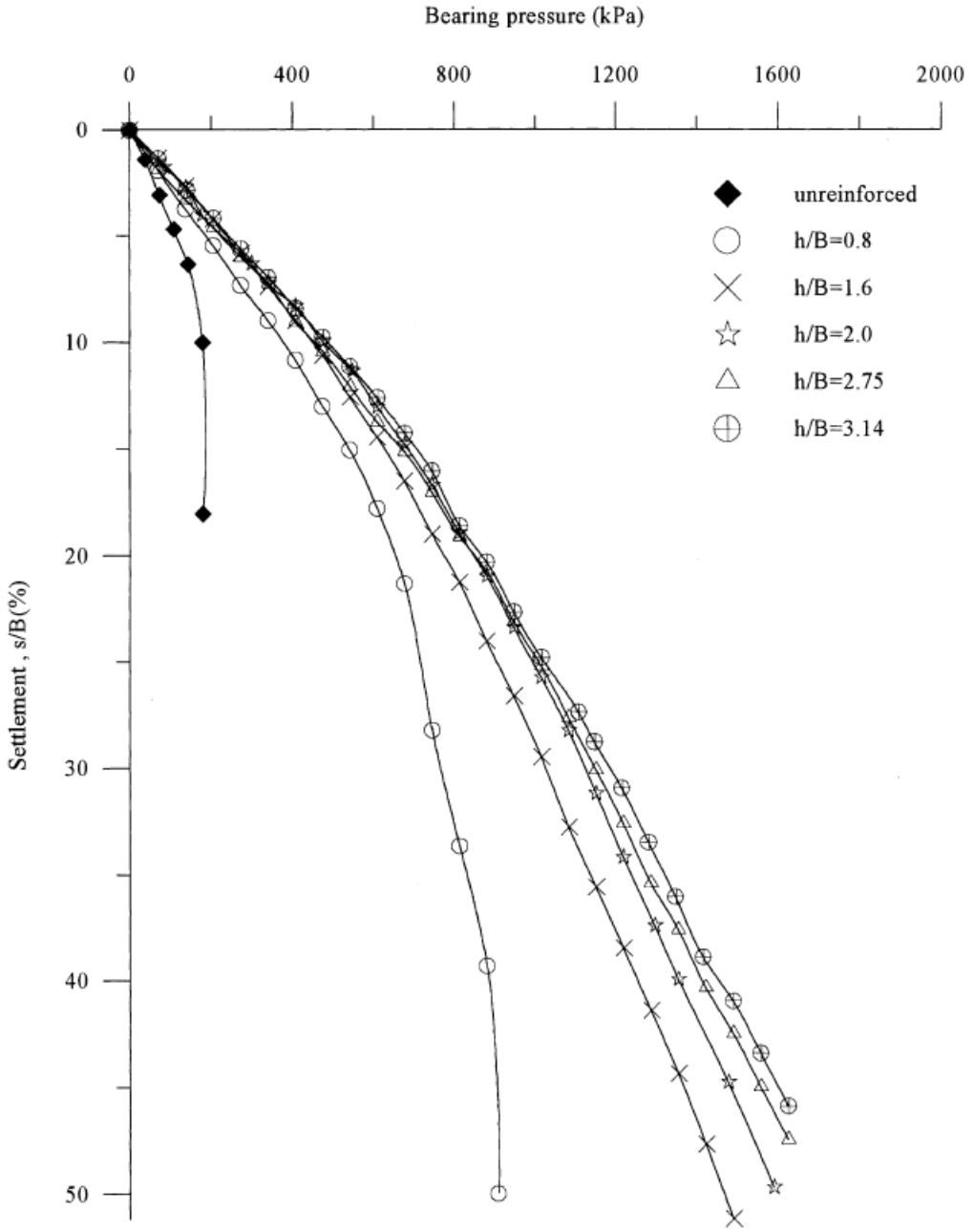

Figure 2.9 Variation of bearing pressure with settlement for different heights of geocell mattress (Dash et. al., 2001a)

Following were inferred by Dash et. al., (2001a) in summary:

- The optimum width of the geocell layer is around 4 times the footing width, at which stage the geocell would intercept all the potential rupture planes formed in the foundation soil as used in that study.
- The performance improvement is significant up to a geocell height equal to 2 times the width of the footing. Beyond that height, the improvement is only marginal.
- The optimum aspect ratio of geocell pockets for supporting strip footings was found to be around 1.67.
- To obtain maximum benefit, the top of geocell mattress should be at a depth of 0.1B from the bottom of the footing.

Dash et al. (2004) studied with three different types of reinforcement which are geocell, planar and randomly distributed mesh elements and compared the results with those of unreinforced tests regarding settlement and ultimate load capacity. Same testing apparatus and materials used in all tests as described in Dash et al. (2001b). Following results achieved from that study; in geocell type reinforcement test, failure was not seen even though the settlement reached 45% of the plate width and that system carried as much 8 as times the load in the unreinforced case. In the cases of planar reinforcement and randomly distributed mesh element type reinforcement, failure was observed when settlement values reached 15% and 10% of loading plate width, respectively. These reinforcements increased the bearing capacity of soil by respective factors of 4 and 1.8 times more, compared to the unreinforced capacity. Thus, the efficiency of geocell reinforcement has been proven with reference to other options.

Dash et al. (2007) performed a series of laboratory model tests by using the same testing apparatus as described in Dash et al. (2001b). filled by geocell reinforced sand under a strip loading. Steel loading plate with a length of 330 mm, a width of 100 mm,

and a thickness of 25 mm was used. Sand was filled by sand raining method. Strain gauges were placed to different locations of geocell walls. The biggest strain was obtained under the loading plate and it was seen that strain was getting smaller when moved away from the plate. Thus, the largest contribution provided from cells just under the loading area, was deduced. Besides, geocell reinforced soil mattresses behaved as a beam, and accordingly, bigger depth of mattresses showed outstanding performance. It was observed that, geocell reinforced zone intersects with possible failure plane of foundation soil and this zone transmit footing pressures deeper into the underlying soil layer. In addition to these, it was discovered that load dispersion angle is affected by factors such as height, weight, pocket size of geocells and placement depth of.

Dash (2010) investigated the effect of relative density of foundation and infill soil on the behavior of unreinforced and geocell reinforced sand basements by using the same testing equipments used in Dash et al. (2001b). In total 10 reinforced and unreinforced tests with five relative densities (30, 40, 50, 60 and 70%) were performed; where type, pattern and placement depth of geocell were constant in the reinforced experiments. It was observed that stiffness of foundation bed increased four times by increasing the relative density from 30% to 70%. This indicated that for effective utilization of geocell reinforcement, basement and infill soil must be compacted and placed as dense as possible.

Dash (2012) investigated the influence of geocell material on the load-carrying mechanism of geocell reinforced sand mattresses under strip foundations. Uniformly graded river sand (Unified Soil Classification System SP) and three different geogrid made geocells formed in a chevron pattern were used in tests. To make a uniform density, sand raining system was used to fill the testing tank and relative density was checked during raining process by placing small metal boxes at different locations. Geocell height, pocket size, width and placement depth were constant in all tests. Effect of strength, stiffness and aperture opening size of geogrids to bearing capacity of soils were investigated. Smaller aperture size of geogrids provide higher confinement to infill soil, hence, increase the performance of geocell behavior.

Similarly, increase in strength of geocell material contributes resistance of soil by ensuring more rigid and stable structures. In addition, it was emphasized that square or rectangular aperture opening geogrids with ribs placed parallel or perpendicular to the loading plate exhibit better performance.

Tafreshi and Dawson (2010a) researched the behavior of three dimensional and planar geotextile reinforced sands and compared them with unreinforced cases under static and repeated loads. Tests were performed by using poorly graded, relatively uniform silica sand and non-woven geotextiles (3D and planar) placed in a rigid testing tank of 750 mm length, 375 mm height and 150 mm width. Optimum placement depths of planar reinforcement and top of the 3D geotextile were obtained as 0.35 times and 0.1 times of footing width, respectively. Increase in the number of planar reinforcement and also height of 3D geotextile, decreased the footing settlement. 3D geotextile reinforcement type performed better compared to planar geotextile while keeping the other variables constant. To show the same performance, 2.85 times as much mass of geotextile had to be used in planar reinforcement compared to 3D geotextile. Moreover, it was found that increase in the amplitude of repeated load, caused settlement increases. In all cases, the largest portion of the settlement occurred after the first ten cycles.

The second study of Tafreshi and Dawson (2010b) named as ”Comparison of bearing capacity of a strip footing on sand with geocell and with planar forms of geotextile reinforcement” deduced the similar results with Tafreshi and Dawson (2010a) such as;

- Using geotextile increases the load carrying capacity of soil and decreases the footing settlement.
- Increase in number of planar geotextile or height of geocell, increases the bearing capacity and decreases the settlement.
- Approximately three times as much mass of geotextile was needed in the case of using planar reinforcement to perform similar results obtained in 3D geotextile.

Otherwise, it was found that increment in bearing capacity reaches 200% and 150% of the unreinforced case, in geocell and planar reinforced soils, respectively. Settlement reduction of 75% was attained 3D reinforcement and 64% with planar reinforcement, in comparison to reference tests on unreinforced soil.

Gurbuz and Mertol (2012) investigated parameters such as width, height, number of layers of geocells and distance between layers of geocells in the case of using more than one layer. A rigid testing tank with 700.5 mm x 700.5 mm square area and 800 mm height was filled with relatively uniform poorly graded sand reinforced with HDPE-made geocells. It was found that if the distance between the geocell layers became 0.142 times of the foundation width, bearing capacity improvement is maximized. Increase in geocell height and number of layers of geocells increase the bearing capacity that is defined as when the plate settlement is equal to 12% of the footing width. Additionally, geocell width had no observable significant effect on the bearing pressure versus settlement behavior.

Hegde and Sitharam (2014) performed a series of uniaxial compression tests with single geocell reinforced soils which are silty clay, sand and the aggregates. Laboratory experiments were validated using numerical simulations carried out using a three-dimensional (3D) finite-difference package Fast Lagrangian Analysis of Continua (FLAC3D 4.00) as shown in Figure 2.10.

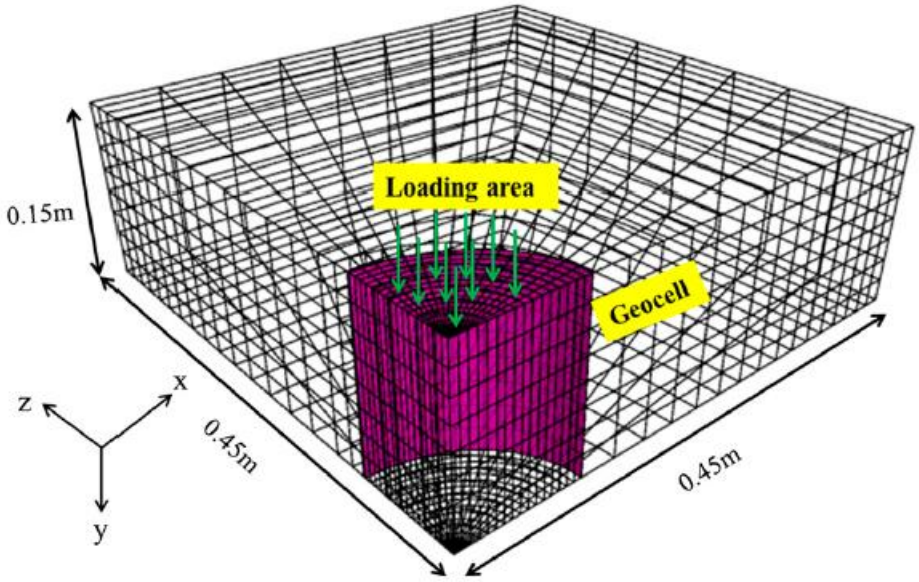

Figure 2.10 Skeleton view of FLAC3D model (Hegde and Sitharam, 2014)

Mainly, effect of infill soil on the load carrying capacity as well as reduction in the deformation of the geocells were investigated in that study. Infill soils with higher friction angle showed better performance in terms of deformation in the geocells. A simple analytical model was also proposed to calculate stresses and strains on the geocell wall using superstructure loads and elastic properties of geocells.

Kargar and Hosseini (2017) investigated the effects of geocell height, geocell width, pocket size of geocells and number of geocell layers on the bearing pressure vs. settlement behavior by using a reduced-scale physical model as shown in Figure 2.11.

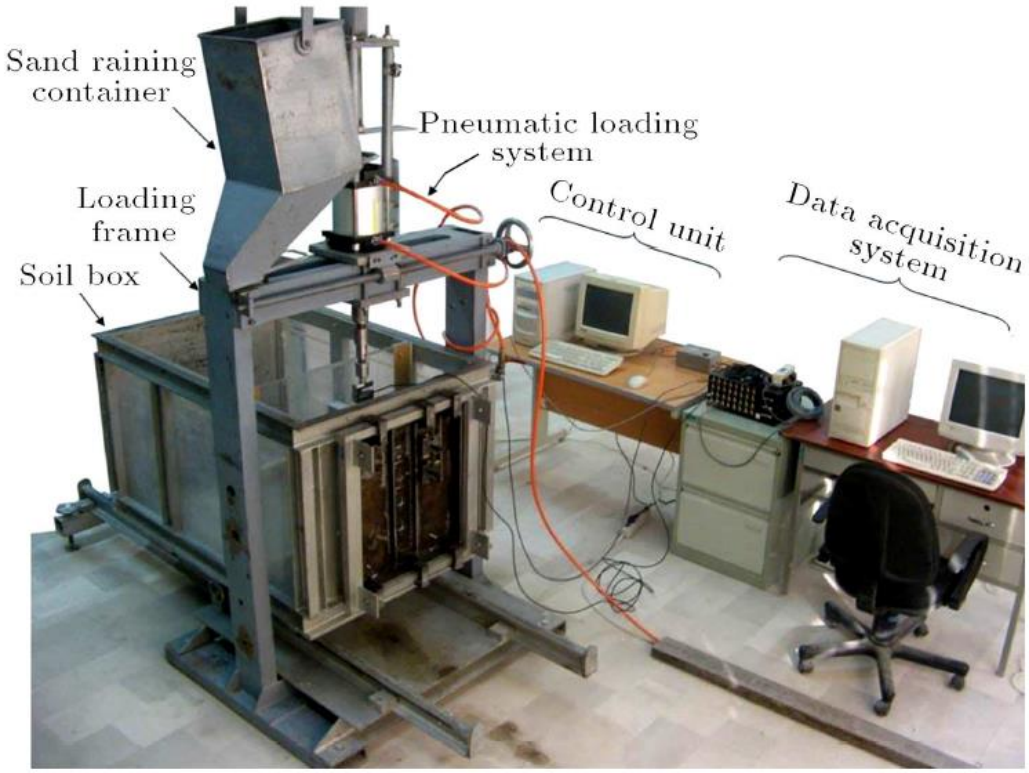

Figure 2.11 Photographic view of general arrangement of the physical model apparatus (Kargar and Hosseini, 2017).

Following results were obtained from that study;

- Most influential parameter was found as height of geocell. Increase in the ratio of geocell height to width of the plate from H/B=0.25 to H/B=1.50, increased the ultimate bearing capacity from 1.6 to 7.1 times the unreinforced capacity.
- Increase in pocket size decreased the performance of geocell reinforcement.
- Considerable improvement in bearing capacity and settlement of geocell-reinforced sand is obtained by increasing the width of geocell layer up to 5B, beyond which further improvement is marginal.
- In practice, using one layer high geocell shows better improvement than using lower height multi-layer geocells.

Neto et al. (2013) proposed a method to calculate bearing capacity of geocell reinforced soils. Contribution of geocell was classified in two ways: confinement effect and stress dispersion effect. An improvement factor was added to classical bearing capacity formula of Terzaghi and Peck, 1967 (Equation 2.4) and hence bearing capacity of geocell reinforced soil was calculated. Steps of calculations are presented below.

$$p_u = cN_cS_c + \frac{1}{2}\gamma BN_\gamma S_\gamma \quad (2.4)$$

p_u, unreinforced subgrade bearing capacity

c, subgrade soil cohesion

γ, subgrade soil unit weight

B, loading width

N_c and N_γ, bearing capacity factors

S_c and S_γ, shape factors

Confinement effect improvement;

$$\Delta F_\tau = 4\frac{h}{d}k_0 pBL \tan\delta \quad (2.5)$$

ΔF_τ, confinement effect improvement

h/d, geocell aspect ratio

k_0, lateral earth pressure of unreinforced soil at rest

δ, interface friction angle between the filling soil and the geocell wall

p, load at the top of the geocell mattress

Stress dispersion effect;

The dispersion effect decrease the applied load on the subgrade soil by spreading the stress over a distance equal to one pocket that is a value equal to “d” for each side of the load as shown in Figure 2.12.

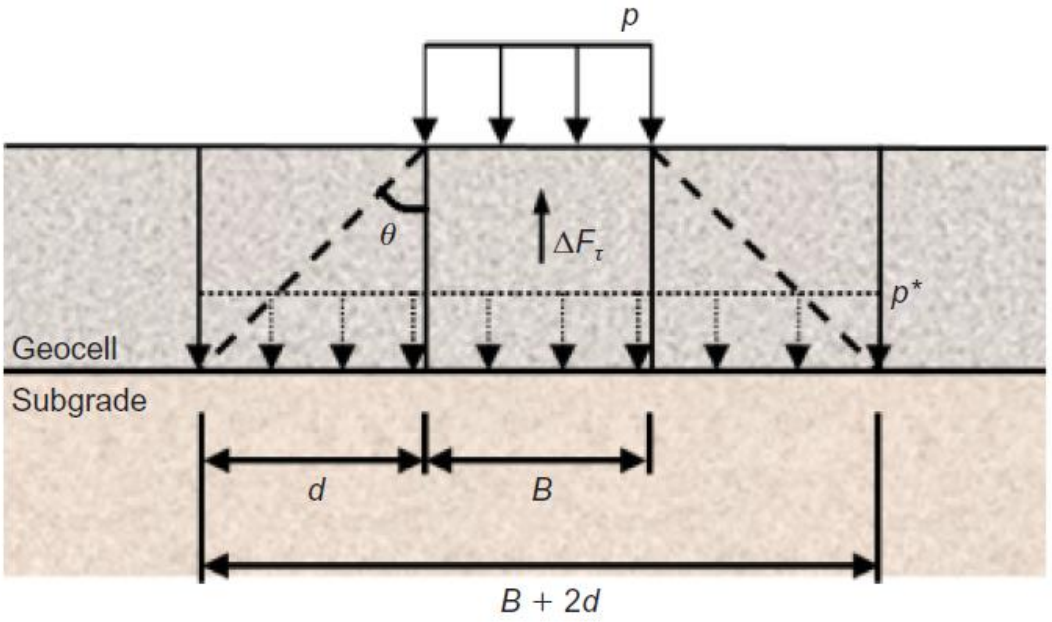

Figure 2.12 Illustration of the stress dispersion effect adopted for the presented method (Neto et al., 2013)

Making a force balance from Figure 2.12, it follows that the force on the geocell mattress bottom (p*), is equal to the load on the surface (p) minus the confinement effect (ΔF_τ).

$$p^*(B + 2d)(L + 2d) = pBL - 4\frac{h}{d}k_0 pBL \tan\delta \quad (2.6)$$

The improvement of the soil due to geocell reinforcement was described as the difference between the stress at top (p) and the bottom (p*) of the geocell.

$$p_r = p_u + (p - p^*) \quad (2.7)$$

Where p_r is bearing capacity of reinforced soil.

2.3 Studies of Geocell Improvement on Cohesive Soils

This section gives an overview of the geocell studies performed on cohesive soils. Each study is briefly summarized below.

Sitharam et al. (2005) investigated the performance of geocell reinforced clayey soils by changing parameters including width, height and placement depth of geocells and also using a planar geogrid under the geocell mattress. A testing tank with inside dimensions of 900 mm x 900 mm x 600 mm (length x width x height), a rigid steel loading plate of 150 mm diameter and 30 mm thickness, low plasticity silty clay and geocells made of biaxial geogrid were used in tests. Clay basement was prepared by placing and compacting 25 cm thick clay layers. To assure uniformity of the clay bed, undisturbed samples were collected from different locations in the tank and they were checked and compared with respect to unit weight, moisture content and vane shear strength. It was found that geocell reinforcement is more effective than planar reinforcement. Load carrying capacity of geocell reinforced clayey bed was 4.8 times the load carrying capacity of unreinforced clay bed. Optimum contributions of geocell were obtained in the case of using geocell which has a height 1.8 times the loading plate width and has a width of geocell layer 4.9 times the loading plate width.

Latha et al. (2006) investigated the performance of geocell reinforced weak soils underlain by earth embankments. Some properties of geocells such as tensile stiffness (four different types), height (100 mm, 150 mm, 200 mm and 250 mm), pocket size (200 mm and 400 mm) and type of infill material (clay and clayey sand) were studied. A steel tank with dimensions of 1800 mm x 800 mm x 1200 mm were used. The clay was mixed with water and consolidated under 10 kPa surcharge pressure for a week. In the case of using geocell with 100 mm height and 400 mm pocket size under the embankment, surcharge capacity of the embankment reached almost twice that in the unreinforced test. It was stated that increase in the ratio of geocell height to pocket size (aspect ratio) significantly increases the ultimate surcharge pressure. Type of infill soil did not substantially effected the behavior of geocell mattress. It was indicated that geocell reinforced soils have an additional “apparent” cohesion term generated due to

confinement effect of geocell on the infill soil. Identification of geocell height and apparent cohesion help us to make a preliminary design, by performing back analyses to decide geocell stiffness and pocket sizes for desired factor of safety value in a slope stability analysis software, was emphasized.

Sireesh et al. (2009) performed a series of laboratory model tests to investigate the effect of loading on a void placed in clay soil bed for both geocell reinforced and unreinforced conditions (Figure 2.13). Low plasticity silty clay (CL) and dry poorly graded sand (SP) were used as subgrade and infill soil, respectively. Testing tank dimensions were 900 mm x 900 mm x 900 mm and dimensions of loading plate were 150 mm in diameter and 30 mm in thickness. Diameter of void in the clay layer was 95 mm. Plan area of geocell mattress, height of geocell and thickness of sand layer overlay of clay subgrade were described in terms of the diameter of footing (D) and effects of these factors on bearing capacity of soil were investigated. A considerable increase was observed by increasing the area of geocell mattress (till the width of geocell layer reaches to 4.9D) because it plays a major role in transmitting the footing pressure to adjacent regions of stable soil mass, in other words it acts as a bridge. As the height of geocell is increased up to 1.8 times the footing width, bearing capacity first increases then it starts to decrease again. Increase in the thickness of sand layer and its relative density increase the bearing capacity. Using planar geogrid reinforcement under geocell layer makes a significant contribution however, influence of geogrid layer on bearing capacity decreases by increasing of geocell height. In this study, it was emphasized that if proper sand and geocell were used, load carrying capacity of the footing increases by about 40 times compared to the case of clay subgrade with void alone.

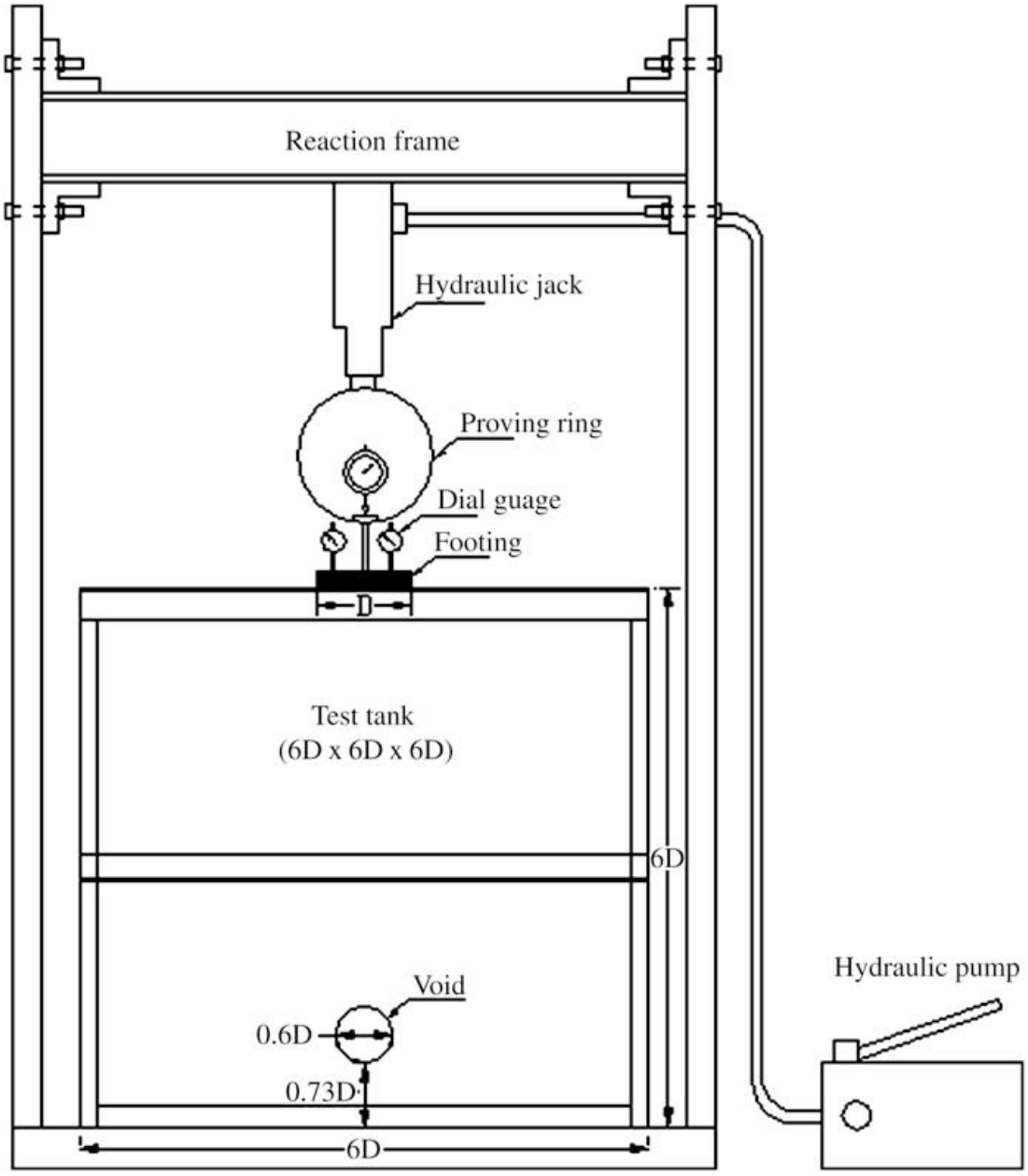

Figure 2.13 Schematic view of the test setup (Sireesh et al., 2009)

Zhang et al. (2010) performed experiments to investigate effect of geocell reinforcement on bearing capacity of soft soils underlain by earth embankments considering either vertical stress dispersion effect or membrane effect of geocell reinforcement shown in Figure 2.14-a and Figure 2.14-b, respectively (p_r is the footing load after the vertical stress dispersion effect; b_n is the width of the uniform load, p_s; T is the tensile force in the reinforcement).

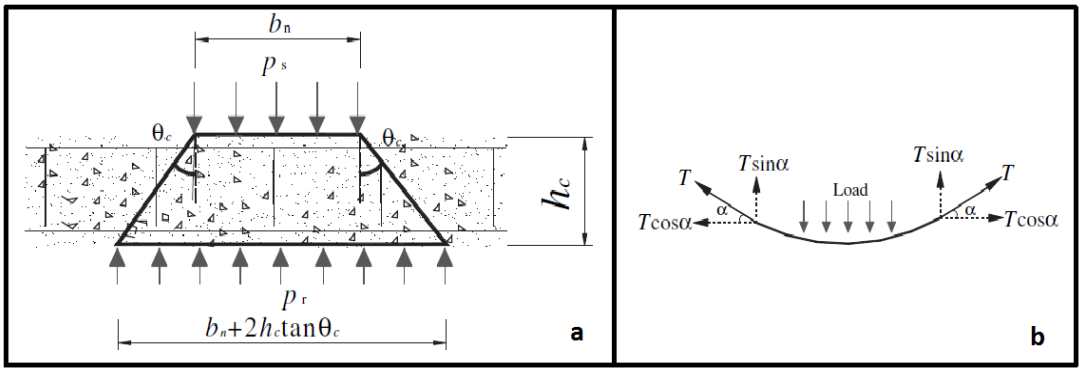

Figure 2.14 Vertical load dispersion effect (a) and membrane effect of geocell reinforcement (b) (Zhang et al., 2010)

A reinforced concrete testing tank with dimensions 1300 mm in length, 650 mm in width and 1000 mm in height was used in tests. Load was applied to the 200 mm high embankment by a rigid steel plate 236 mm in diameter and 10 mm in thickness. Soils were soft clay, crushed stone and clayey sand for subgrade soil, infill material and embankment, respectively. The use of geocell in the crashed stone layer increased the ultimate bearing capacity of embankment by 78.22% as shown in Figure 2.15. It was indicated that vertical dispersion effect is valid for small amount of settlements, whereas membrane effect of geocell is valid for big and differential embankment settlements. Therefore when the membrane effect was considered in proposed calculation method for large settlements, very close results were obtained compared to experimental results.

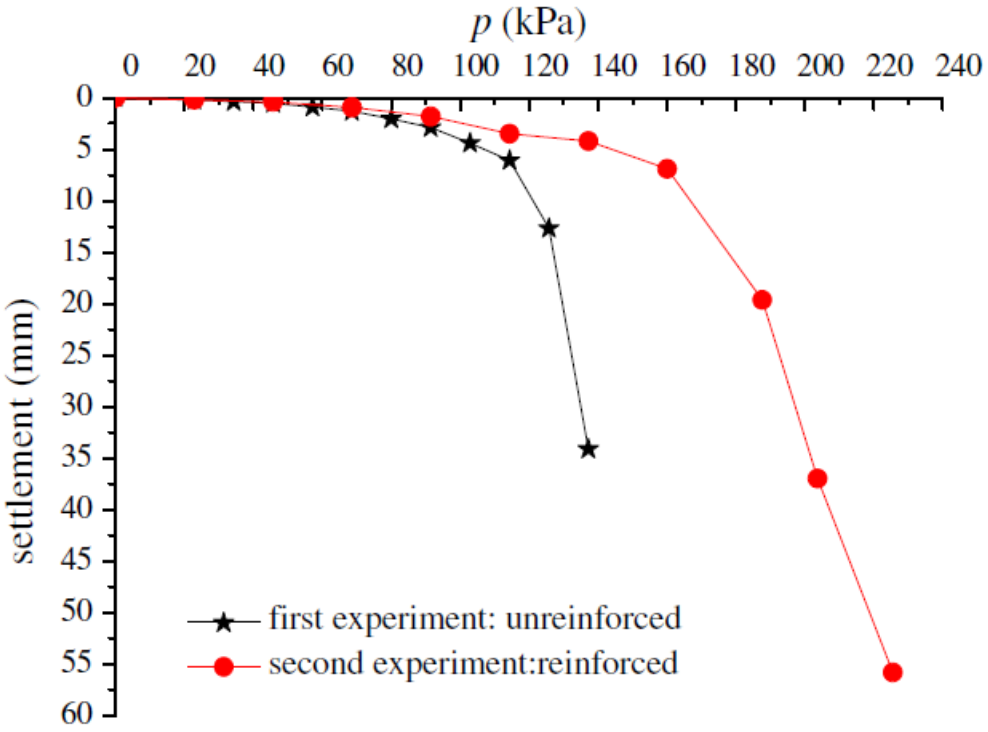

Figure 2.15 Load settlement curves of the embankment surface (Zhang et al., 2010)

Emersleben and Meyer (2008) performed a series of large scale model tests and in-situ field tests to research the behavior of geocell reinforcement over soft soils. A big testing tank with dimensions of 2.0 x 2.0 x 2.0 m, a steel plate with a diameter of 30 cm, an artificial mixed (Glyben) as soft subgrade material and two different types of geocell made from high density polyethylene (HDPE) were used in model tests. Five inductive displacement gauges and eight earth pressure cells were used to measure heave and settlement of the soil surface and stress distribution under the geocell layers, respectively. Following results were obtained from large scale model tests;

- Increasing height and decreasing width of geocell increase the load carrying capacity.
- Using proper geocell height and diameter improved the load carrying capacity up to 1.5 times compared to unreinforced one.

- In the unreinforced tests, it was observed that stresses concentrated below the loading plate rather stresses distributed over a larger area in the case of geocell reinforcement.

In addition to laboratory model tests, two in-situ field tests were carried out. Comparison tests were prepared to observe effect of geocell reinforcement by using different heights of gravel layers overlain on soft subgrade. Following results obtained from in-situ tests;

- Stresses on the subgrade soil were reduced approximately 30% by using geocells in the gravel layers.
- Surface deflections significantly decreased.
- Using geocell in the gravel increased the modulus of gravel layer.

Tanyu et al. (2013) conducted large scale laboratory experiments with four different types of geocells. Deflections, modulus of subgrade reaction and resilient modulus of each layer were investigated. Tests were performed in terms of two loading conditions which are loads due to construction equipments and traffic load due to vehicle passes. Following results obtained from that study;

- Geocell use improved the resilient modulus by 30-50%.
- Presence of geocell decreased the plastic deflection by 30-50% compared to unreinforced case.
- Geocells contributed to decrease rutting.
- Modulus of subgrade reaction increased by use of geocell reinforcement in gravel layer.

CHAPTER 3

LABORATORY EXPERIMENTS

A series of laboratory model tests are conducted to understand the behavior of geocell reinforced sands under static load. To perform these tests, a test setup, a soil and geosynthetic materials were needed. In this chapter, details of required test setup and materials are presented in details.

3.1 Testing Equipment

The test setup is designed and manufactured for this study. Pieces of the test setup are: (1) a sand raining system that can fill the testing tank at the desired relative density value in each test, (2) a testing tank that can carry the desired loads as well as that allows the operation of the sand raining system, (3) a loading system which enables to apply static loads and repeated loads in future studies. Measuring equipment such as data logger and dial gauges are procured to make necessary measurements during tests. This section gives information about the design process and methodology of testing equipments used in this study. To design the testing tank structurally, forces acting on testing tank surfaces should be known. So, these forces and stresses are calculated according to the maximum amount of loading to be used in experiments. Maximum 55 cm sand height will be used in tests but for further studies, testing tank is designed as if it will be filled to 100 cm height. Hereunder, vertical stress below the center of a circular footing can be achieved analytically by using the equation shown in Equation 3.1 (Poulos and Davis, 1974).

$$\sigma_z = p\left[1 - \left\{\frac{1}{1+\left(\frac{a}{z}\right)^2}\right\}^{3/2}\right] \quad (3.1)$$

Where;

σ_z = Vertical stress due to loading (kPa)

p = Uniform stress over circular area at surface (kPa)

a = Radius of circular loading area (m)

z = Depth from surface (m)

Horizontal stress below the center of a circular footing can be achieved analytically as shown in Equation 3.2 (Poulos and Davis, 1974). Unidentified symbols are the same in Equation 3.1.

$$\sigma_r = \sigma_\theta = \frac{p}{2}\left[(1+2\nu) - \frac{2(1+\nu)z}{(a^2+z^2)^{(1/2)}} + \frac{z^3}{(a^2+z^2)^{3/2}}\right] \quad (3.2)$$

σ_r = Horizontal stress in plane due to loading (kPa)

σ_θ = Horizontal stress out of plane due to loading (kPa)

ν = Poisson's ratio

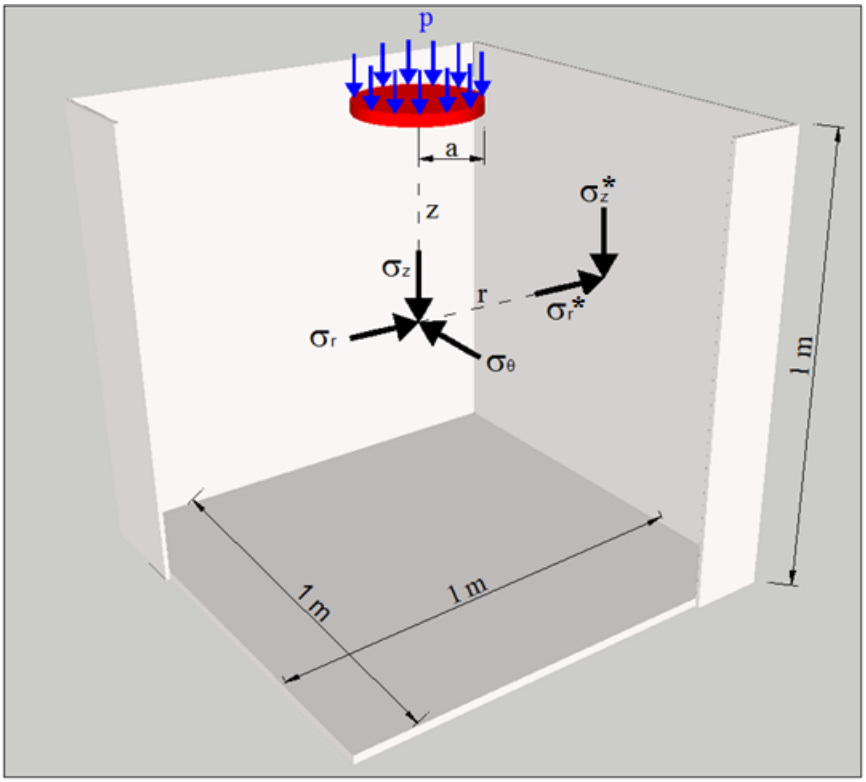

Figure 3.1 Stresses acting on the test tank

Uniform stress under loading plate, p was tempered to capacity of loading system which can be used maximum at 8 bar. Piston has 32 cm diameter and loading plate has 26 cm diameter, so maximum applicable stress due to the limitations of loading system is calculated as 1210 kPa. Poisson ratio, ν, is taken as 0.3 from a previous study performed with Çine Sand (Ulgen, 2011). All stresses are calculated at 20 locations throughout tank depth in every 5 cm and results are shown in Table 3.2. Vertical and horizontal stresses due to soil are calculated separately and added to stresses based upon additional plate loading. Internal friction angle, ϕ is taken as 37° which corresponds the value at 64% relative density obtained from direct shear tests by making linear interpolation between 59% (ϕ = 35.1°) and 67% (ϕ = 37.9°) relative densities. Selected relative density is specified by calculating the arithmetic value of the top and the bottom relative density values in testing tank found from sand

raining tests presented in following subsections. Similarly, unit weight, γ is calculated as 16 kN/m³ making linear interpolation according to 64% relative density by assuming minimum (γ = 13.78 kN/m³) and maximum (γ = 17.31 kN/m³) unit weight values were found at 0% and 100% relative densities, respectively.

Lateral earth pressure coefficient at rest condition, K_0 is used to convert vertical stresses to horizontal stresses due to either presence of soil loading or additional plate loading.

$$K_0 = 1 - \sin\phi \tag{3.3}$$

$$\sigma_{zs} = \gamma z \tag{3.4}$$

$$\sigma_{rs} = \gamma z K_0 \tag{3.5}$$

Where;

σ_{zs} = Vertical stress due to presence of soil

σ_{rs} = Horizontal stress due to presence of soil

z = Depth from surface

σ_z* is calculated by using Table 3.1 which gives σ_z*/p accordingly z/a and r/a (Scott, 1963). Values at the right and the bottom of the table were used if r/a is bigger than 1.5 and z/a is bigger than 2.0.

Schematic view of test set up without sand raining system is shown in Figure 3.2.

Table 3.1 σ_z*/p versus z/a and r/a for uniform stress on circular area

z/a \ **r/a**	**0**	**0.5**	**1.0**	**1.5**
0.0	1.00	1.00	1.00/0	0.00
0.25	0.99	0.96	0.50	0.03
0.5	0.91	0.83	0.41	0.07
1.0	0.65	0.56	0.34	0.11
1.5	0.42	0.37	0.24	0.13
2.0	0.28	0.26	0.19	0.13

Table 3.2 All stresses throughout tank depth

	Stresses due to plate loading				Stress due to presence of soil		Total stresses			
							Below at the center of plate		At the face of the tank	
z (m)	**σ_z (kPa)**	**σ_r, σ_θ (kPa)**	**σ_z* (kPa)**	**σ_r* (kPa)**	**σ_{zs} (kPa)**	**σ_{rs} (kPa)**	**σ_{ztotal} (kPa)**	**σ_{rtotal} (kPa)**	**σ_{ztotal}* (kPa)**	**σ_{rtotal}* (kPa)**
0.05	1154.03	431.31	60.5	24.08	0.80	0.32	1154.83	431.63	61.30	24.40
0.10	935.74	146.05	108.9	43.34	1.60	0.64	937.34	146.69	110.50	43.98
0.15	687.83	40.39	133.1	52.97	2.40	0.96	690.23	41.35	135.50	53.93
0.20	496.81	5.72	157.3	62.61	3.20	1.27	500.01	6.99	160.50	63.88
0.25	364.97	-5.07	157.3	62.61	4.00	1.59	368.97	-3.48	161.30	64.20
0.30	275.28	-7.95	157.3	62.61	4.80	1.91	280.08	-6.04	162.10	64.52
0.35	213.23	-8.18	157.3	62.61	5.60	2.23	218.83	-5.95	162.90	64.83
0.40	169.18	-7.57	157.3	62.61	6.40	2.55	175.58	-5.02	163.70	65.15
0.45	137.08	-6.74	157.3	62.61	7.20	2.87	144.28	-3.87	164.50	65.47
0.50	113.09	-5.92	157.3	62.61	8.00	3.18	121.09	-2.74	165.30	65.79
0.55	94.75	-5.20	157.3	62.61	8.80	3.50	103.55	-1.70	166.10	66.11
0.60	80.46	-4.56	157.3	62.61	9.60	3.82	90.06	-0.74	166.90	66.43
0.65	69.13	-4.02	157.3	62.61	10.40	4.14	79.53	0.12	167.70	66.74
0.70	60.00	-3.56	157.3	62.61	11.20	4.46	71.20	0.90	168.50	67.06
0.75	52.55	-3.17	157.3	62.61	12.00	4.78	64.55	1.61	169.30	67.38
0.80	46.39	-2.83	157.3	62.61	12.80	5.09	59.19	2.26	170.10	67.70
0.85	41.25	-2.54	157.3	62.61	13.60	5.41	54.85	2.87	170.90	68.02
0.90	36.90	-2.29	157.3	62.61	14.40	5.73	51.30	3.44	171.70	68.34
0.95	33.21	-2.08	157.3	62.61	15.20	6.05	48.41	3.97	172.50	68.66
1.00	30.04	-1.89	157.3	62.61	16.00	6.37	46.04	4.48	173.30	68.97

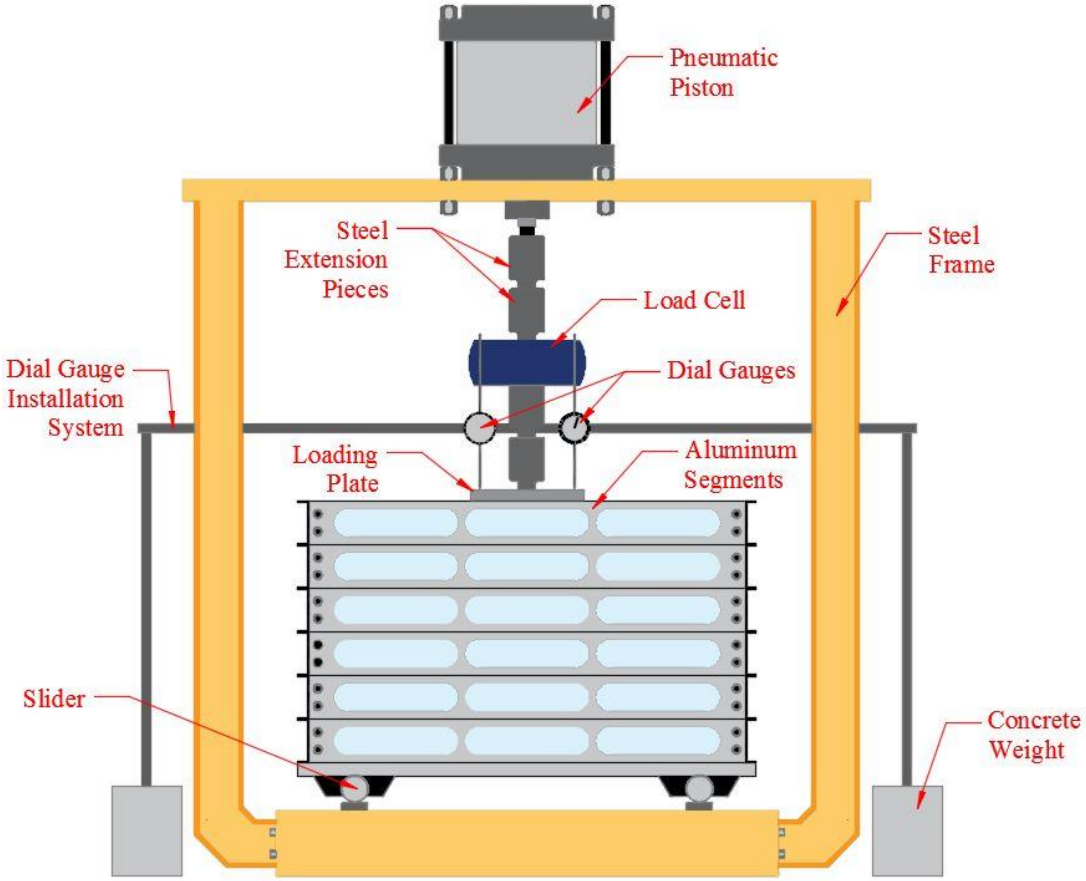

Figure 3.2 Schematic view of test set up

3.1.1 Sand Raining (Pluviation) System

A sand raining system is considered necessary to fill such a large scale testing tank with sand in same relative densities in each test for repeatability. Small scale trial sand raining tests are performed with different sieves having different dimensions between their holes. The most proper dimension between holes for sand raining is determined as 15 mm from center to center and when grain size distribution of Çine Sand is taken into consideration, sieve hole diameter is selected as 2.8 mm. Retained mass on the raining system sieve is not used during tests. Raining sieve is designed bigger than testing tank. Dimensions of the sieve are 110 cm x 110 cm. The sieve is divided into nine equal compartments to prevent accumulation of the sand in the center of the sieve

during raining process. In this way uniform raining is carried out. To arrange raining height by changing position of sieve, it is tied to a spool with steel wires. Four rubber vibration isolators are placed near to the corners of sieve to prevent the transmission of the vibration generated by vibration motor to the sand filled testing tank thus prohibit densifying of sand. A photographical view of sand raining system is shown in Figure 3.3. Bolted joints are preferred instead of welded joints because vibration causes metal fatigue and cracks. A single phase micro series vibration motor is used to vibrate the sieve. Technical details of the vibration motor is shown in Table 3.3.

Table 3.3 Mechanical and electrical data of vibration motor

MECHANICAL DATA						**ELECTRICAL DATA**			
RPM at 50 Hz	TYPE	Centrifugal Force		Static Moment	Weight	Rated Current	Rated Voltage	Capacitor	Max Input Power
	-	kg	N	kgmm	kg	A	V	μF	W
3000	VX 20	21	206	2.10	1.60	0.12	230	1	25

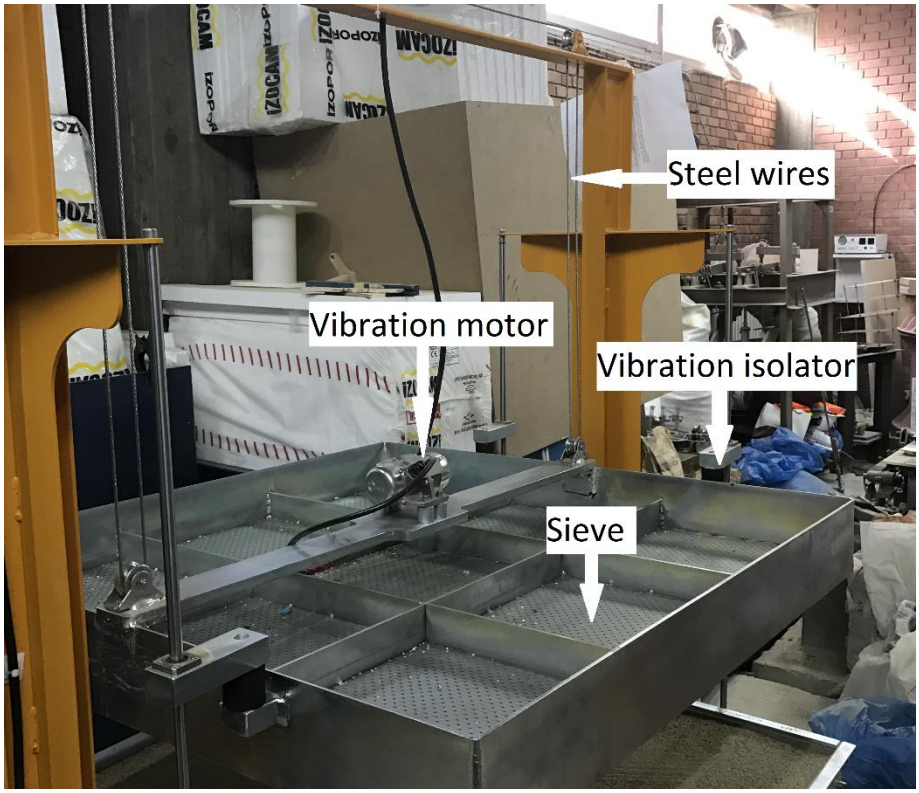

Figure 3.3 View of sand raining system

3.1.2 Loading System

Loading system consists of three main parts which are an air compressor that has capacity of 8 bar pressure, 100 lt pressured air storage and 1000 cycles/minute used to provide and store pressurized air, a pneumatic double acting piston with a diameter of 320 mm and a stroke length of 100 mm and a manually controlled pressure valve that has a capacity of 8 bar. The piston is attached to a strong steel frame which does not deflect during loading. Steel extension pieces are produced to adjust loading plate at any elevation. Threaded design allows adding pieces to each other and also make more precise height adjustment. Pieces of loading system are shown in Figure 3.4.

Figure 3.4 Pieces of the loading system (a: pressure regulator valve, b: pneumatic piston, c: air compressor)

3.1.3 Testing Tank

Testing tank is one of the main parts of the setup therefore several factors are taken into account during design:

- Favorability to the realization of a low elevation sand raining process in order to achieve low relative density values,
- Easy mobility and mountability,
- Resistant against loads during tests,
- At least one side transparent to observe inside of the tank during tests,
- Large enough for multi-geocell system and also not be effected from boundary conditions.

In some previous studies in the literature, single cell geocells were tested. To represent real behavior of geocell system, cells must support each other through horizontal direction. Because of the above stated reason, the cell, placed on the center of the tank, must be supported by other cells as shown in Figure 3.5. Load will be acting at the middle of the cell and its joint in different tests and deformations will be recorded from here. Most common cell dimensions in the market are between 200 mm and 450 mm. To use multicell system during tests, tank sizes are selected as 1000 mm x 1000 mm x

1000 mm. Due to size of loading plate (260 mm), 600 mm tank depth will be enough and stress will not be transferred till the base of the tank. However in order to perform multi layered geocell tests in future studies, tank depth is selected as 1000 mm. The tank consists of 10 segments made of aluminum and each segment has 100 mm height. One side of each segment is made of plexiglass to observe inside the tank during tests, when needed, as shown in Figure 3.6. After one layer of sand is deposited, tank height is increased by adding these 10 cm high segments until the tank reaches to desired height. Base of the tank, which is 30 mm thick steel, was placed on two steel sliders in order to move the tank horizontally between the sand raining system, loading system and open space to fill or empty the tank.

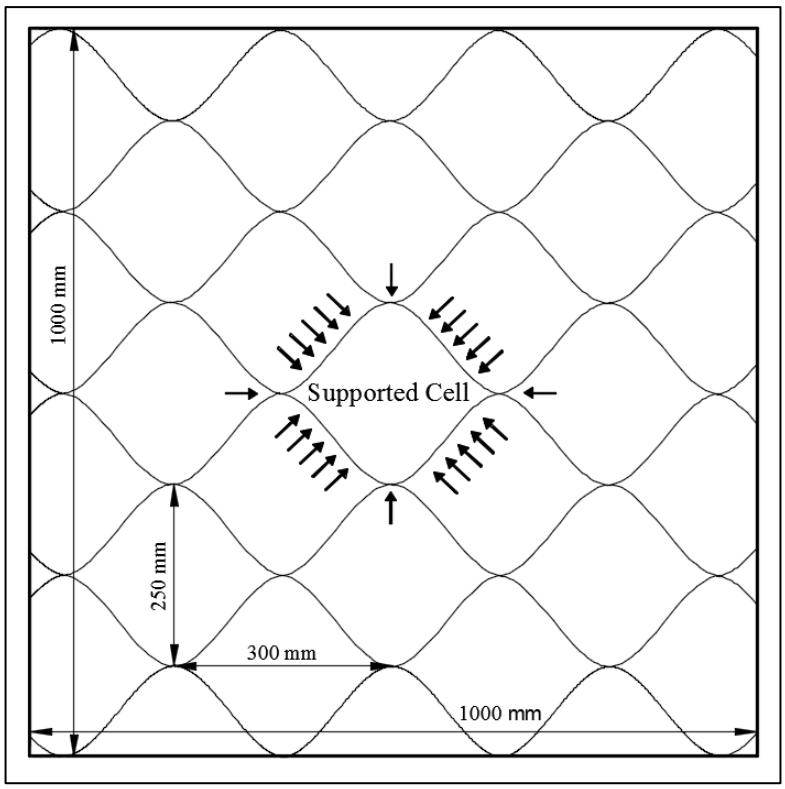

Figure 3.5 Plan view of testing tank

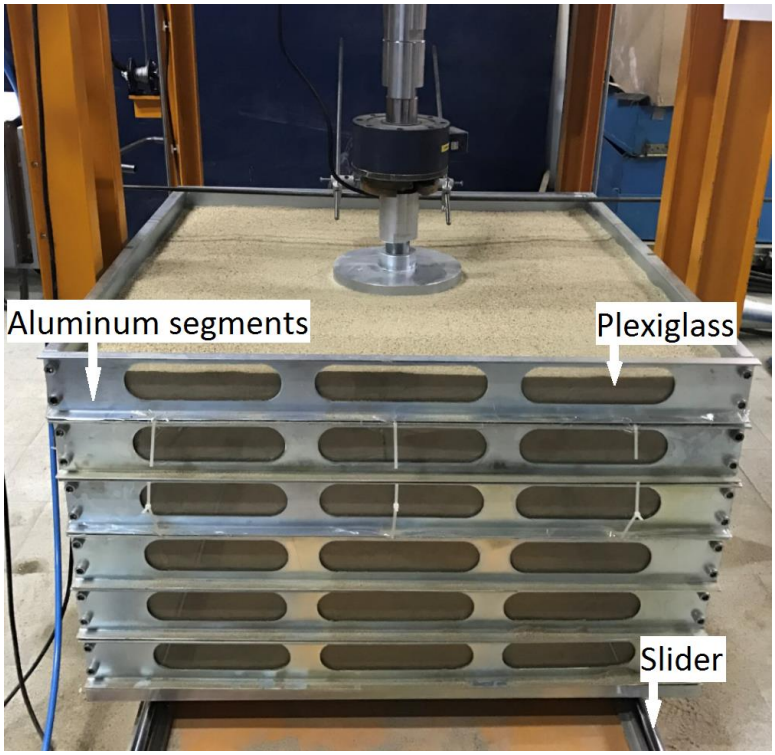

Figure 3.6 View of testing tank showing 6 aluminum segments, 10 cm high each

3.1.4 Measuring Instruments

Since the main purpose of this study is to examine the load-displacement characteristics of geocell reinforced and unreinforced sandy soil under static load, displacement of the loading plate as well as the force on the plate are measured by using two dial gauges and a load cell connected to a data logger, respectively.

3.1.4.1 Dial Gauges

Two dial gauges, each with measuring range up to 100 mm and 0.01 mm scale interval, are used in all tests to measure settlement of the loading plate. Two dial gauges are used in order to avoid errors in the case of differential settlement or tilting of the loading plate. So they are placed on either side of the center line of the plate and average value of the readings taken from dial gauges are used as the plate settlement.

Dial gauges are attached to reference frame (dial gauge installation system) that consists of two vertical steel bars fixed to concrete blocks and horizontal bars to adjust dial gauges to desired elevation and location. Dial gauge installation system is independent from test setup in order to use in every kind of test as well as not be affected from any deflection, expansion or vibration caused by any other part of the test setup.

3.1.4.2 Load Cell

An electronic annular type load cell that has a capacity of 20000 kg and 2.0006 mV/V output voltage as capacity is placed between the piston and the loading plate. It is connected to a computer-aided data logger and each load step is recorded in a coordinated manner with settlement readings.

3.1.4.3 Data Logger

TESTBOX 1001 data acquisition system developed by Teknik Destek Grubu (TDG), is used in tests to read applied load to the load cell it has 8 channels and enables 8 times data readings in a second. Only one channel of data logger is used to get readings from load cell in mV. The load cell is calibrated by the manufacturer and calibration information is provided in the product datasheet. Channel gain and output voltage are adjusted as 890 and 5V, respectively as suggested in the software.

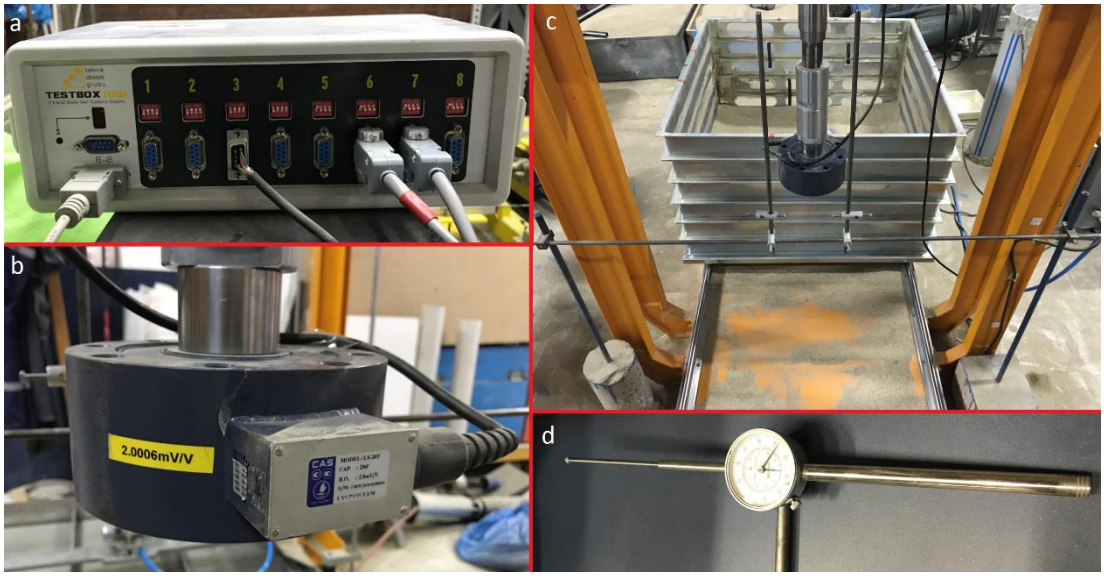

Figure 3.7 Elements of measuring instruments (a: data logger, b: load cell, c: dial gauge installation system, d: dial gauge)

3.2 Materials Used

In this section, details of laboratory tests performed in order to determine physical and strength properties of Çine Sand and geocell material are presented. Properties of materials have an influence in design process either by hand calculations or finite element analysis. Hence, correct specification of material properties is directly influential in achieving accurate results.

3.2.1 Sand

In all laboratory tests, Çine Sand collected from banks of Çine River in Turkey is used as either basement soil or infill soil of geocells. Çine Sand consists of colorless and white color quartz, yellow, white and pink color feldspar and black and gray color rock fragment (Figure 3.8). Particle shape of Çine Sand is classified as sub-angular to angular as shown in Figure 3.8.

Figure 3.8 Photomicrograph of Çine Sand

To specify characteristics of the sand, some laboratory tests are performed. These are; sieve analysis, determination of specific gravity, determination of minimum and maximum dry densities and unit weights, direct shear tests and California Bearing Ratio tests. All sand tests are performed according to related American Society for Testing and Materials (ASTM) standards.

3.2.1.1 Sieve Analysis

To determine the grain size distribution, sieve analysis is conducted according to ASTM D6913 / 6913M-17 standard. The amount of required sample is determined in accordance with ASTM C702 / C702M-11 standard and using “quartering” method. Sample is mixed three times and material heap is flattened by a shovel (Figure 3.9-a). The heap of material is divided into four equal parts (Figure 3.9-b). Opposite quarters of sample are combined into a representative half, therefore reducing the amount.

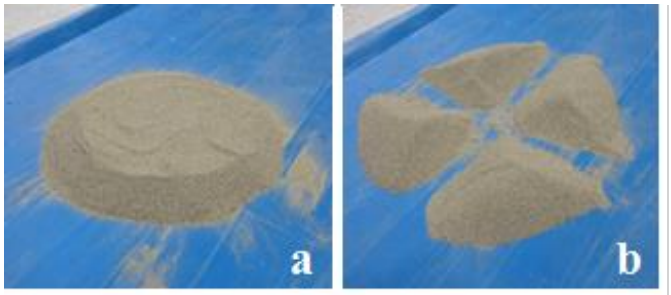

Figure 3.9 Quartering of the sample

Overloading limits of the sieves are taken into account. All of these stages are repeated three times on three different samples to minimize mistakes during testing and also to check and compare the test results. Resulting grain size distribution data chart and curve are shown in Table 3.4 and Figure 3.10, respectively.

Table 3.4 Sieve analysis test results

		Test 1	Test 2	Test 3	Average	
Sieve Size	**4.75 mm**	100.00	100.00	100.00	100.00	% Passing
	2.0 mm	99.79	99.85	99.94	99.86	
	0.6 mm	72.86	72.84	71.12	72.27	
	0.3 mm	37.70	37.55	36.91	37.39	
	0.212 mm	21.50	21.88	20.69	21.36	
	0.15 mm	1158	11.85	11.18	11.54	
	0.075 mm	1.32	1.44	1.32	1.36	
D_{10} (mm)		0.16	0.15	0.16	0.16	
D_{30} (mm)		0.26	0.26	0.27	0.26	
D_{50} (mm)		0.36	0.37	0.38	0.37	
D_{60} (mm)		0.43	0.44	0.46	0.44	
C_u		2.69	2.93	2.88	2.83	
C_c		0.98	1.02	0.99	1.00	
Fines Content (%)		1.32	1.44	1.32	1.36	
USCS		SP	SP	SP	SP	

D_{10}, D_{30}, D_{50} and D_{60} are grain size diameters at 10%, 30%, 50% and 60% passing, respectively. C_u and C_c represent coefficient of uniformity and coefficient of curvature, respectively. Material is classified as clean, poorly graded sand (SP) according to Unified Soil Classification System (USCS).

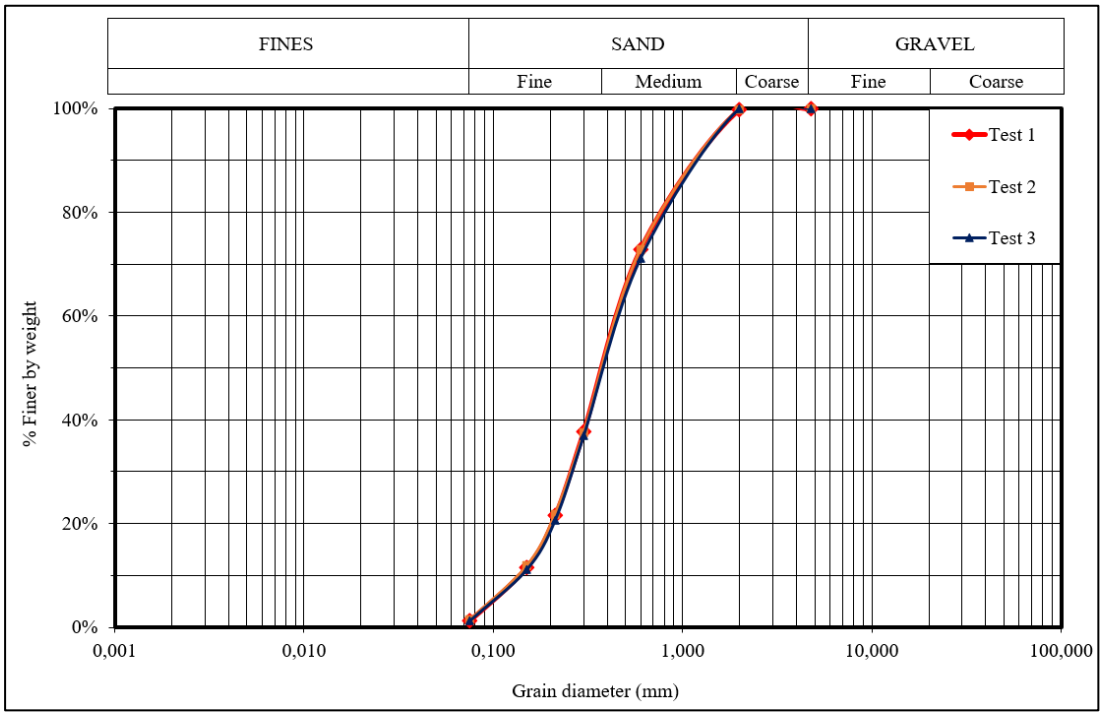

Figure 3.10 Grain size distribution

3.2.1.2 Determination of Specific Gravity

Specific gravity is the ratio of the density of soil particles to density of distilled water at test temperature. Specific gravity is shown as "G_s" and is used on density calculations of soil. The test is conducted according to "ASTM D 854 – 14, Standart Test Methods for Specific Gravity of Soil Solids by Water Pycnometer" and G_s is found as 2.66. Photos taken during the test are shown in Figure 3.11.

Figure 3.11 Specific gravity test

3.2.1.3 Maximum Dry Density and Unit Weight

Results of sieve analysis indicate that fine content of soil is approximately 1.36%. Due to low fines content, capacity of water absorbtion of the soil is very low therefore Standard Proctor Test cannot be applied to compact the soil. Air dry water content (w) of soil is found as 0.03 %. Soil is assumed as dry because of low water content. Vibrating hammer is used to compact to soil to determine minimum void ratio (e_{min}) accordingly maximum dry density (ρ_{dmax}). This test is performed according to the ASTM D7382-08 - Method A. Dimensions of the mold is measured by a calipers in order to use them in volume calculations as illustrated in Figure 3.12-a. After that, the mold is filled in three layers and each layer is compacted for 60 seconds as shown in Figure 3.12-b and Figure 3.12-c, respectively. Just after the compaction of final layer, collar removed from the mold and surface of the sand is flattened as illustrated in Figure 3.12-d. Finally, mass of soil-filled mold is recorded. Vibrating hammer test is repeated twice and average values are used to evaluate maximum dry density. Results are provided in Table 3.5.

Table 3.5 Obtained values from maximum dry density and unit weight tests

Test number	**1**	**2**	**Average**
Weight of mold (g)	4566.80	4566.80	4566.80
Weight of sample (g)	3734.20	3717.00	3725.60
Diameter of mold (mm)	152.11	152.11	152.11
Height of mold (mm)	115.90	115.90	115.90
Volume of mold (ml)	2106.15	2106.15	2106.15
Maximum dry density, ρ_{dmax} (g/ml)	1.77	1.76	1.765
Maximum unit weight, γ_{max} (kN/m³)	17.36	17.26	17.31
Minimum void ratio, e_{min}	0.50	0.51	0.505

Figure 3.12 Determination process of maximum dry density and unit weight

3.2.1.4 Minimum Dry Density and Unit Weight

These tests are performed according to the ASTM D4254-14 Method A including a funnel pouring device. Sample is placed to mold as low as possible height following a spiral path in order to obtain the loosest condition (Figure 3.13). Test is repeated twice and average values are used for evaluating minimum dry density. Results are shown in Table 3.6.

Table 3.6 Obtained values from minimum dry density and unit weight tests

Test number	**1**	**2**	**Average**
Weight of mold (g)	4540.30	4540.30	4540.30
Weight of sample (g)	2971.30	2986.6	2978.95
Diameter of mold (mm)	152.06	152.06	152.06
Height of mold (mm)	116.74	116.74	116.74
Volume of mold (ml)	2120.02	2120.02	2120.02
Minimum dry density, ρ_{dmin} (g/ml)	1.40	1.41	1.405
Minimum unit weight, γ_{min} (kN/m³)	13.73	13.83	13.78
Maximum void ratio, e_{max}	0.90	0.88	0.89

Figure 3.13 Placement of soil using a funnel

3.2.1.5 Direct Shear Test

Direct shear tests are performed as defined in ASTM D3080-04 Standard Test Method for Direct Shear Test of Soils Under Consolidated Drained Conditions by using relative densities obtained from randomly selected soil masses. Corresponding relative densities are found as 34%, 42%, 50%, 59% and 67%. Direct shear tests are performed under these five different relative densities and five different normal stresses (50 kPa, 100 kPa, 200 kPa, 400 kPa and 700 kPa) at each density. Shearing speed is set to 0.61 mm/min. A view of direct shear test machine and used equipments are shown in Figure 3.14-a and Figure 3.14-b, respectively. Effective internal friction angle, ϕ' values of Çine Sand are obtained for each relative density and presented in Table 3.7. Comparison of results of Çine Sand with other sands taken from literature is shown in APPENDIX A.

Figure 3.14 Direct shear test apparatus

Table 3.7 Effective friction angle of Çine Sand

Relative Density (%)	Friction Angle, ϕ' (°)
34	32.6
42	33.1
50	34.5
59	35.1
67	37.9

3.2.1.6 California Bearing Ratio (CBR) Test

California Bearing Ratio (CBR) Test is a simple strength test done by comparing bearing capacity of prepared sample and well graded crushed stone. CBR test is performed to specify the bearing capacity of sample which is prepared by sand raining system. ASTM D1883-16 Standard Test Method for California Bearing Ratio (CBR) of Laboratory Compacted Soils is followed during the test. A steel penetration piston with 49.7 mm diameter is used (Figure 3.15-a). Because no pavement weight is specified, 4.54 kg surcharge weights are used (Figure 3.15-b). When the test results are analyzed, it is observed that bearing ratio at 0.2 inch penetration is greater than bearing ratio at 0.1 inch penetration, and the test is repeated. The second test results are obtained similar to the first test. Accordingly, ratio at 0.2 inch penetration is accepted as CBR ratio and average value of two tests (CBR=17.3%) are used. Results of tests are shown in Table 3.8. Besides, due to concave upward shaped curve, corrections are applied to result graphs as shown in APPENDIX B.

Table 3.8 Results of CBR tests

	Penetration		**Pressure Reading**		**Corrected Pressure**	**Standard Pressure**	**CBR**
	inch	**mm**	**kN**	**MPa**	**MPa**	**MPa**	**%**
Test 1	0.1	2.5	1.24	0.64	0.93	6.90	13.5
	0.2	5.0	2.92	1.51	1.70	10.00	17.0
Test 2	0.1	2.5	1.07	0.55	1.04	6.90	15.1
	0.2	5.0	2.14	1.51	1.76	10.00	17.6

Figure 3.15 California Bearing Ratio (CBR) test

3.2.2 Geocell

HDPE type, small perforated and ultrasonic welded geocells are procured from GEOPLAS Plastic Soil Technics and Chemistry Industry and Trade Limited Co. (Figure 3.16). Popular sizes of geocells widely used in market are preferred. The reason of scantiness of different cell opening of geocells was except these sizes become custom manufacturing accordingly it was time consuming and expensive. Two different products are used: Geocell 40 with 25 x 30 cm openings and 1.1 mm material thickness, and Geocell 60 with 35 x 40 cm openings and 1.3 mm material thickness. Each geocell is tried in cell heights of 10, 15 and 20 cm. Technical details of geocells used in tests are presented in Table 3.10. A tensile test is performed on a sample of each perforated geocell material that has 105 mm length, 102 mm width and 1.2 mm thickness with 50 mm/min deformation rate to represent the mechanical behavior of both Geocell 40 and Geocell 60 (Figure 3.17). Results of this tests are presented in

Table 3.9. All technical data and tensile strength value are taken from manufacturer. No additional material tests are done in material laboratory.

Figure 3.16 A view of geocells used in this study

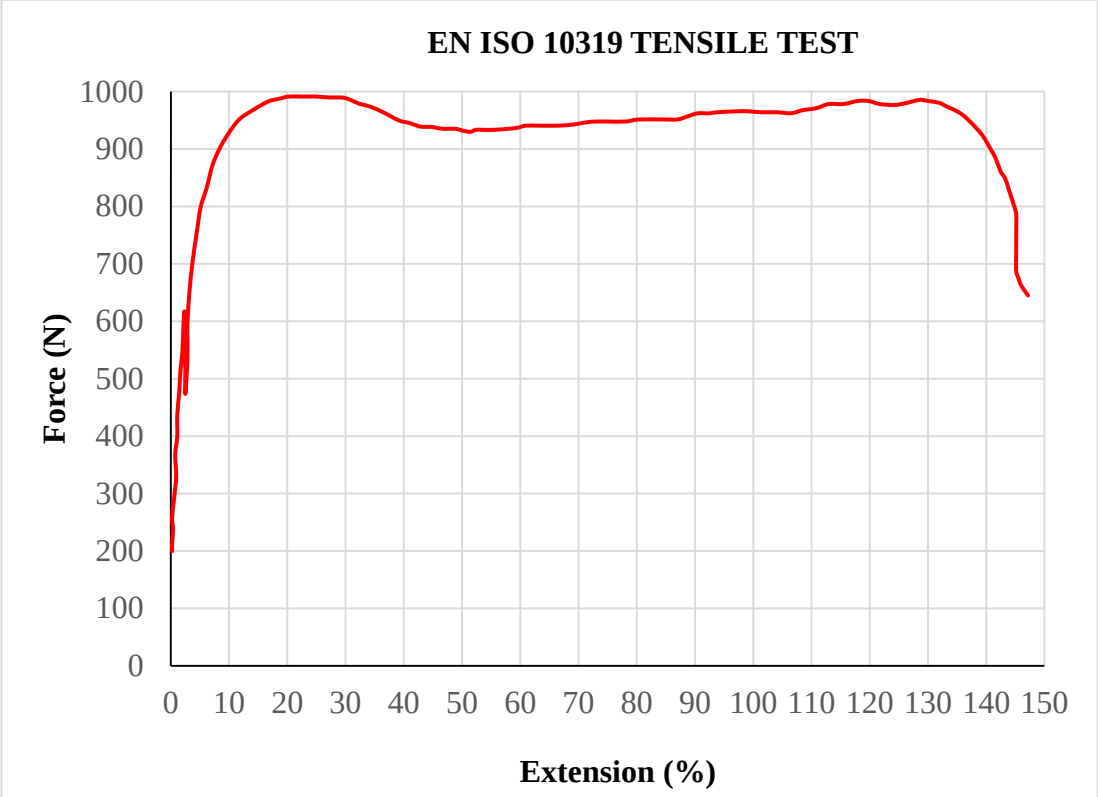

Figure 3.17 Tensile test result

Table 3.9 Results of tensile test

Extension at maximum force (%)	25.22
Extension at break (%)	146.61
Ultimate tensile strength (kN/m)	9.72
Tensile Strength at 2% extension (kN/m)	5.61
Tensile Strength at 5% extension (kN/m)	7.79

Table 3.10 Properties of geocells (Geoplas, www.geoplas.com.tr, last visited on September,2017)

Specifications of Geocell				
	Unit	**Value**		**Tolerance**
Row Material		High Density Polyethylene (HDPE)		
Geocell Types		GEOCELL 40	GEOCELL 60	
Weld Distance	cm	40	60	-10%
Rated Cell Length/Width (L/W)	mm	250 x 300	350 x 450	-10%
Area Of Cell	cm^2	382	846	-10%
Height Of Cell	mm	50 - 100 - 150 - 200		-10%

Physical Properties				
	Test Method	**Unit**	**Values**	**Tolerance**
Polymer Density	EN ISO 1183-1/A	g/cm^3	0.935-0.965	-10%

Mechanical Properties							
	Test Method	**Unit**	**Values**				**Tolerance**
Thickness	EN ISO 9863-1	g/cm^3	1.0	1.2	1.5	2.0	-10%
Tensile Strength - Unperforated	EN ISO 10319	kN/m	10	15	20	25	-10%
Tensile Strength - Perforated	EN ISO 10319	kN/m	5	7	10	12	-10%
Stress Of Internal Structural Junctions	EN ISO 13426-1 (method B)	kN/m	5	7	10	12	-10%

Chemical Properties				
	Test Method	**Unit**	**Values**	**Tolerance**
Oxydative Induction Time (OIT)	ASTM D 3895	Minute	>20	-10%
Carbon Black Content	ASTM D 1603	%	1-3	-

CHAPTER 4

MODEL TESTS AND RESULTS

This chapter mainly consists of two sections. In the first one, relative density tests carried out and relative density values determined according to different sand raining heights which will be used in laboratory model tests are evaluated. Additionally, sample preparation process including sand raining, adjusting of geocell sizes, placement of monitoring equipments etc. are presented in detail. In the second part, under static loads, unreinforced and geocell reinforced model tests are studied and effect of the aspect ratios, cell sizes and loading locations such as exact center of the cell and intersection of polymer boundaries of cell are examined.

4.1 Sample Preparation

This section includes procedures and purposes of sand raining tests and relative density values obtained from these tests.

4.1.1 Relative Density Tests

Considering the geocell heights and design of the testing tank, the sand raining elevations vary from 5 cm to 25 cm. The aim of using different elevations is to observe the difference between relative density values. As indicated in Section 3.1.1, the sieve is divided into nine equal compartments to prevent the accumulation of the sand in the center of the sieve during raining process. The nine compartments can be classified as three type of compartments which are corner, edge and center, and relative density boxes are placed at each type of these compartments to measure the density. Schematic and real view of relative density box placement are shown in Figure 4.1-a and Figure

4.1-b, respectively. Thus, relative density values are calculated and compared at different zones of testing tank and also checked if homogeneous raining is obtained. That placement system of the boxes is repeated after each 10 cm sand raining process at different elevations.

Metal cylindrical relative density boxes are used. Diameters and heights of these boxes are measured three times by a clipper and volumes of boxes are calculated using average values (Figure 4.2-a,b). Otherwise, using distilled water and a measuring cylinder, volumes of relative density boxes are measured (Figure 4.2-c,d). Details and physical properties of density boxes are presented in APPENDIX C. Arithmetic means of clipper measured and water measured volumes are accepted as final volumes and they are used for relative density calculations. These calculations are carried out by using Equation 4.1.

$$\text{Relative Density, R. D. (\%)} = \frac{e_{max} - e}{e_{max} - e_{min}} \text{ x } 100 \qquad (4.1)$$

Beginning of sand raining process, horizontality of sieve is checked using a bubble level. Five relative density tests are performed to specify the effect of raining elevation on the variance of the relative density values. First relative density test, test 1, is performed to represent maximum sand height (55 cm) will be used in tests and also to observe relative density variance between the bottom and the top levels of testing tank due to sand weight. Second relative density test, test 2, is performed again to understand relative density change by comparing with relative density test 1. Other relative density tests, test 3, test 4 and test 5 are carried out to elucidate the effect of the raining elevation on relative densities because as it was stated before, sand raining elevations vary from 5 to 25 cm because of geocell heights and design of the testing tank. Details of these tests are presented in the following sections. Relative density boxes designated as 3, 6, 9, 12, 15 and 18 could not be shown in schematic views of relative density tests since they are placed at the center of the testing tank.

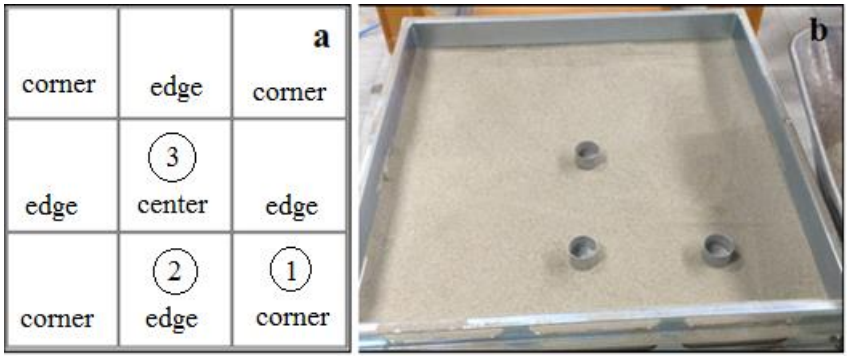

Figure 4.1 Placement of relative density boxes in each 10 cm depth of testing tank (a: schematic view, b: real view)

Figure 4.2 Volume determination of relative density boxes

4.1.1.1 Relative Density Test 1

As described in Section 3.1.3, testing tank comprises of ten pieces and each of them has 100 mm height. The sieve, vibrated by the motor and used for raining, is placed 5 cm above from the tank to prevent soil compaction by touching. Thus, raining height is arranged as 5 cm and 15 cm to the top and the base of the tank, respectively. Three relative density boxes designated as 1, 2 and 3 are placed at the bottom of the tank which is at corner, edge and center, respectively (Figure 4.4-Phase1). After completion of 10 cm height of raining process, a new segment of the tank is added just above of the existing tank segment and raining sieve is repositioned at 5 cm above of the new tank segment for second stage of raining process. In the same way, three relative density boxes designated as 4, 5 and 6 are placed on the sand deposited inside the first segment, such that number 4 is at the corner, number 5 is at the edge and number 6 is at the center (Figure 4.4-Phase2). The process is continued until five segments are filled, with 3 density boxes embedded in each layer (Figure 4.4-Phase3~Phase5). Sixth segment is filled till sand level covers the relative density boxes and reachs up approximately 5 cm (Figure 4.4-Phase6). Thereby total rained sand height is obtained as 55 cm. After the deposition process, sand is dug by a small shovel carefully and relative density boxes are unearthed individually without shaking them (Figure 4.3-a). Sand placed in the boxes is scraped off by a straight-edge (Figure 4.3-b), full boxes are weighed and relative density values are calculated (Figure 4.3-c). Calculated relative density values are presented in Table 4.1. Results show that; average relative density values are obtained as 62% and 67% from the top and the bottom level density boxes, respectively. These differences are caused by increase in sand height, hence compaction of underlying layers due to overburden pressure.

Relative density differences between the boxes placed to corner, edge and corner at the same elevation are not higher than 2%. It shows that a uniform sand raining was carried out at the any location of the testing tank.

That test represents the possible minimum raining elevation and maximum sand height condition. The same procedures are followed in the rest of relative density tests as stated in following sections.

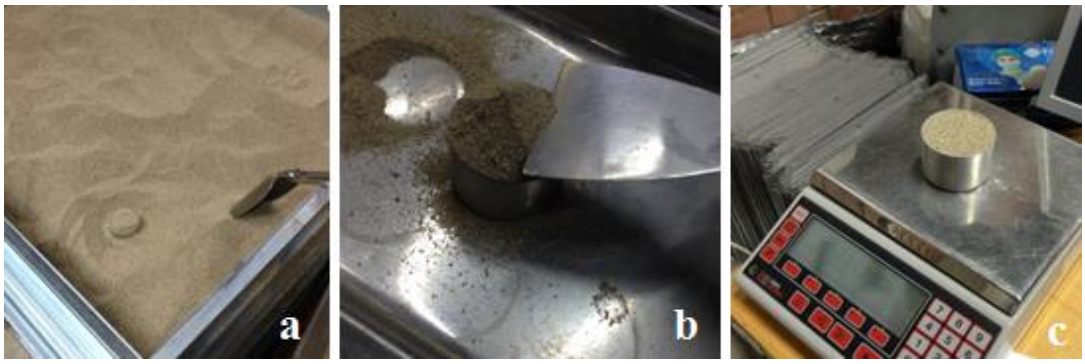

Figure 4.3 Steps of relative density tests

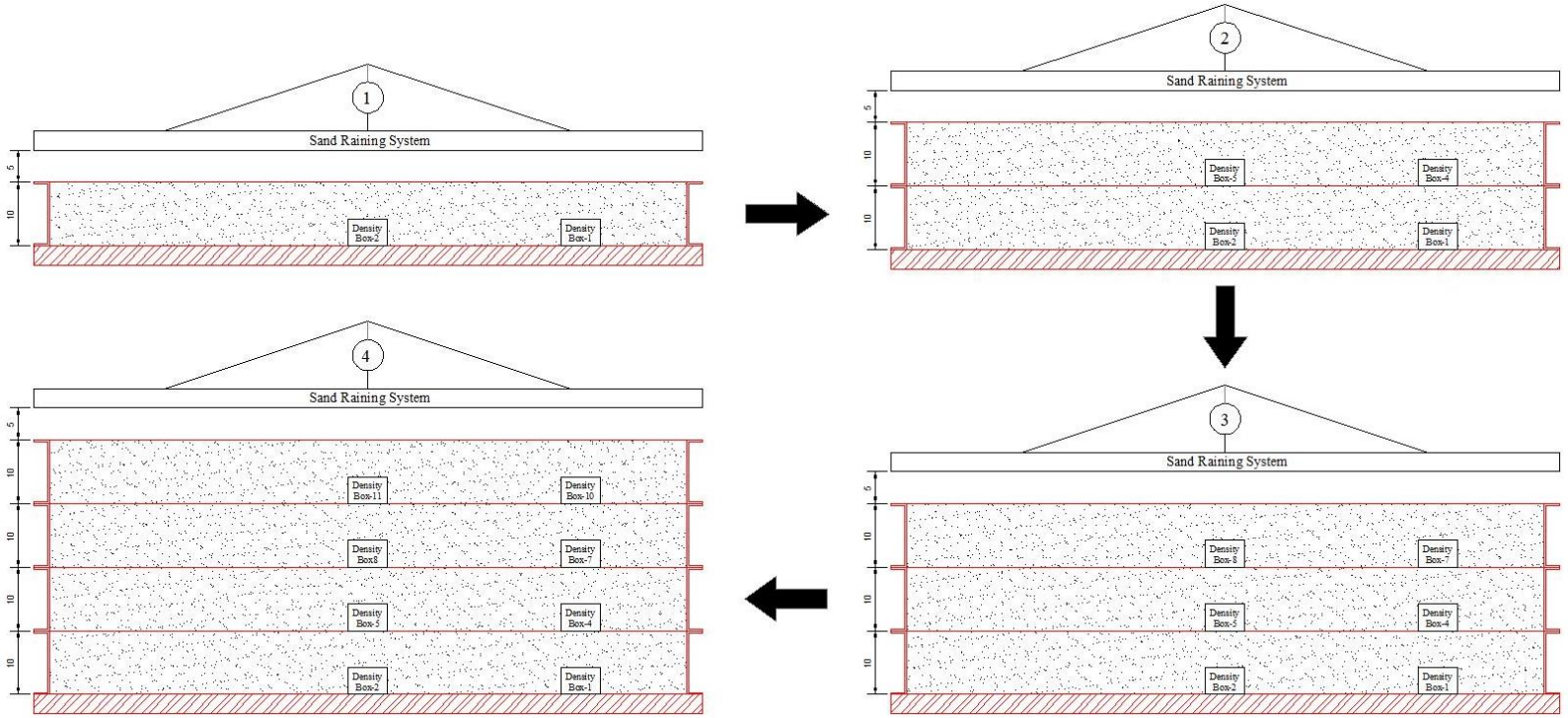

Figure 4.4 Schematic view and phases of relative density test 1

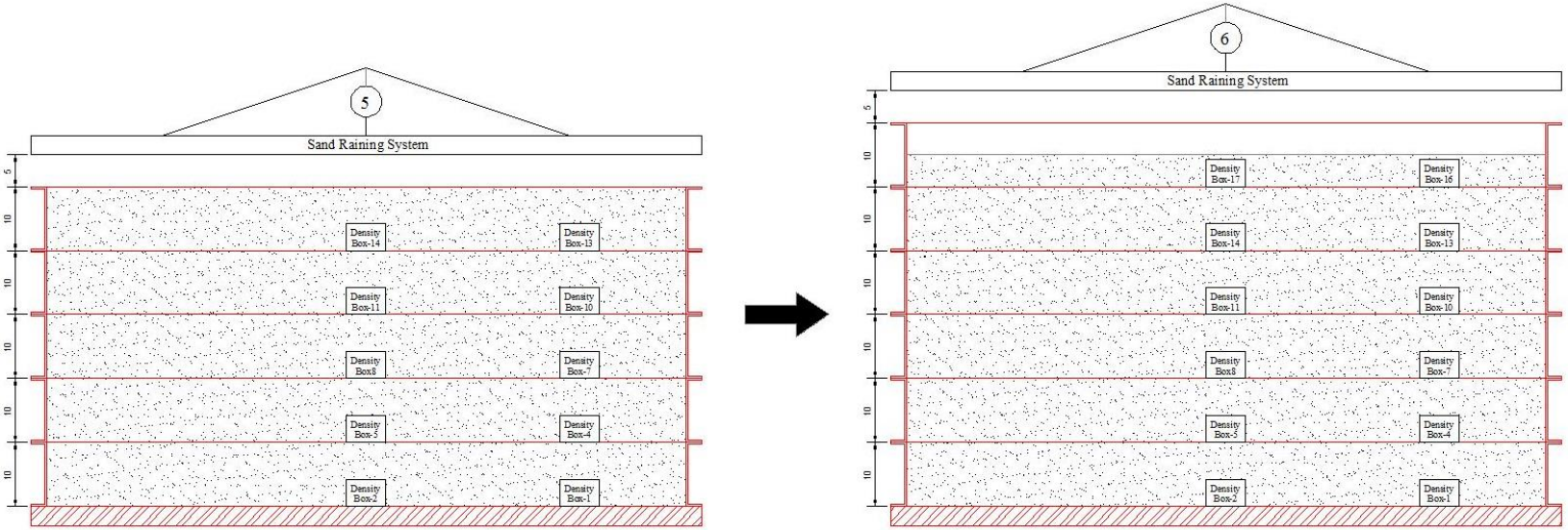

Figure 4.4 (continued)

Table 4.1 Results of relative density test 1

Layer No (from bottom)	Box No	V_{final} (cm^3)	m (g)	m_{full} (g)	m_{soil} (g)	ρ (g/cm^3)	ρ_{ort} (g/cm^3)	RD (%)
1	1	132.74	29.62	247.81	218.19	1.64	1.63	67
	2	132.95	31.87	247.33	215.46	1.62		
	3	131.89	30.7	244.82	214.12	1.62		
2	4	131.18	32.38	246.90	214.52	1.64	1.63	66
	5	130.95	31.47	243.31	211.84	1.62		
	6	130.80	31.65	244.36	212.71	1.63		
3	7	130.84	30.41	242.38	211.97	1.62	1.62	64
	8	130.78	31.76	243.22	211.46	1.62		
	9	131.34	31.06	243.91	212.85	1.62		
4	10	129.80	30.44	243.76	213.32	1.64	1.61	62
	11	132.61	31.77	245.23	213.46	1.61		
	12	131.18	30.07	241.74	211.67	1.61		
5	13	131.77	32.15	242.57	210.42	1.60	1.61	62
	14	130.62	32.09	243.32	211.23	1.62		
	15	131.22	31.04	243.30	212.26	1.62		
6	16	130.69	32.83	242.73	209.90	1.61	1.61	62
	17	129.00	31.78	241.20	209.41	1.62		
	18	129.63	31.91	240.12	208.2	1.61		

4.1.1.2 Relative Density Test 2

Second relative density test, test 2, is performed in a similar procedure as relative density test 1. Twelve relative density boxes are used and placed to testing tank as stated at test 1. The only difference is that 35 cm sand is deposited to understand the effect of sand weight to relative density at the bottom levels of testing tank by comparing 55 cm rained sand carried out in previous test. Schematic view and obtained relative density values are shown in Figure 4.5 and Table 4.2, respectively.

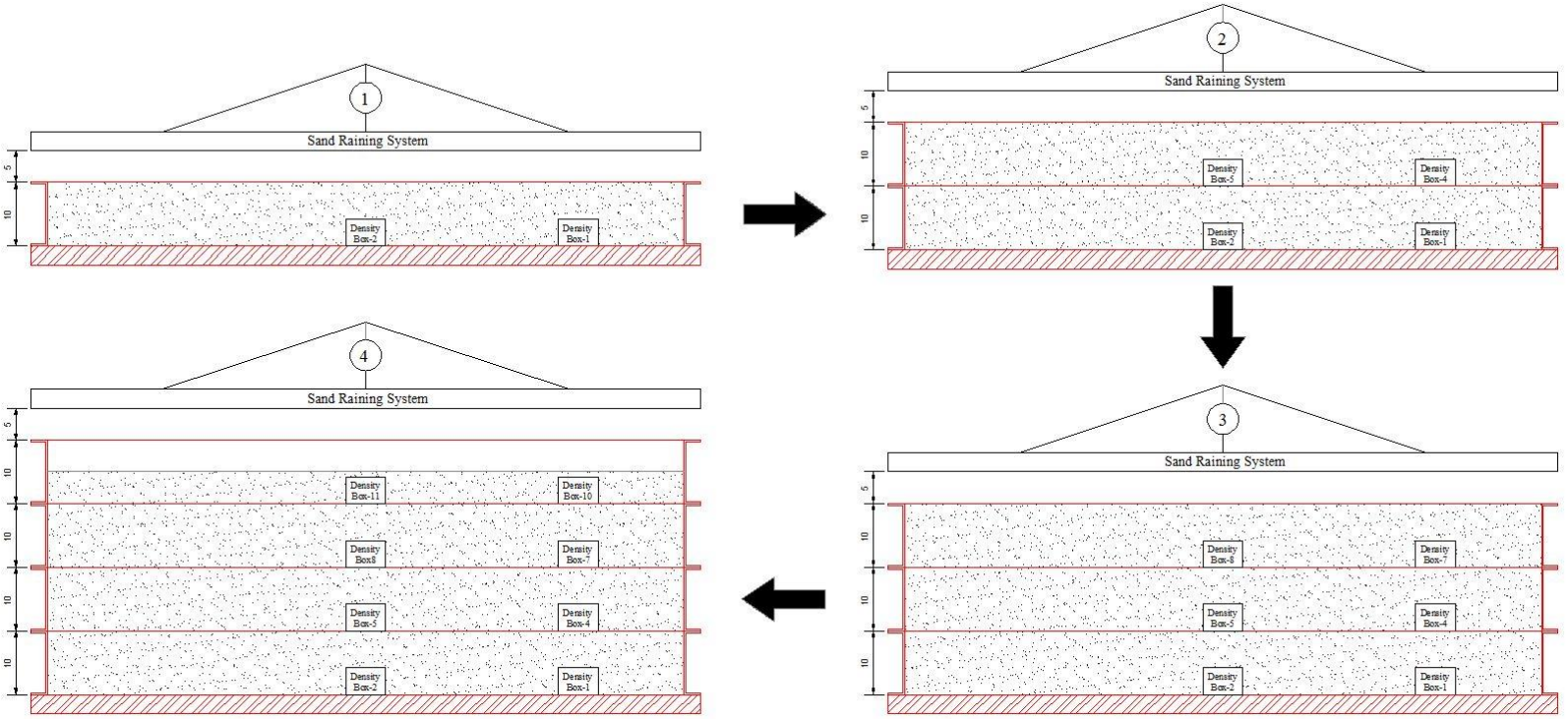

Figure 4.5 Schematic view and phases of relative density test 2

Table 4.2 Results of relative density test 2

Layer No (from bottom)	Box No	V_{final} (cm^3)	m (g)	m_{full} (g)	m_{soil} (g)	ρ (g/cm^3)	ρ_{ort} (g/cm^3)	RD (%)
1	1	132.74	29.62	246.91	217.29	1.64	1.63	67
	2	132.95	31.87	247.81	215.94	1.62		
	3	131.89	30.70	245.34	214.64	1.63		
2	4	131.18	32.38	247.28	214.90	1.64	1.63	67
	5	130.95	31.47	243.98	212.51	1.62		
	6	130.80	31.65	244.78	213.13	1.63		
3	7	130.84	30.41	242.97	212.56	1.62	1.62	65
	8	130.78	31.76	245.88	214.12	1.64		
	9	131.34	31.06	241.80	210.74	1.60		
4	10	129.80	30.44	245.98	215.54	1.66	1.61	61
	11	132.61	31.77	244.69	212.92	1.61		
	12	131.18	30.07	241.48	211.41	1.61		

4.1.1.3 Relative Density Test 3

In this test, testing tank is filled only its 10 cm height by raining at 5 cm raining elevation from the top of the testing tank. Three relative density boxes are used designated as 1, 2 and 3 which placed at corner, edge and center of the testing tank, respectively. Schematic view and obtained relative density values are shown in Figure 4.6 and Table 4.3, respectively.

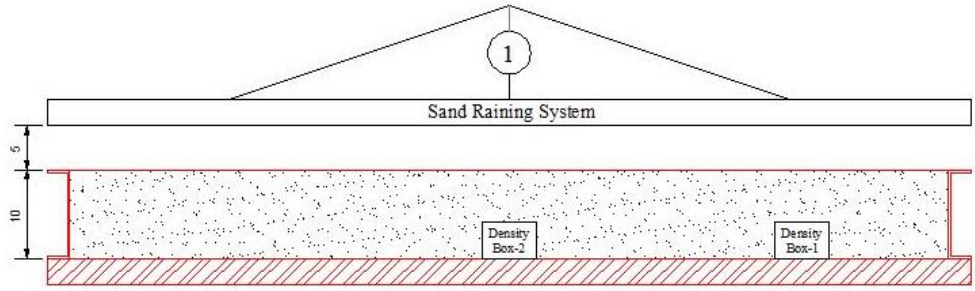

Figure 4.6 Schematic view of relative density test 3

Table 4.3 Results of relative density test 3

Box No	V_{final} (cm^3)	m (g)	m_{full} (g)	m_{soil} (g)	ρ (g/cm^3)	ρ_{ort} (g/cm^3)	RD (%)
1	132.74	29.62	242.70	213.08	1.61	1.61	61
2	132.95	31.87	245.33	213.46	1.61		
3	131.89	30.70	243.69	212.99	1.61		

4.1.1.4 Relative Density Test 4

This test is performed in a similar way as relative density test 3. The only difference between these tests is raining elevation. At this test, the sieve is placed 15 cm higher than the top of the testing tank as shown in Figure 4.7. Thus, the distances to the bottom and the top of the testing tank from raining sieve are 25 cm and 15 cm, respectively. Relative density boxes 1, 2 and 3 are used. Results are shown in Table 4.4.

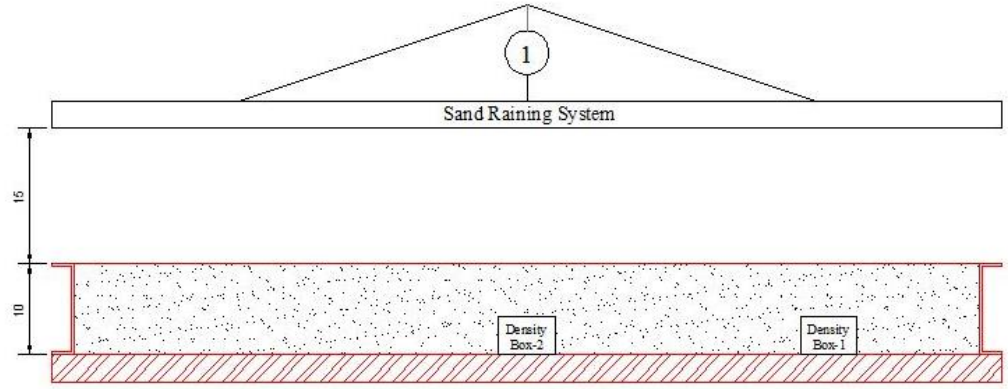

Figure 4.7 Schematic view of sand raining test 4

Table 4.4 Results of sand raining test 4

Box No	V_{final} (cm^3)	m (g)	m_{full} (g)	m_{soil} (g)	ρ (g/cm^3)	ρ_{ort} (g/cm^3)	RD (%)
1	132.74	29.62	242.05	212.43	1.60	1.61	62
2	132.95	31.87	245.60	213.73	1.61		
3	131.89	30.70	244.34	213.64	1.62		

4.1.1.5 Relative Density Test 5

The final relative density test is done to understand how much relative density variance will be observed when raining elevation is arranged to 35 cm height from the bottom of the testing tank. This raining height will not be used during tests, but nevertheless to comprehend the alteration of relative density value by raining height increasing, that test is needed. The same relative density boxes are used as the previous test. Schematic view and the test results are shown in Figure 4.8 and Table 4.5, respectively.

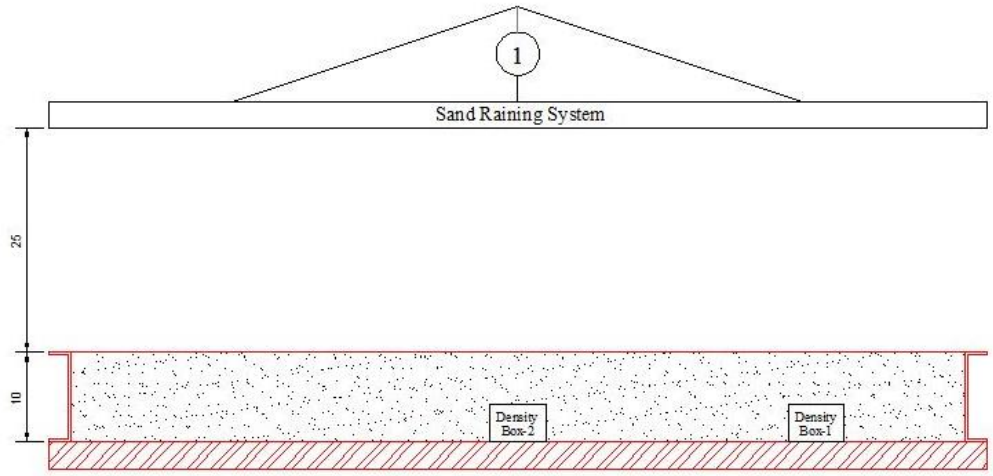

Figure 4.8 Schematic view of sand raining test 5

Table 4.5 Results of sand raining test 5

Box No	V_{final} (cm^3)	m (g)	m_{full} (g)	m_{soil} (g)	ρ (g/cm^3)	ρ_{ort} (g/cm^3)	RD (%)
1	132.74	29.62	242.93	213.31	1.61	1.62	64
2	132.95	31.87	246.99	215.12	1.62		
3	131.89	30.70	245.42	214.72	1.63		

4.1.1.6 Discussion of the Results of Relative Density Tests

Geocell reinforced tests will be performed with 10, 15 and 20 cm heights of geocells. Accordingly, raining elevation will vary between 5 cm and 25 cm at any level of testing tank in all reinforced and unreinforced tests. When considering relative density test 1, it is observed that relative density values increase at the bottom levels of testing tank because of sand weight. Obtained values are 62% and 67% at the uppermost and lowermost of the tank, respectively. As indicated before, that test represents the maximum sand height condition in all tests. In other words, relative density will not be more than 67% in any test at the base of the tank. Results of second test support that theory. In relative density test 2, relative density value at the bottom of the tank is

obtained as 67%, similar to test 1. In brief, relative density test 1 and test 2 are performed to observe relative density variance by depth due to sand weight.

Other relative density tests 3, 4 and 5 are performed to understand the effect of raining height to relative density. Because, geocells have different heights and accordingly different raining elevations will be used in each test. Relative density values are found as 61%, 62% and 64% from test 3, test 4 and test 5, respectively. Increase in raining elevation slightly increases the relative density.

If the relative density results of the top levels of test 1 and test 2 and also result of test 3 which all obtained by filling at a sieve elevation of 5 cm from the top of the tank, are compared, it can be seen that the results are compatible (61% and 62%). That small difference was probably due to measurement error.

This set of tests show that there is a limited effect of raining elevation and sand depth (accordingly sand weight) on relative density. In any case, relative density values change between 61% and 67% in all tests. That variance can be neglected because the difference is so small. As shown in Figure 4.9, if the relative density value increases from 61% to 67%, the value of the internal friction angle increases by less than 1° in the case of using a linear relation in relative density vs friction angle relation obtained in direct shear tests.

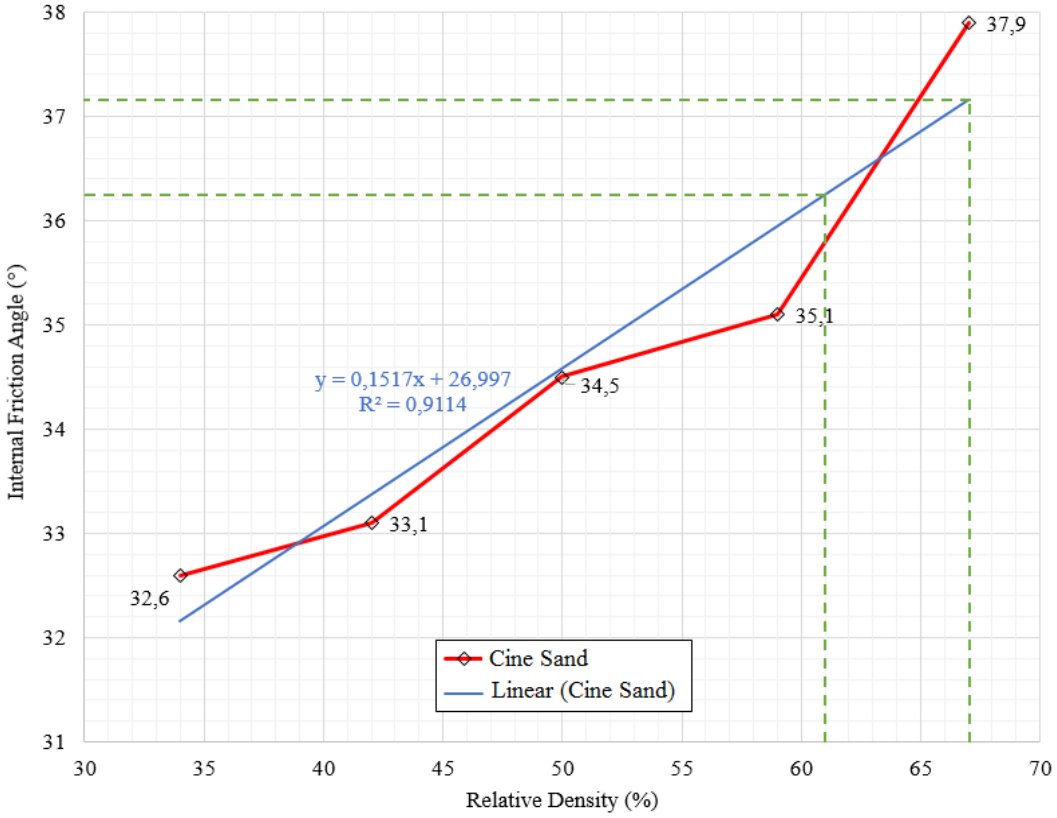

Figure 4.9 Change of internal friction angle with relative density of Çine Sand

Moreover; the variance of the relative density values is not important for this thesis purpose, as it aims to compare the unreinforced and geocell reinforced cases, which will have the same raining procedure in all tests. Furthermore, too close dry density values are obtained in all relative density boxes placed at the same level, in a sense homogeneous raining can be performed at the corner, edge and the center of the tank by the new sand raining system.

In addition, to perform CBR tests, bigger molds than relative density boxes are used. These molds are filled by the same raining procedure as stated relative density tests. Before starting CBR tests, volume and weight of molds are saved and after filling of molds, relative density values are calculated by measuring full weight. Relative density values are obtained as 64% and 67% in two CBR tests. Hence, it was proved that the relative density values can be obtained independently from box and mold sizes.

4.1.2 Preparation of an Experiment

Sample preparation process starts with filling the first segment of testing tank with sand by using sand raining system. Similar with the relative density tests, filling the tank segment, adding new 10-cm high segment and repositioning of the sieve continued till the setup reached to the desired height. With the difference of unreinforced tests, geocell is placed in the pre-determined levels in geocell reinforced tests. In all geocell reinforced tests, 30 cm height (3 segments of testing tank) of sand basement and 5 cm height of sand cover above the geocell are kept constant as these are the relatively more compressible layers of the problem. Only height of geocells are changed between these sand layers and hence final height of sands are obtained as 45 cm, 50 cm and 55 cm for geocells that have 10 cm, 15 cm and 20 cm heights, respectively. Segments of the tank are taped to each other both externally and internally to prevent sand flowing out during loading (Figure 4.10). Geocells are tied with plastic clamps to the edge of the segment of the tank to keep the cells open and also stressed during the sand raining process (Figure 4.11). Geocell tied segments are added to filled testing tank (Figure 4.12). After sand filling is completed, these clamps are cut and thus, getting additional strength of geocells are prevented. Filled testing tank is moved over the slider from under the raining sieve to under the loading piston for the start of the loading process.

After testing tank is moved to loading system, and placed under the piston, a steel loading plate that has a diameter of 260 mm and a thickness of 25 mm is placed at the center of the tank on the ground surface. Connection of the loading plate and the piston is carried out by steel extension pieces. Load cell is placed between these pieces (Figure 4.13). Two dial gauges are positioned on a line passing through the center and near the edges of the loading plate by using dial gauge installation frame. Free movement of the rod of the dial gauges is checked by hand and it is controlled to not to touch anywhere during the loading process. Calibration of load cell is done by using the software of the data logger, TESTBOX 1001. The piston is moved down till all pieces touch each other. After touching, load cell reading that corresponds to weight of the piston and the extension pieces is recorded. That value is set to zero and the zero

values of dial gauges are noted. Compressor tank is filled by pressurized air till it reaches to 8 bars. Valve of the compressor is opened. After all of these stages are completed, the system is ready for loading by opening the pressure valve manually (Figure 4.14). After an experiment finishes, all monitoring experiments and loading plate are removed and sand is transferred back to sand storage tank by a shovel (Figure 4.15).

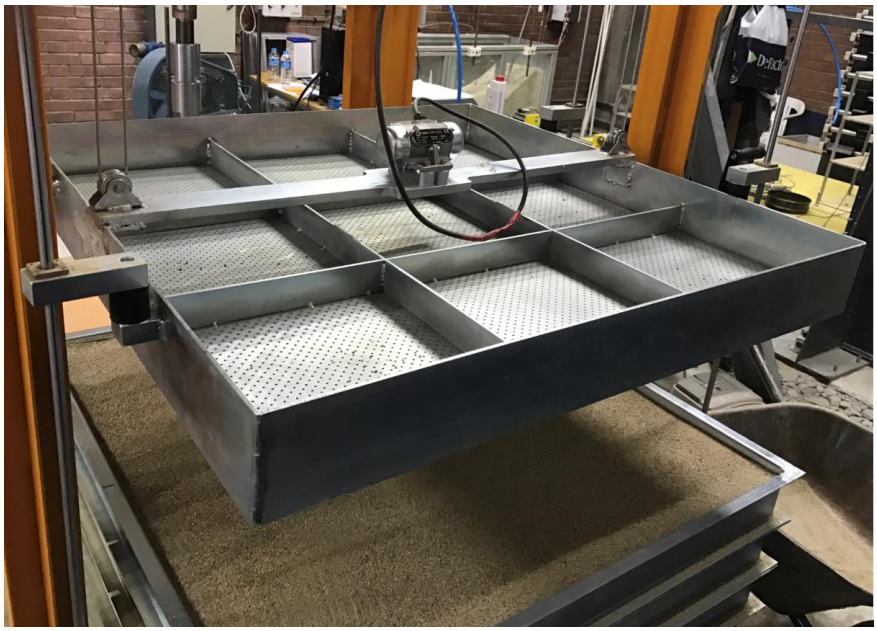

Figure 4.10 Sand raining process

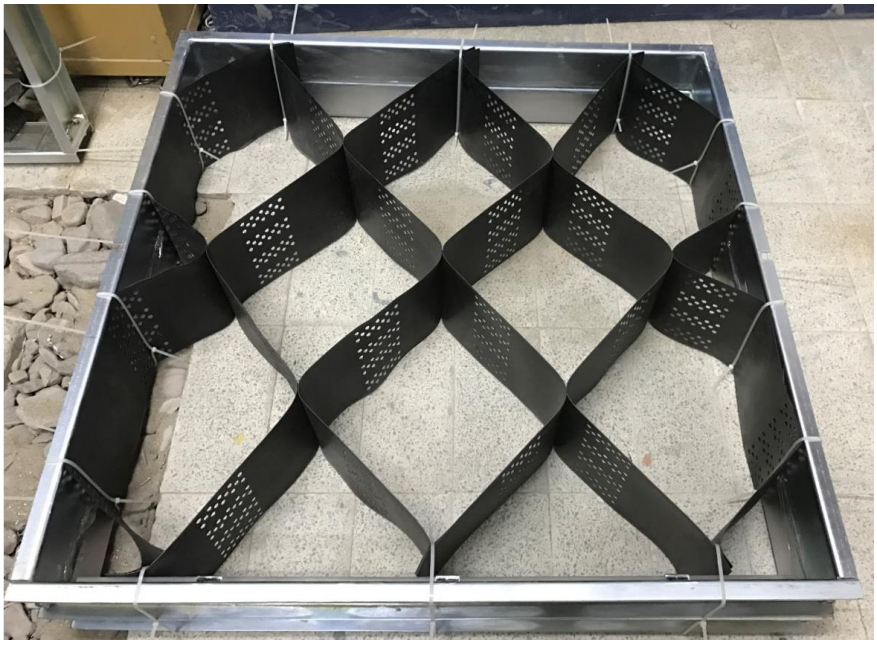

Figure 4.11 Tying of geocells by plastic clamps

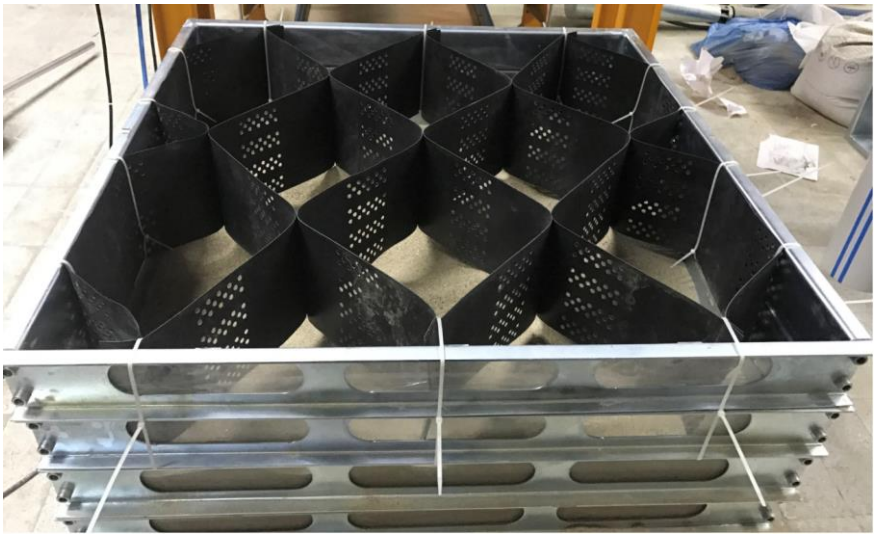

Figure 4.12 Placement of geocell tied segments to sand filled testing tank

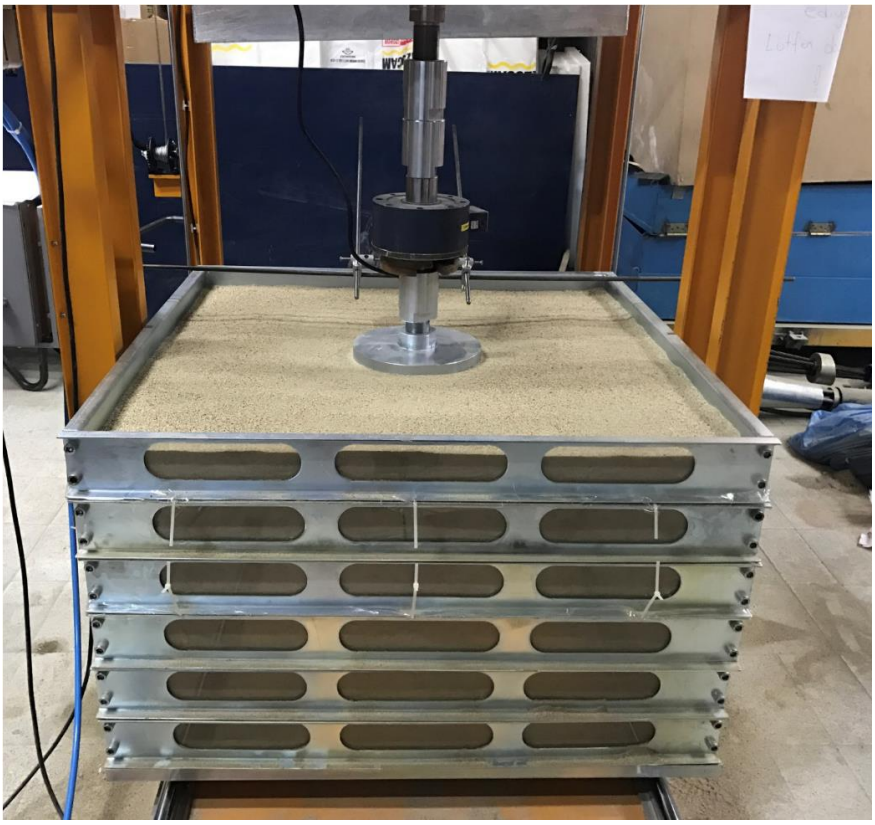

Figure 4.13 Filling of the tank to desired height, placement of loading plate and load cell

Figure 4.14 Placement of dial gauges by using dial gauge installation system

Figure 4.15 Removal of the sand from the tank by a shovel at the end of the test

4.2 Laboratory Model Tests

Contribution of geocell reinforcement on the behavior of bearing capacity and settlement of the footing is investigated in this study. Amount of the contributions of the geocells are examined with regards to height of the cell, width of the cell and loading location of the footing. In four series of plate load tests, a total of 13 experiments are performed as shown in Table 4.6.

Table 4.6 Summary of static plate load tests

Test Series	Test Name	Test Type	Total Sand Height (cm)	Geocell Width (cm)	Geocell Height (cm)	Loading Location	Stress at settlement 20% of plate diameter (kPa)
1	Test 1	Unreinforced	45	-	-	-	430
	Test 2	Unreinforced	50	-	-	-	457
	Test 3	Unreinforced	55	-	-	-	480
2	Test 4	Reinforced	45	35 x 40	10	center	603
	Test 5	Reinforced	45	35 x 40	10	intersection	585
	Test 6	Reinforced	50	35 x 40	15	center	655
	Test 7	Reinforced	50	35 x 40	15	intersection	665
	Test 8	Reinforced	55	35 x 40	20	center	753
	Test 9	Reinforced	55	35 x 40	20	intersection	825
3	Test 10	Reinforced	45	25 x 30	10	center	620
	Test 11	Reinforced	50	25 x 30	15	center	730
	Test 12	Reinforced	55	25 x 30	20	center	830
4	Test 13	Reinforced (Repeat)	55	35 x 40	20	center	736

First test series is carried out on unreinforced sands for three different heights which are 45 cm, 50 cm and 55 cm corresponding to different heights of geocells in geocell reinforced tests. Second test series is performed with GEOCELL 60 type geocell to compare the effect of loading location on the behavior of load-settlement. Center and

intersection represent the conditions in which geocell is placed the way that projection of plate does not touch the geocell material and projection of plate is exactly centered at the welded parts of geocell materials, respectively. Loading location effect could not be studied with GEOCELL 40 type geocell due to loading plate could not be placed exactly at the center of the cell. Third test series is conducted to understand the effects of the width of the cell on the performance of geocell reinforcement by comparing the results with second test serial at the same cell heights. Additionally, these test series allowed to study the effect of geocell height for different geocell widths. The last test series is a repeat test to ensure the repeatability of tests. Details of these test series are presented in following sections.

The plate settlement reported here is the average value of the readings taken at the two different points. Dial gauge results for two randomly selected experiments (one of them is unreinforced (Test 2) the other one is geocell reinforced (Test 6)) are presented individually as shown in Figure 4.16. As can be seen in the figure, no differential settlement or no tilting of the loading plate is observed during tests.

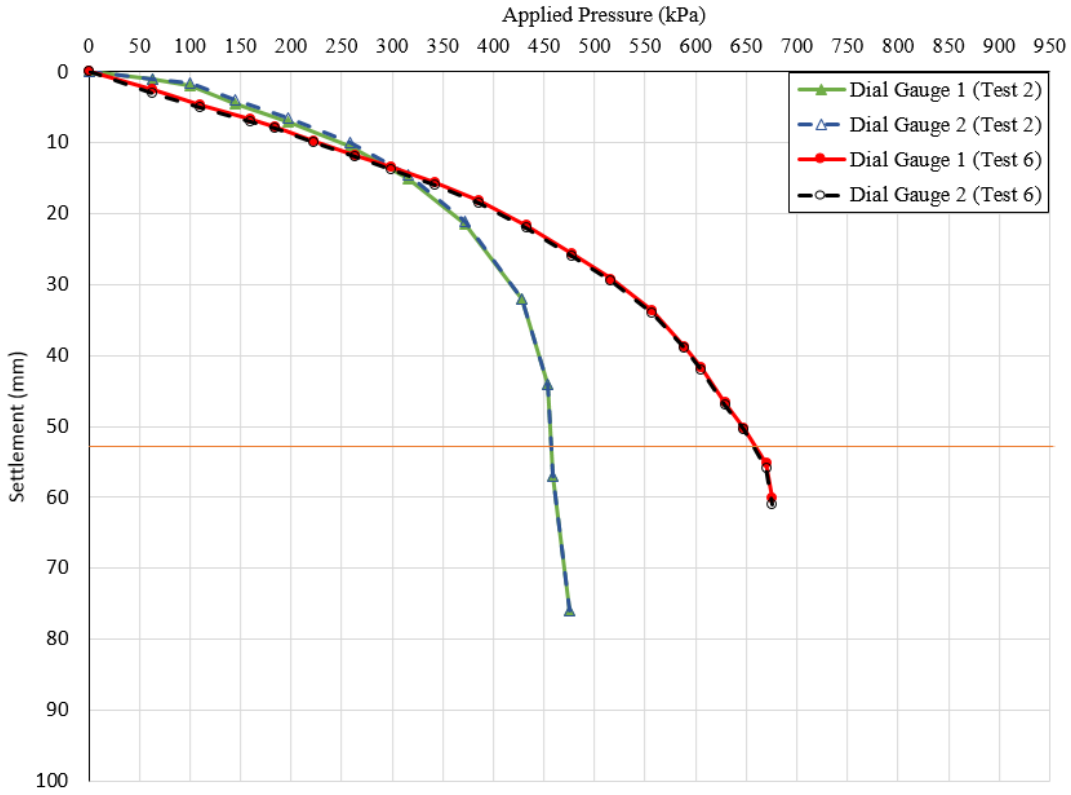

Figure 4.16 Individual results of dial gauges on loading plate

A rigid steel loading plate 260 mm in diameter is selected and used to simulate truck tire contact area.

Ultimate bearing capacity of the footing (loading plate) is assumed as the bearing capacity value corresponding to 52 mm settlement of plate which is 20% diameter of it, as used in the study of Gurbuz & Mertol (2012). 52 mm settlement of the plate is shown an additional line on the graphs.

4.2.1 Test Series 1 (Unreinforced Experiments)

This series of tests is carried out to decide on the amount of improvement of geocell reinforcement as compared with other test series. Three unreinforced tests are performed corresponding to three different sand heights varying due to geocell heights. All tests are performed with the same procedure. A clear failure is observed in

unreinforced tests unlike geocell reinforced ones. 430 kPa, 457 kPa and 480 kPa stress values are obtained under the loading plate at the 52 mm settlement of it for Test 1, Test 2 and Test 3, respectively. It is estimated that these differences might be caused by small testing errors. Results of the unreinforced tests are presented in Figure 4.17.

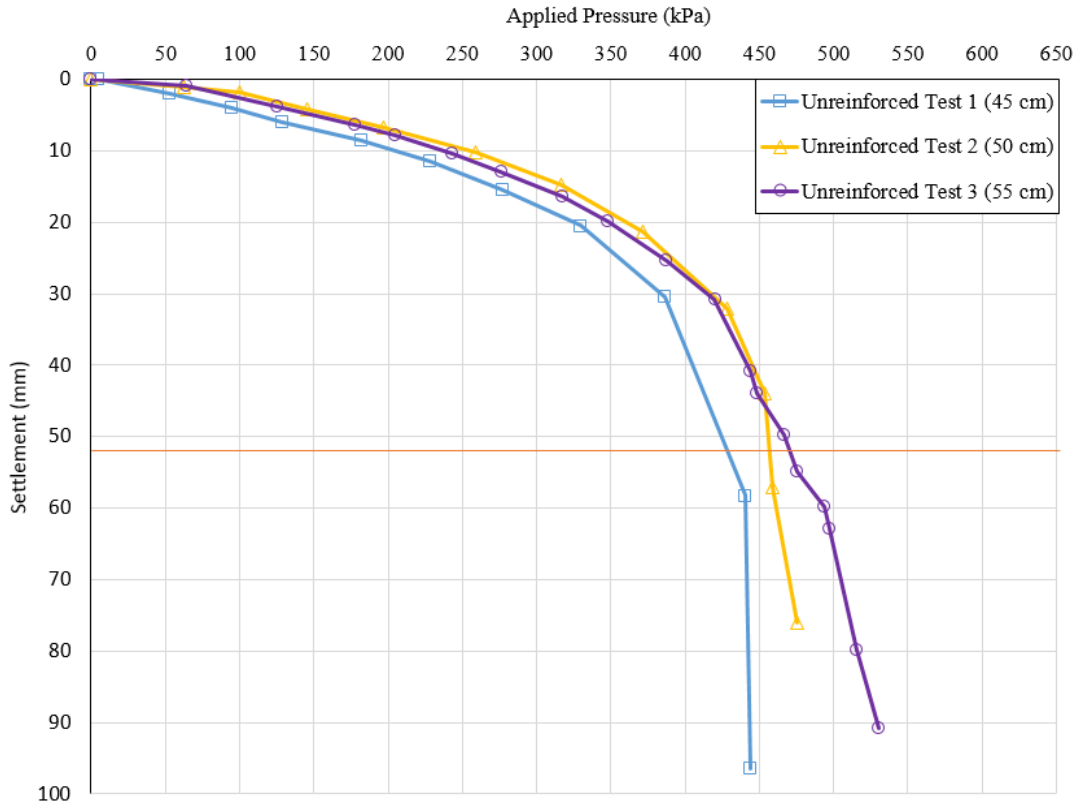

Figure 4.17 Results of test series 1 (unreinforced tests)

4.2.2 Test Series 2

Geocells have bigger openings compared with other geosynthetics such as geogrid, geonet etc. Consequently the behavior of geocell may be affected from loading an area smaller than geocell openings area (Figure 4.18). This series of tests are mainly conducted to understand effect of loading location on the behavior of the bearing capacity and the settlement of a footing. Two limit loading types which are at the center

of the cell and at the intersection of polymer boundaries of cells are applied to sand reinforced by GEOCELL 60. Other type of geocell (GEOCELL 40) could not be used in these tests because the loading plate is bigger than the geocell opening area accordingly plate could not be located at the center of the cell exactly, as can be seen in Figure 4.18.

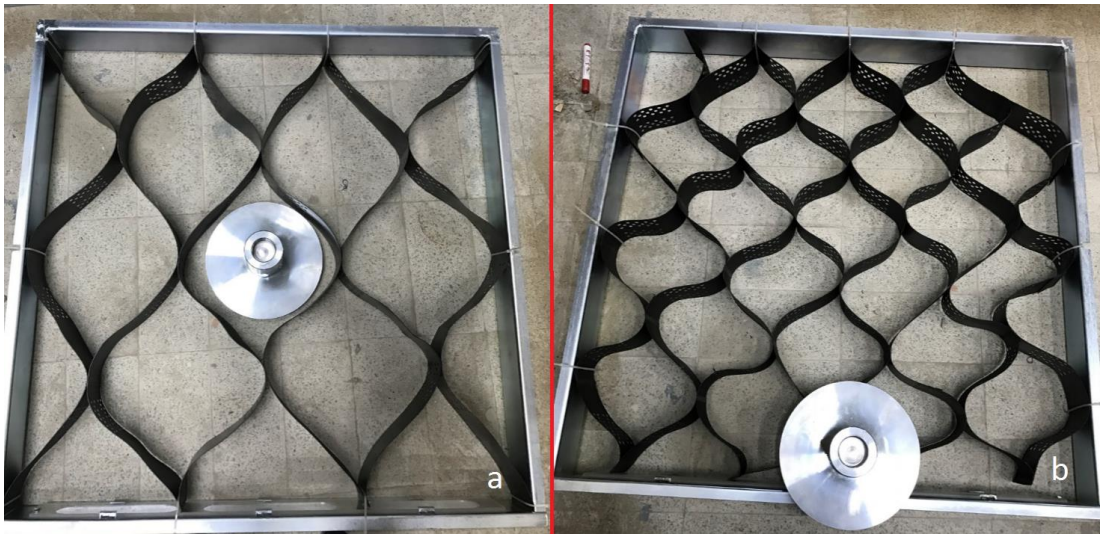

Figure 4.18 Placement of the loading plate (a: GEOCELL 60, b: GEOCELL 40)

Graph of test 4 is extended till it touches to the line that represents the settlement of 52 mm due to experiment is finished before reaching to that settlement value. Results are evaluated and compared according to bearing capacity corresponding to 52 mm of plate settlement. For 10 cm, 15 cm and 20 cm geocell heights, -3.1%, 1.5% and 9.6% more load carrying capacities are obtained when loading plate placed at the intersection of the polymer boundaries rather than geocell center. Percentage of improvement of smallest geocell height condition is shown in minus because of boundary intersection loading gave lower value compared to center loading. For 10 cm height of geocell, boundary intersection loading test ended with buckling of geocell material. Hence, smaller ultimate bearing capacity is obtained compared to centerly loaded one. Other height of geocells gave the exact opposite of the result of 10 cm

height of geocell. This is because, if height of geocell increases, geocell starts to act as a load carrying beam, and this effect increases the load carrying capacity until settlement of plate reaches to 52 mm (Figure 4.19).

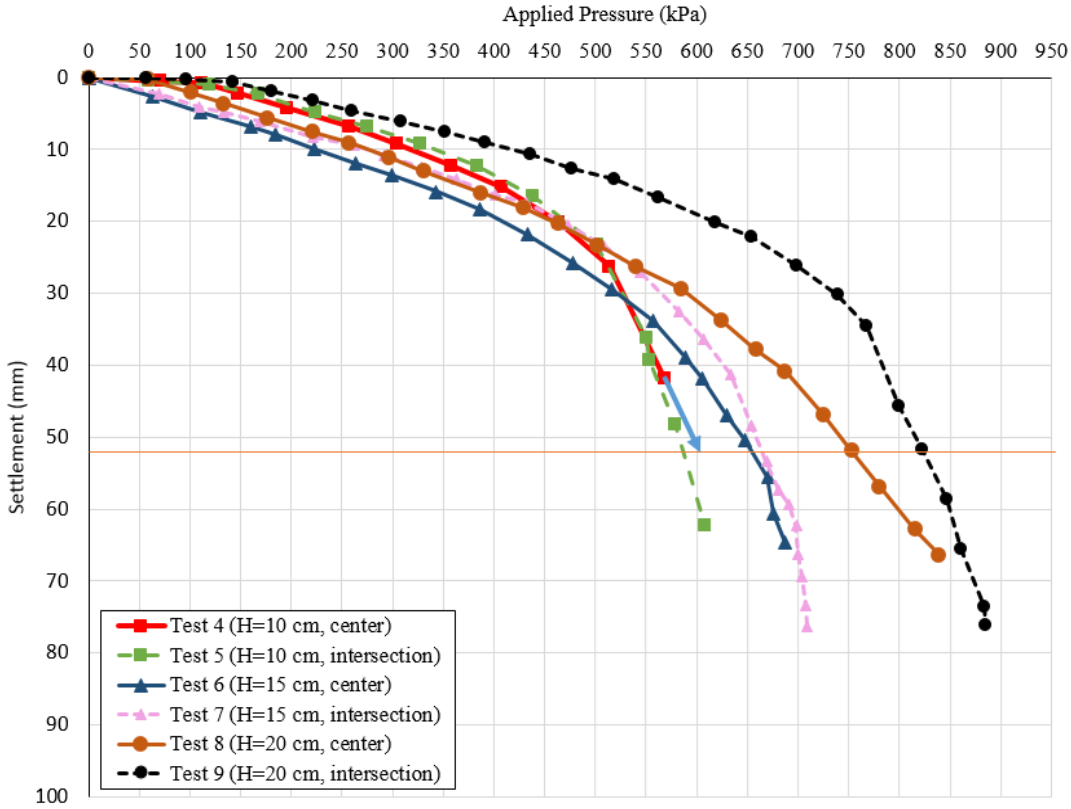

Figure 4.19 Results of test series 2

4.2.3 Test Series 3

This series of tests are carried out to compare the results with the results of test series 2 to understand the effect of the geocell width. At the same time this series of experiments also provided an opportunity to us to observe the effect of geocell height on a geocell with different cell opening. The loading plate is placed in the way that the center of the plate overlapped with the center of the cell. Three loading tests performed on GEOCELL 40 type geocells with three different heights of them. 620 kPa, 730 kPa

and 830 kPa stresses are obtained at 52 mm displacement of the plate from Test 10, Test 11 and Test 12, respectively (Figure 4.20). Each test gives a higher bearing capacity compared to larger of the same height.

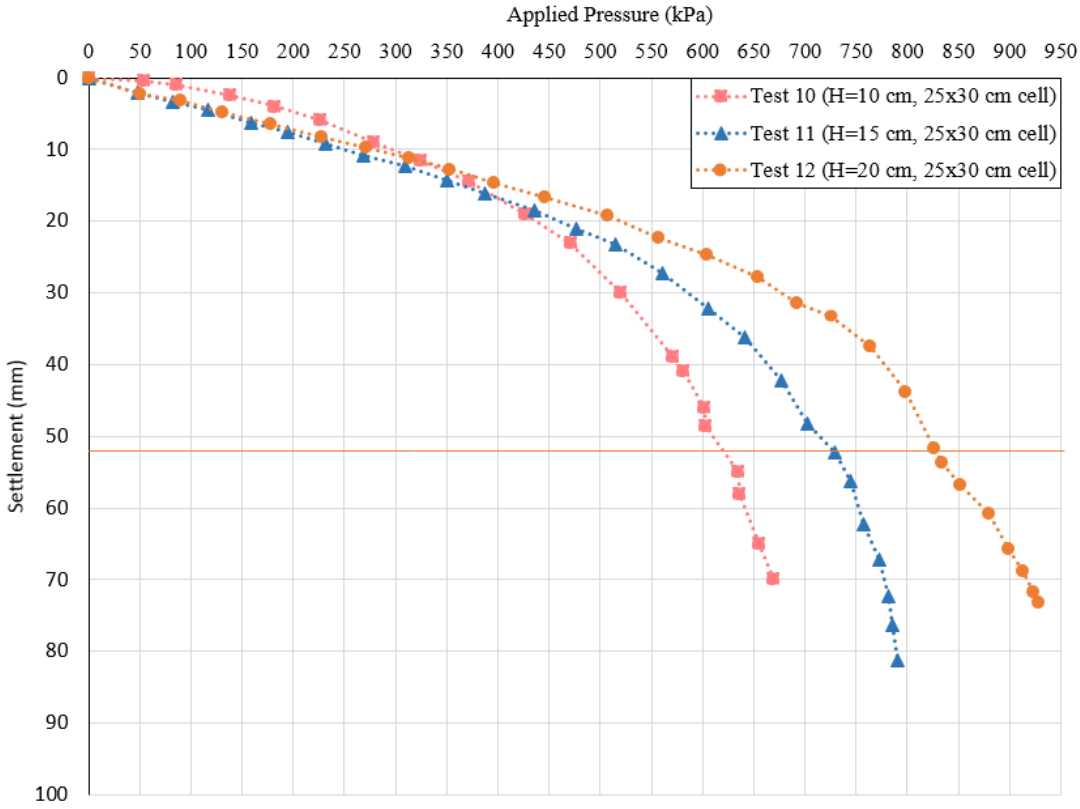

Figure 4.20 Results of test series 3

4.2.4 Test Series 4

Test series 4 consists of only Test 13 performed to understand the repeatability of the tests. Test 8 is repeated at the same conditions. 753 kPa and 736 kPa stress values under the loading plate at 52 mm settlement are obtained in Test 8 and Test 13, respectively. Difference between the test results is 2.3% and it can be said that tests are repeatable. Results of Test 8 and Test 13 are shown together in Figure 4.21.

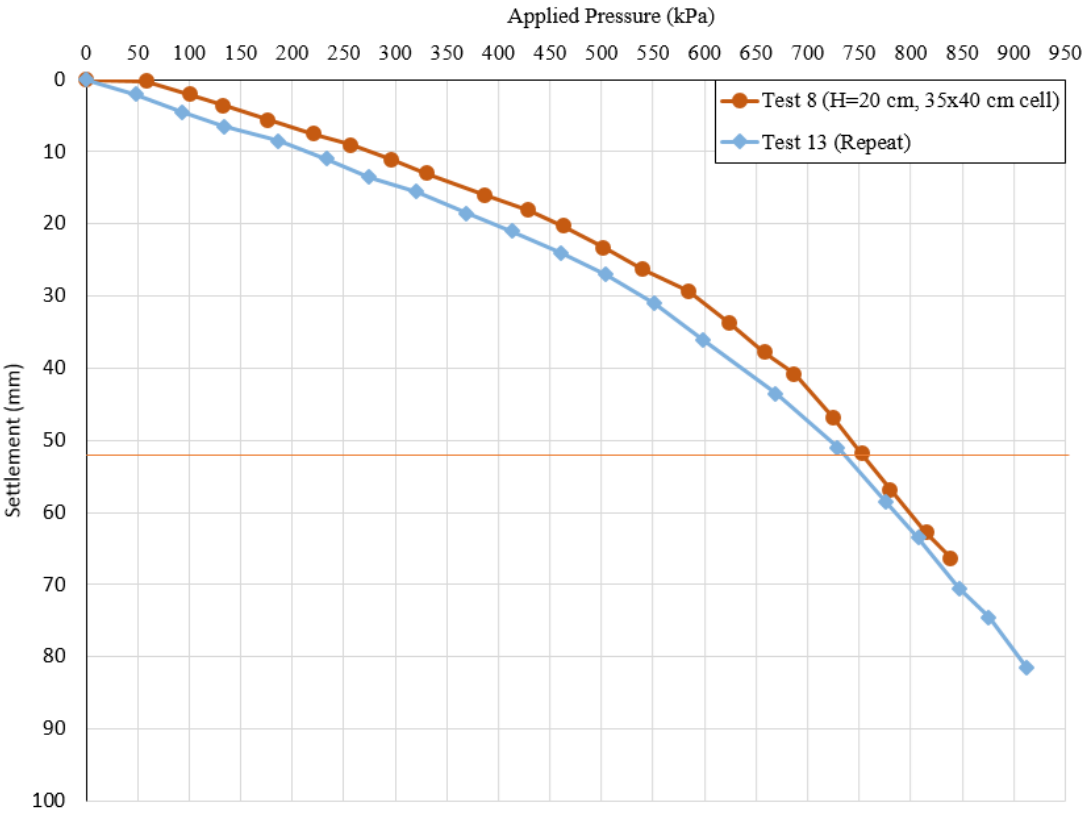

Figure 4.21 Results of test series 4

4.2.5 Discussion of the Results

Test results are evaluated regarding three different factors which are effect of geocell height, effect of geocell width and effect of loading location. Effects of these factors are presented in following subsections. All the experimental results are shown together in Figure 4.22. Average result of identical tests 8 and 13 is used instead of either test.

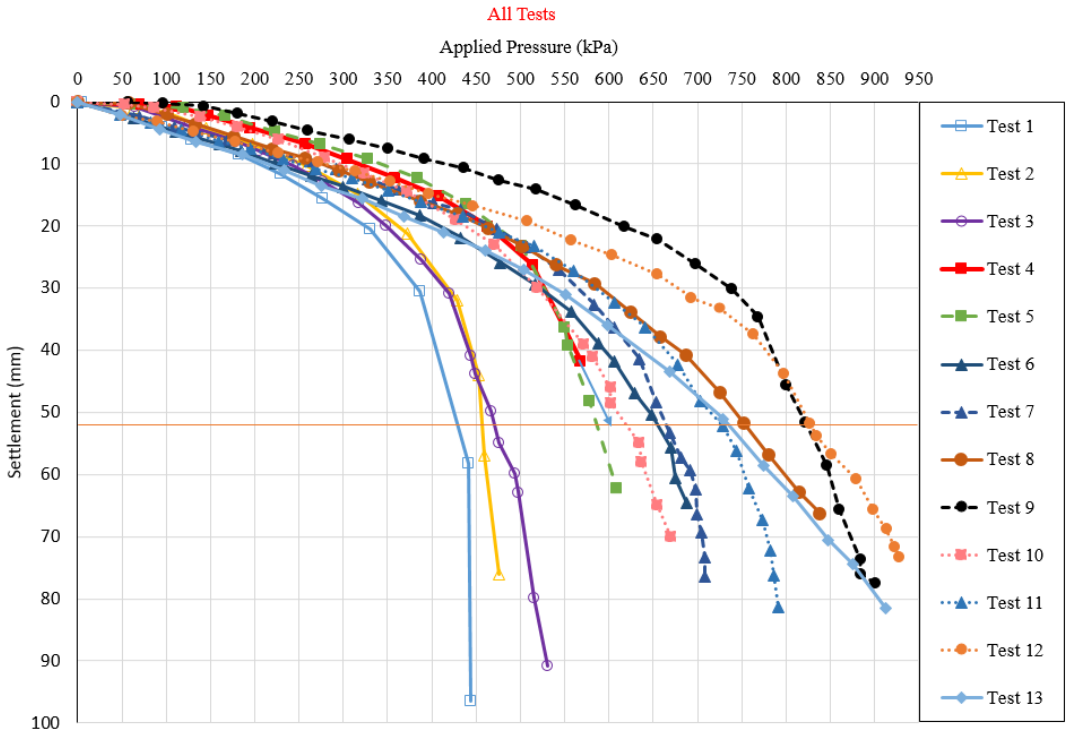

Figure 4.22 Results of all experiments

4.2.5.1 Effect of the Geocell Height

Effect of geocell height is examined on the both GEOCELL 60 and GEOCELL 40 type geocells. Three different heights which are 10 cm, 15 cm and 20 cm were used for each. In test series 2, there are two test results for each height of geocell due to load being applied to either the center of geocell or intersection of polymer boundary of the cell. Average of the results in test series 2 is used to compare and understand the effect of geocell height. Geocell reinforced test results are compared with corresponding unreinforced ones and amount of improvement is presented as percentage (%). As can be seen in Table 4.7, independently from geocell width, increase in geocell height increases the load carrying capacity of the footing at the same settlement value.

Additionally, for bigger geocell width (GEOCELL 60 – from Test 4 to Test 9), percentage of improvement increases when geocell height increases. In other words, in the case of using 15 cm height geocell instead of 10 cm, improvement percentage

increases from 38.14% to 44.42%. In a similar manner, using of 20 cm height geocell instead of 15 cm, that improvement percentage increases from 44.42% to 63.54%.

Table 4.7 Amount of the effect of the geocell height

Test Series	Test Name	Geocell Height (cm)	Stress at settlement 20% of plate diameter (kPa)	Improvement Percentage (%)
1 (No Geocell)	Test 1	-	430	-
	Test 2	-	457	-
	Test 3	-	480	-
2 (GEOCELL 60)	Average of Test 4 and Test 5	10	594	38.14
	Average of Test 6 and Test 7	15	660	44.42
	Average of Test 8 and Test 9	20	785	63.54
3 (GEOCELL 40)	Test 10	10	620	44.19
	Test 11	15	730	59.74
	Test 12	20	830	72.92

4.2.5.2 Effect of the Geocell Width

This effect is examined by comparing the results of test series 2 and test series 3 with the same heights of geocells. Similarly, average values of Test 4 and Test 5, Test 6 and Test 7 and also Test 8 and Test 9 are used for test series 2. For 10 cm and 20 cm height of geocell usage, buckling effect and load carrying beam effect which described previously could be carried out, respectively. But in any case, as it can be seen in Table

4.8, independently from geocell height, decrease in geocell width, increases the load carrying capacity of the footing.

Table 4.8 Amount of the effect of the geocell width

Test Series	Test Name	Geocell Height (cm)	Geocell Width (cm)	Stress at settlement 20% of plate diameter (kPa)	Improvement Percentage (%)
1 (No Geocell)	Test 1	-	-	430	-
	Test 2	-	-	457	-
	Test 3	-	-	480	-
2 (GEOCELL 60)	Average of Test 4 and Test 5	10	35 x 40	594	38.14
	Average of Test 6 and Test 7	15	35 x 40	660	44.42
	Average of Test 8 and Test 9	20	35 x 40	785	63.54
3 (GEOCELL 40)	Test 10	10	25 x 30	620	44.19
	Test 11	15	25 x 30	730	59.74
	Test 12	20	25 x 30	830	72.92

4.2.5.3 Effect of the Loading Location

This effect was examined in test series 2 using GEOCELL 60 type geocells. It is observed that loading on the intersection showed better performance in the case of using geocells with bigger heights. When using geocell with 10 cm height, gave better result in the case of center loading. If a geocell with a cell height more than 20 cm is

used, this difference might increase. However, it has not been evaluated within the scope of this study since these are not commonly used heights in the market.

In a similar way with load carrying beams, increase in height increases the load carrying capacity, because boundary of geocell is confined with sand and it acts like a structural beam. However, for the small height of geocells (10 cm), buckling and displacement is observed although it is confined with sand too. Because friction is small due to little cell surface area and under big loads, it buckled and deflected easily as shown in Figure 4.23.

Figure 4.23 A view of the tank after Test 5

Table 4.9 Amount of the effect of the loading location

Test Series	Test Name	Test Type	Geocell Height (cm)	Loading Location	Stress at settlement 20% of plate diameter (kPa)	Improvement Percentage (%)
2 (GEOCELL 60)	Test 4	Reinforced	10	center	603	-3.07
	Test 5	Reinforced	10	intersection	585	
	Test 6	Reinforced	15	center	655	1.53
	Test 7	Reinforced	15	intersection	665	
	Test 8	Reinforced	20	center	753	9.56
	Test 9	Reinforced	20	intersection	825	

Results are shown in Table 4.9. For 10 cm, 15 cm and 20 cm geocell heights, -3.07%, 1.53% and 9.56% more load carrying capacities are obtained in the case of loading plate is placed at the intersection of the polymer boundaries, respectively as stated before. Percentage of improvement of smallest geocell height condition is shown in minus because of boundary intersection loading gave lower value compared to center loading. It can be obviously deduced that geocells perform a uniform behavior and in any case, loading location did not effect the ultimate bearing capacity more than 10% for that kind of loading condition.

CHAPTER 5

SUMMARY AND CONCLUSIONS

5.1 Summarized Points and Conclusions

The aim of this study is to investigate the effect of geocell reinforcement on the behavior of sandy soils under static load. For this purpose, a total of 13 static load experiments are conducted; three of them are unreinforced, nine of them are geocell reinforced with different sizes of geocells and the last of them is a repeat test. The results are presented in terms of load versus settlement plots and bearing capacity and settlement performance of geocell reinforcement are investigated as compared to unreinforced conditions. Additionally, a series of soil mechanics tests including sieve analysis, minimum-maximum dry density and void ratio, determination of specific gravity, direct shear test and California Bearing Ratio (CBR) tests are performed to specify the properties of the Çine Sand.

A test set up that contains a sand raining system for fillling the tank by sand in all tests at the same relative density, a testing tank whose height is adjustable by adding aluminum segments to each other, and a pneumatic loading system is designed and manufactured to perform static load tests.

Geocells with two different widths and three different heights are used in tests. Influence of geocell height, geocell width on the bearing capacity of a rigid plate in a predetermined settlement value is investigated. In addition, the effect of loading location was investigated (i.e. at the exact center of the cell versus at intersection of polymer boundaries of the geocells) in the case of loading plate being smaller than the cell area. This topic was never studied before in the literature.

Major conclusions upon an evaluation of data obtained from the static plate load tests are summarized as given below:

1) Geocell reinforcement in any sizes contributed to bearing capacity of the footing corresponding to settlement value of 20% of diameter of it compared to unreinforced ones.
2) A clear failure is observed in unreinforced tests however, the same behavior could not be observed in geocell reinforced tests in the other words geocell reinforced sand showed a ductile behavior.
3) Bearing capacity of the system increased with increasing geocell height independently from geocell width.
4) Decreasing of geocell width increased the bearing capacity of the footing independently from geocell height.
5) Importance of the location of the loading plate is investigated in this study with the difference of previous studies. Geocell with 20 cm height gave the better result in the case of intersection of material boundary of a geocell is loaded. However, exact opposite behavior is observed in the event of using geocell with 10 cm height. This behavior can be expressed similarly as expressed at previous item. In any case, no more than 10% difference on the bearing capacity of the footing at 52 mm displacement of it is not observed and it can be concluded that, geocell shows almost homogenous behavior regardless of loading location relative to geocell structure.

In summary, for a predetermined settlement value, presence of the geocells increased the bearing capacity of the footing by 38% to 73% compared to unreinforced cases.

It should be noted that only one type of loading plate, one type of geocell with different heights and widths and one type of sand were used in this study; therefore, the results obtained from this study may be different than those of full-scale tests in field and also using of different materials.

5.2 Recommendations for Future Studies

Scale model type experimental studies are very important to obtain correlations for designs. But their results are limited to use in all projects in the other words they are project specific. Since a different test setup cannot be prepared for the materials to be used in each project, it is important and necessary to obtain quick and easy-to-use design tools. Because of these reasons following topics are recommended for future studies:

- Behavior of geocell reinforced soils under repeated loads represent to truck wheel loads.
- Wide field in-situ tests to get real behavior of geocell reinforcement because they are worthwhile for designers.
- Instrumentation of geocells with strain gauges and earth pressure cells.
- 3D numerical analysis verifying the results of experimental studies and also making parametric studies on them.
- Transferring geocell behavior to 2D numerical model and develop easy hand calculations that can be used by anyone.

REFERENCES

ASTM D6913 / D6913M-17 Standard Test Methods for Particle-Size Distribution (Gradation) of Soils Using Sieve Analysis, ASTM International, West Conshohocken, PA, 2017, www.astm.org

ASTM C702 / C702M-11, Standard Practice for Reducing Samples of Aggregate to Testing Size, ASTM International, West Conshohocken, PA, 2011, www.astm.org

ASTM D1883-16, Standard Test Method for California Bearing Ratio (CBR) of Laboratory-Compacted Soils, ASTM International, West Conshohocken, PA, 2016, www.astm.org

ASTM D3080-04, Standard Test Method for Direct Shear Test of Soils Under Consolidated Drained Conditions, ASTM International, West Conshohocken, PA, 2004, www.astm.org

ASTM D4254-14, Standard Test Methods for Minimum Index Density and Unit Weight of Soils and Calculation of Relative Density, ASTM International, West Conshohocken, PA, 2014, www.astm.org

ASTM D854-14, Standard Test Methods for Specific Gravity of Soil Solids by Water Pycnometer, ASTM International, West Conshohocken, PA, 2014, www.astm.org

Avesani Neto, J. O., Bueno, B. S., & Futai, M. M. (2013). A bearing capacity calculation method for soil reinforced with a geocell. Geosynthetics International, 20(3), pp. 129-142.

Bathurst, R.J. & Karpurapu, R. (1993). Large-scale triaxial compression testing of geocell-reinforced granular soils. Geotechnical Testing Journal, ASTM, 16(3), pp. 296-303.

Chen, R.-H., Huang, Y.-W., & Huang, F.-C. (2013). Confinement effect of geocells on sand samples under triaxial compression. Geotextiles and Geomembranes, 37(Supplement C), pp. 35–44.

Dabiryan, H., Kargar, M., Aghabeigi, E., Mir Mohammad Hosseini, S. M., & Hosseini Varkiyani, S. M. (2017). Evaluating the performance of geocells made from needle punched nonwoven layers in the bearing capacity of reinforced soil. The Journal of The Textile Institute, 108(10), pp. 1747–1752.

Dash, S. K., Krishnaswamy, N. R., & Rajagopal, K. (2001a). Bearing capacity of strip footings supported on geocell-reinforced sand. Geotextiles and Geomembranes, 19(4), pp. 235-256.

Dash, S. K., Rajagopal, K., & Krishnaswamy, N. R. (2001b). Strip footing on geocell reinforced sand beds with additional planar reinforcement. Geotextiles and Geomembranes, 19(8), pp. 529-538.

Dash, S. K., Rajagopal, K., & Krishnaswamy, N. R. (2004). Performance of different geosynthetic reinforcement materials in sand foundations. Geosynthetics International, 11(1), pp. 35-42.

Dash, S. K., Rajagopal, K., & Krishnaswamy, N. R. (2007). Behaviour of geocell-reinforced sand beds under strip loading. Canadian Geotechnical Journal, 44(7), pp. 905-916.

Dash, S. K. (2010). Influence of relative density of soil on performance of geocell-reinforced sand foundations. Journal of Materials in Civil Engineering, 22(5), pp. 533-538.

Dash, S. K. (2012). Effect of geocell type on load-carrying mechanisms of geocell-reinforced sand foundations. International Journal of Geomechanics, 12(5), pp. 537-548.

Emersleben, A., & Meyer, N. (2008). The use of geocells in road constructions over soft soil: Vertical stress and falling weight deflectometer measurements. Paper No. 132, EuroGeo4, Edinburgh, Scotland.

Gilbert, P.A. (1984). Investigation of Density Variation in Triaxial Test Specimens of Cohesionless Soil Subjected to Cyclic and Monotonic Loading. U.S. Army Engineer Waterways Experiment Station, United States.

Gurbuz, A., & Mertol, H. C. (2012). Interaction between assembled 3D honeycomb cells produced from high density polyethylene and a cohesionless soil. Journal of Reinforced Plastics and Composites, 31(12), pp. 828–836.

Han, J., Yang, X., Leshchinsky, D., & Parsons, R. (2008). Behavior of geocell-reinforced sand under a vertical load. Transportation Research Record: Journal of the Transportation Research Board 2045, pp. 95-101.

Hegde, A., & Sitharam, T. G. (2014). Joint strength and wall deformation characteristics of a single-cell geocell subjected to uniaxial compression. International Journal of Geomechanics, 15(5), 04014080.

Henkel, D. J., & Gilbert, G. D. (1952). The effect measured of the rubber membrane on the triaxial compression strength of clay samples. Geotechnique, 3(1), pp. 20-29.

Kargar, M. & Hosseini, S. M. M. M. (2017). Effect of reinforcement geometry on the performance of a reduced-scale strip footing model supported on geocell-reinforced sand. Scientia Iranica A, 24(1), pp. 96-109.

Koerner, R.M. (2012). Designing with Geosynthetics (Vol. I). Xlibris Corporation.

Madhavi Latha, G., Rajagopal, K., & Krishnaswamy, N. R. (2006). Experimental and Theoretical Investigations on Geocell-Supported Embankments. International Journal of Geomechanics, 6(1), pp. 30-35.

Madhavi Latha, G., Rajagopal, K., & Krishnaswamy, N. R. (2006). Experimental and theoretical investigations on geocell-supported embankments. International Journal of Geomechanics, 6(1), pp. 30-35.

Mengelt, M.J. & Edil, T.B., Benson, C.H. (2000). Reinforcement of Flexible Pavements Using Geocells. Geo Engineering Report No. 00-04. Geotechnical Engineering Program, Department of Civil & Environmental Engineering, University of Wisconsin-Madison, Madison, Wisconsin, USA.

NAPA (1994). “Guidelines for Use of HMA Overlays to Rehabilitate PCC Pavements.” Information Series 117, National Asphalt Pavement Association (NAPA).

Parvathi, K., & P. K. Jayasree. (2017) "Geocells: A Recent Technique of Soil Strengthening–A Review." International Conference on Geotechniques for Infrastructure Projects, 27th & 28th February, Thiruvananthapuram.

Pokharel, S. K., Han, J., Leshchinsky, D., Parsons, R. L., & Halahmi, I. (2010). Investigation of factors influencing behavior of single geocell-reinforced bases under static loading. Geotextiles and Geomembranes, 28(6), pp. 570-578.

Pokharel, S. K., Han, J., Parsons, R. L., Qian, Y., Leshchinsky, D. & Halahmi, I. (2009). Experimental study on bearing capacity of geocell-reinforced bases. 8th International Conference on Bearing Capacity of Roads, Railways and Airfields, Champaign, IL, USA, June 2009, pp. 1159-1166.

Poulos, H.G. & Davis, E.H. (1974). Elastic Solutions for Soil and Rock Mechanics. New York: John Wiley & Sons.

Rajagopal, K., Krishnaswamy, N. R., & Latha, G. M. (1999). Behaviour of sand confined with single and multiple geocells. Geotextiles and Geomembranes, 17(3), pp. 171-184.

Riaund, J.L. & Miran, J. (1992). “The Cone Penetrometer Test.” Technical report: FHWA-SA-91-043, Federal Highway Administration Office of Technology Applications, 400 Seventh Street, SW Washington, D.C, 20590.

Scott, R.F. (1963). Principles of Soil Mechanics. Addison-Wesley Publishing Company, Inc.

Shetgar, C. A., & Sharma, V. (2017). Comparative Model Studies on Circular & Square Footing Supported on Geocell Reinforced Sand. International Journal of Engineering Technology Science and Research, 4(4), pp. 420-427.

Shin, E. C., Kang, H. H., & Park, J. J. (2017). Reinforcement efficiency of bearing capacity with geocell shape and filling materials. KSCE Journal of Civil Engineering, 21(5), pp. 1648-1656.

Sireesh, S., Sitharam, T. G., & Dash, S. K. (2009). Bearing capacity of circular footing on geocell–sand mattress overlying clay bed with void. Geotextiles and Geomembranes, 27(2), pp. 89-98.

Sitharam, T. G., Sireesh, S., & Dash, S. K. (2005). Model studies of a circular footing supported on geocell-reinforced clay. Canadian Geotechnical Journal, 42(2), pp. 693-703.

Sitharam, T. G., Sireesh, S., & Dash, S. K. (2005). Model studies of a circular footing supported on geocell-reinforced clay. Canadian Geotechnical Journal, 42(2), pp. 693-703.

Tafreshi, S. M., & Dawson, A. R. (2010a). Behaviour of footings on reinforced sand subjected to repeated loading–Comparing use of 3D and planar geotextile. Geotextiles and Geomembranes, 28(5), pp. 434-447.

Tafreshi, S. N. M., & Dawson, A. R. (2010b). Comparison of bearing capacity of a strip footing on sand with geocell and with planar forms of geotextile reinforcement. Geotextiles and Geomembranes, 28(1), pp. 72-84.

Tanyu, B. F., Aydilek, A. H., Lau, A. W., Edil, T. B., & Benson, C. H. (2013). Laboratory evaluation of geocell-reinforced gravel subbase over poor subgrades. Geosynthetics International, 20(2), pp. 47-61.

Terzaghi, K. & Peck, R. B. (1967). Soil Mechanics in Engineering Practice, 3rd edition, Wiley, New York, NY, USA.

Tingle, J.S. & Jersey, S. R. (2007). Empirical Design Methods for Geosynthetic-Reinforced Low-Volume Roads, Journal of the Transportation Research Board. No. 1989, 2, pp. 91-101.

Ulgen, D. (2011). “An experimental study on the behavior of box-shaped culverts buried in sand under dynamic excitations” PhD. Thesis, Middle East Technical University, Ankara, Turkey.

Wesseloo, J., Visser, A. T., & Rust, E. (2009). The stress–strain behaviour of multiple cell geocell packs. Geotextiles and Geomembranes, 27(1), pp. 31-38.

Zhang, L., Zhao, M., Shi, C., & Zhao, H. (2010). Bearing capacity of geocell reinforcement in embankment engineering. Geotextiles and Geomembranes, 28(5), pp. 475-482.

APPENDIX A

COMPARISON OF RESULTS OF ÇİNE SAND WITH OTHER SANDS TAKEN FROM LITERATURE

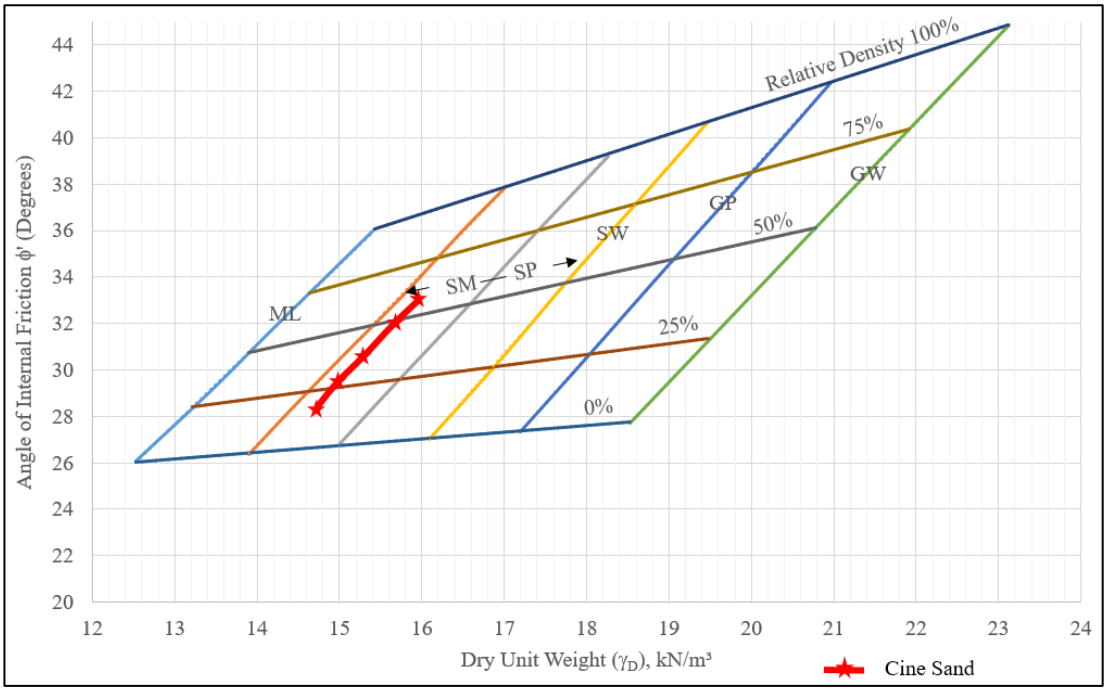

Figure A.1 The relation between friction angle and relative density (Riaund & Miran, 1992)

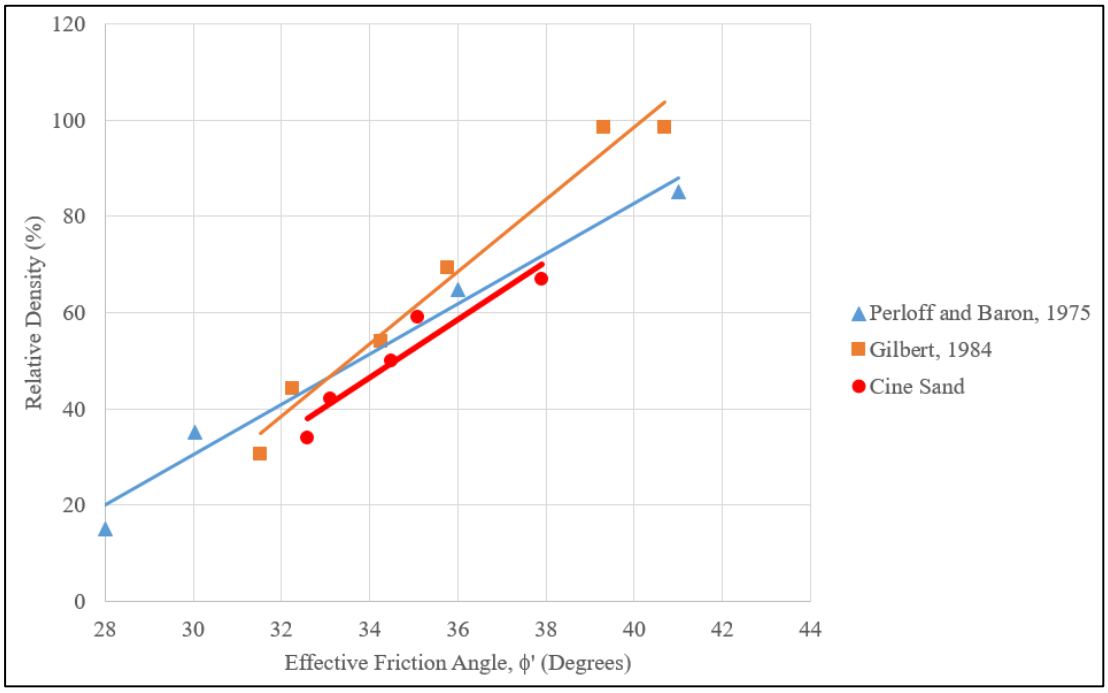

Figure A.2 Investigation of Density Variation in Triaxial Test Specimens of Cohesionless Soil Subjected to Cyclic and Monotonic Loading (Gilbert, 1984)

APPENDIX B

CORRECTIONS AND COMPARISONS OF CALIFORNIA BEARING RATIO (CBR) TESTS

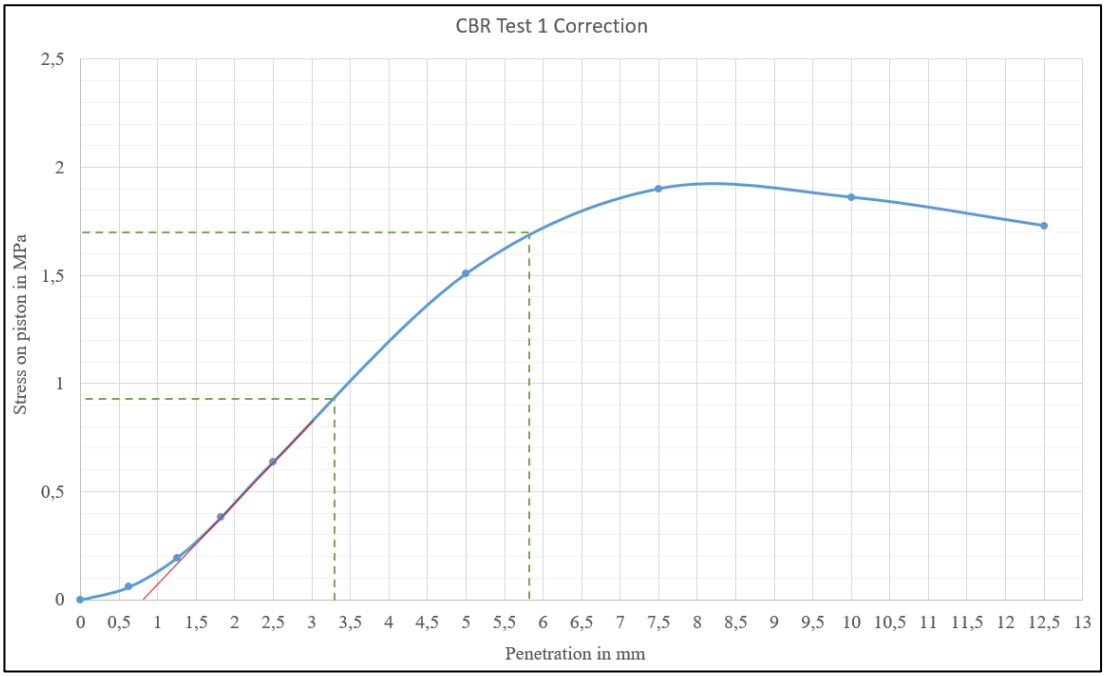

Figure B.1 Correction of CBR Test 1

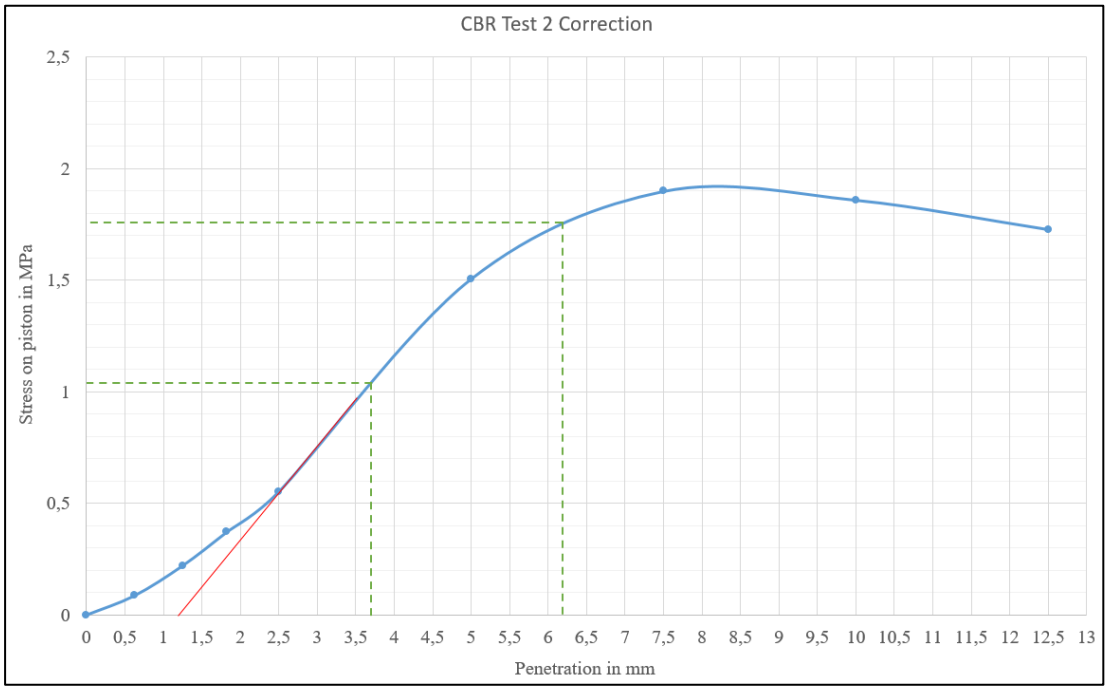

Figure B.2 Correction of CBR Test 2

COMPARISON OF CBR TEST RESULTS WITH UNIFIED SOIL CLASSIFICATION SYSTEM

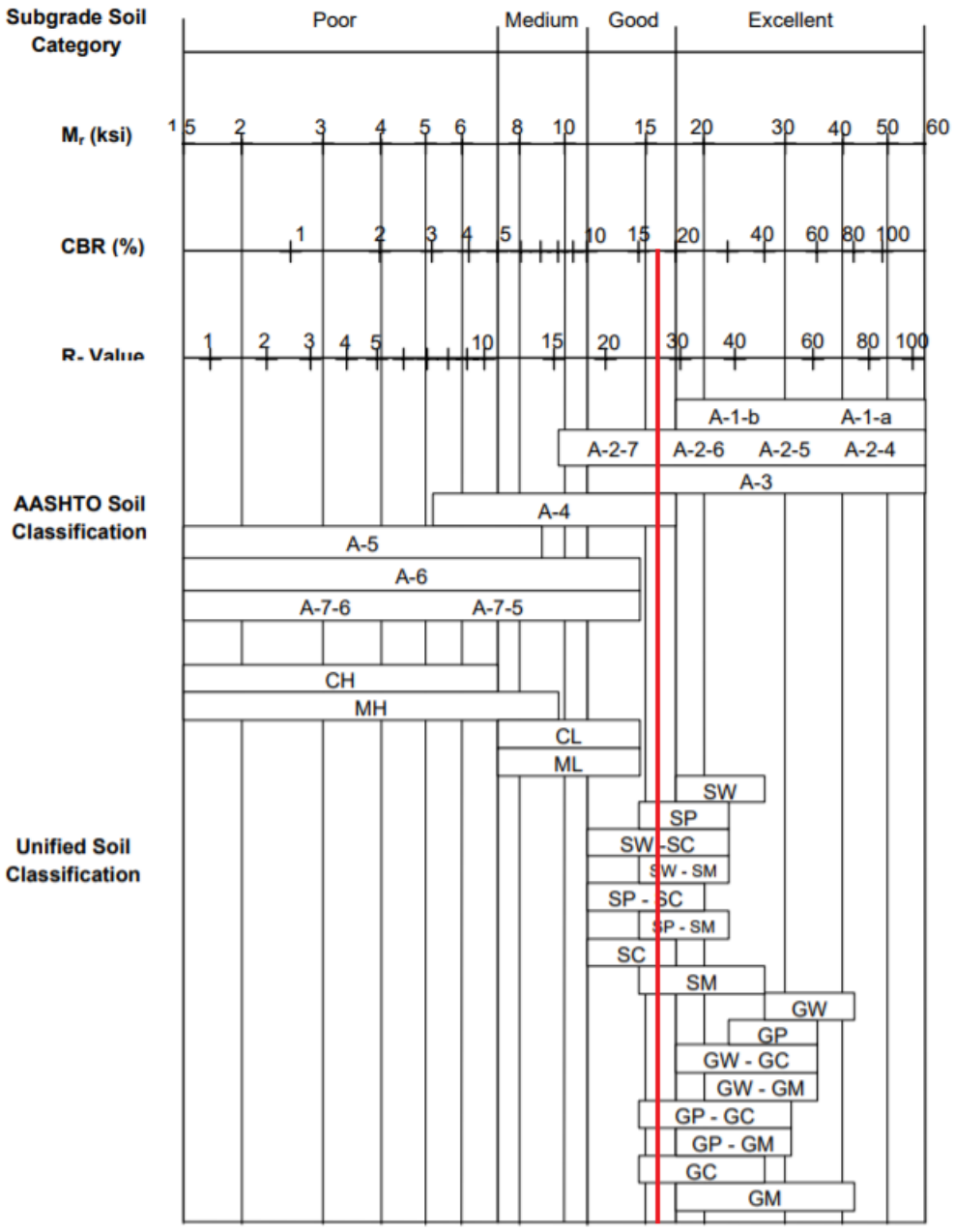

Figure B.3 Guidelines for Use of HMA Overlays to Rehabilitate PCC Pavements (NAPA, 1994)

APPENDIX C

PHYSICAL PROPERTIES OF RELATIVE DENSITY BOXES

Table C.1 Physical properties of relative density boxes

Box No	Test No	Diameter D (mm)	Height H (mm)	D_{ave} (mm)	H_{ave} (mm)	Volume			Mass (g)
						$V_{calipper}$ (cm^3)	V_{water} (cm^3)	V_{final} (cm^3)	
1	1	62.83	42.63	62.68	42.61	131.48	134.00	132.74	29.62
	2	62.44	42.59						
	3	62.77	42.61						
2	1	62.72	43.08	62.93	43.05	133.90	132.00	132.95	31.87
	2	63.17	43.02						
	3	62.91	43.04						
3	1	62.57	42.76	62.82	42.85	132.79	131.00	131.89	30.70
	2	62.73	42.92						
	3	63.15	42.86						
4	1	63.52	42.96	63.02	42.75	133.35	129.00	131.18	32.38
	2	62.43	42.75						
	3	63.12	42.53						
5	1	62.45	42.53	62.71	42.38	130.90	131.00	130.95	31.47
	2	62.92	42.31						
	3	62.77	42.29						
6	1	62.86	42.69	62.79	42.56	131.80	129.80	130.80	31.65
	2	62.80	42.38						
	3	62.71	42.62						
7	1	63.19	42.68	62.76	42.56	131.69	130.00	130.84	30.41
	2	61.73	42.49						
	3	63.37	42.52						
8	1	62.51	42.83	62.56	42.64	131.07	130.50	130.78	31.76
	2	62.71	42.29						
	3	62.45	42.81						
9	1	62.31	43.02	62.29	43.05	131.18	131.50	131.34	31.06
	2	62.30	43.05						
	3	62.25	43.08						

Table C.1 (continued)

Box No	Test No	Diameter D (mm)	Height H (mm)	D_{ave} (mm)	H_{ave} (mm)	Volume			Mass (g)
						$V_{calipper}$ (cm^3)	V_{water} (cm^3)	V_{final} (cm^3)	
10	1	61.95	42.88	62.21	42.97	130.61	129.00	129.80	30.44
	2	62.39	42.88						
	3	62.29	43.15						
11	1	63.05	42.62	62.97	42.77	133.21	132.00	132.61	31.77
	2	62.78	42.77						
	3	63.09	42.92						
12	1	62.51	42.68	62.38	42.72	130.56	131.80	131.18	30.07
	2	62.45	42.62						
	3	62.17	42.87						
13	1	62.65	42.62	62.81	42.78	132.54	131.00	131.77	32.15
	2	63.27	42.71						
	3	62.51	43.00						
14	1	61.52	42.76	62.10	42.73	129.44	131.80	130.62	32.09
	2	62.61	42.77						
	3	62.18	42.66						
15	1	62.23	42.77	62.30	42.79	130.44	132.00	131.22	31.04
	2	62.29	42.62						
	3	62.37	42.99						
16	1	62.43	42.82	62.37	42.80	130.77	130.60	130.69	32.83
	2	62.47	42.85						
	3	62.21	42.74						
17	1	62.35	42.54	62.16	42.54	129.11	128.90	129.00	31.78
	2	61.63	42.46						
	3	62.50	42.63						
18	1	62.35	42.42	62.38	42.46	129.77	129.50	129.63	31.92
	2	62.50	42.58						
	3	62.29	42.38						